Aus dem Institut für Medizinische Mikrobiologie
und Krankenhaushygiene
der Heinrich-Heine-Universität Düsseldorf
Direktor: Univ.-Prof. Dr. med. Klaus Pfeffer

Characterization of the impact of the transcription factor BATF on antigen cross-presentation of plasmacytoid dendritic cells

Dissertation

Zur Erlangung des Grades eines Doktors der Medizin
der Medizinischen Fakultät der Heinrich-Heine-Universität Düsseldorf

vorgelegt von

Jasmin K. Weber

2024

Als Inauguraldissertation gedruckt mit der Genehmigung der
Medizinischen Fakultät der Heinrich-Heine-Universität Düsseldorf

gez.:
Dekan: Prof. Dr. Nikolaj Klöcker
Erstgutachter: Prof. Dr. Stefanie Scheu
Zweitgutachter: Prof. Dr. Ingo Drexler

Zusammenfassung

Der Prozess der Antigen-Kreuzpräsentation (ACP) bestimmt die Immunantwort, insbesondere die Abwehr von Virusinfektionen und Tumoren durch den Wirt. Die Identifizierung von Faktoren, die die Funktionen von kreuzpräsentierenden Zellgruppen bestimmen, könnte gezielt eingesetzt werden und dadurch neue therapeutische Optionen für die Behandlung von Krebs und Virusinfektionen bieten.

Plasmazytoide dendritische Zellen (pDCs) stellen ein interessantes Ziel dar, da ihre Fähigkeit zur Antigen-Kreuzpräsentation noch nicht ausreichend untersucht wurde. Bei einem Forschungsansatz zur Identifizierung von Faktoren, die die Entwicklung und die Funktionen von pDCs regulieren, wurde festgestellt, dass BATF in aktivierten pDCs stark exprimiert wird. BATF ist ein Transkriptionsfaktor, der zur Superfamilie der Aktivator Proteine 1 gehört und laut Vorarbeiten zu diesem Projekt die Entwicklung von pDCs und ihre Fähigkeit, IFN I zu produzieren, kontrolliert. In Bezug auf die Entwicklung von pDCs bestimmt BATF die quantitative Differenzierung von pDCs zu Gunsten anderer dendritischer Zelluntergruppen, was die Frage nach einer BATF-abhängigen Funktionsverschiebung zwischen diesen Untergruppen aufwirft.

Ziel dieser Arbeit war es, die Rolle des Transkriptionsfaktors BATF in ACP in pDCs zu charakterisieren. Zu diesem Zweck wurden FACS-sortierte pDCs aus dem Knochenmark von *Batf*$^{+/+}$ und *Batf*$^{-/-}$ Mäusen in einer Zeitverlaufsstudie mit CpG stimuliert und Transkriptomstudien mittels Next Generation-Sequencing dieser Zellen durchgeführt. Unterschiedliche Expressionsmuster von ACP bestimmenden Faktoren wurden untersucht und mittels Real-Time PCR verifiziert. Anschließend wurde ein ACP-Versuch durchgeführt, um die direkte ACP-Fähigkeit von pDCs zu analysieren. Der Einfluss von BATF-Expression sowie Zellstimulation wurde im Hinblick auf die ACP-Kapazität, die Antigenaufnahmerate und die MHC I Molekülexpression der pDCs untersucht. Die daraus resultierenden Daten belegen die ACP-Fähigkeit von pDCs und zeigen, dass sie durch die Reifung der pDCs durch Aktivierung weiter gesteigert werden kann. Darüber hinaus wird BATF als entscheidender negativer Regulator von ACP sowie der Antigenaufnahmekapazität in pDCs charakterisiert, indem er die Expression mehrerer Gene koordiniert. In dieser Arbeit wird BATF zum ersten Mal als ausschlaggebender Suppressor von ACP in pDCs positioniert.

BATF erscheint somit als vielversprechender Kandidat für zukünftige Forschungen, da ein völlig neues Verständnis des Zusammenspiels zwischen IFN I, ACP und BATF zu neuen Therapieoptionen führen könnte, insbesondere im Bereich der zielgerichteten Therapien.

Abstract

The process of antigen cross-presentation (ACP) has a major impact on the immune response, especially regarding the host's defense against viral infections and tumors. The identification of factors determining the functional range of cell subsets conducting efficient ACP may be used in a targeted manner to provide new therapeutic options for the treatment of cancer and virus infections.

Plasmacytoid dendritic cells (pDCs) form an interesting target since their capacity to cross-present antigen has not been well studied. A research approach for the identification of factors regulating the development and functions of pDCs found BATF to be highly expressed in activated pDCs. BATF is a transcription factor belonging to the activator protein 1 superfamily that was found to contribute to the control of pDC development and their capacity to produce IFN I in preliminary studies leading to this project. Considering pDC development, BATF restricts pDC differentiation in terms of quantity in favor of other dendritic cell subsets raising the question of a BATF-dependent function shift between these subsets.

This thesis aimed to characterize the role of the transcription factor BATF in ACP in pDCs. For this purpose, FACS-purified bone marrow derived pDCs from *Batf*$^{+/+}$ and *Batf*$^{-/-}$ mice were stimulated with CpG in a time course study and transcriptome analyses using Next Generation-Sequencing of these cells were performed. Differential expression patterns of ACP controlling factors were studied and verified using real-time PCR. Subsequently, an ACP assay was performed analyzing the direct ACP ability of pDCs. The influence of BATF expression as well as cell stimulation was investigated with regard to ACP capacity, antigen uptake rate and MHC I molecule expression of pDCs.

Taken together, the data presented in this thesis verifies the ACP capability of pDCs that can be further enhanced by pDC maturation via activation. In addition, it characterizes BATF as a crucial negative regulator of ACP as well as antigen uptake capacity in pDCs by coordinating the expression of multiple genes. This thesis positions BATF for the first time as a critical suppressor of ACP in pDCs.

BATF thus appears to be a promising candidate for future research as a completely novel understanding of the interplay between IFN I, ACP and BATF may lead to new therapy options, especially in the field of targeted therapies.

List of abbreviations

abbreviation	meaning
-	negative
%	percentage
°C	degree celcius
+	positive
ACP	antigen cross-presentation
ACPC	antigen cross-presenting cell
AICDA	activation induced cytidine deaminase
AICE	activator preotin 1 interferon regulatory composite element
AP	antigen presentation
AP-1	activator protein 1
APC	antigen presenting cell
ARF	ADP ribosylation factor
BATF	basic leucine zipper transcription factor, activating transcription factor-like
BDCA3	blood dendritic cell antigen 3
Bip	immunoglobulin-binding protein
bp	base pair
bZIP	basic region and leucine zipper
cDC	classical/conventional dendritic cell
cDNA	complementray deoxyribonucleic acid
CH	chronic hepatitis
CHO	chinese hamster ovary
CLEC	C-type lectin domain family
cm	centimeter
CMV	cytomegalievirus
COP	coat protein complex
COVID-19	coronavirus disease 19
CSR	class switch recombination
CTL	cytotoxic T lymphocytes
DC	dendritic cell
DC-SIGN	cendritic cells specific ICAM-3 grabbing non-integrin
ER	endoplasmic reticulum
ERAD	endoplasmic reticulum associated degradation
ERAP	endoplasmic reticulum associated aminopeptidase
ERC	Endocytic recycling compartement
ERGIC	endoplasmic reticulum golgi intermediate compartment
Fig.	figure
FITC	fluorescein isothiocynate
Flt3-L	Fms-like tyrosine kinase 3 ligand
h	hour
HIV	human immunodeficiency virus
HSP	heat shock protein
HSV	herpes simplex virus
IBD	inflammatory bowel disease
Id2	inhibitor of DNA bining 2

IFN I	type I interferons
IFNγ	interferon-gamma
IKFZ	ikaros family zinc finger
IL	interleukin
ILC2	tissue resident group 2 innate lymphoid cell
IRAP	insulin-responsive aminopeptidase
IRF	interferon regulatory factor
ISG	interferon-stimulated genes
ITAM	Immunoreceptor tyrosine-based activation motif
KEGG	Kyoto Encyclopedia of Genes and Genomes
LCMV	lymphocytic choriomeningitis virus
M	molar
MERS	Middle east respiratory syndrome
MHC (I/II)	major histocompatibility complex (class I/II)
min	minute
mRNA	messenger ribonucleic acid
MVA	modified virus Ankara
NCBI	National Center of Biotechnology Information
NF-κB	nuclear factor kappa B
NGS	Next-generation sequencing
nm	nanometer
NOX	NADPH oxidase
NSCLC	non-small cell lung cancer
OVA	ovalbumin
PAMP	pathogen-associated molecular pattern
PD-1	programmed death 1
pDC	plasmacytoid dendritic cell
pFDR	P value corrected for the false discovery rate
PRR	pattern recognition receptors
PUVA	psoralen and ultraviolet A
R	receptor
Rac	Ras-related C3 botulinum toxin substrate
ROS	reactive oxygen species
rpm	rounds per minute
RT PCR	real-time PCR
SARS	revere acute respiratory syndrome
sec	second
SNARE	N-ethylmaleimide-sensitive factor attachment receptor
β_2m	β-microglobulin
TAP	transporter associated with antigen processing
TF	transcription factor
T_{FH}	T follicular helper cell
T_H cell	T helper cell
$T_H$xx	interleukin xx producing T helper cell
TLR	Toll-like receptor
U	units
Δ	delta
µl	microliter

Table of contents

List of figures

List of tables

1. Introduction

1.1 BATF

1.1.1 BATF: affiliation and functional principle

The basic leucine zipper transcription factor ATF (activating transcription factor)-like (BATF) was first isolated from a complementary deoxyribonucleic acid (cDNA) library prepared from messenger ribonucleic acid (mRNA) derived from human B cells which were infected with Epstein-Barr virus. BATF is an 125 amino acid protein that was first described by Michael Dorsey in 1995 [1] followed by the characterization of the murine homolog in 2001 [2].The *Batf* gene is located on mouse chromosome 12q and human chromosome 14q with a 96% human to mouse amino acid sequence identity of BATF [3].

The BATF-family comprises BATF, BATF2 and BATF3, all sharing the characteristic trait of containing a basic region and a leucine zipper (bZIP) domain [3]. However, they are lacking the transactivation domain, which is a common feature of most transcription factors [4]. Proteins with a bZIP domain all belong into one super family and regulate numerous cellular processes by mediating dimerization, DNA binding and therefore steering transcriptional regulation [5].

BATF belongs to the activator protein 1 (AP-1) superfamily. AP-1 is a collective term referring to dimeric transcription factors (TF) made up of Jun, FOS or ATF subunits [6]. These TFs display similar DNA binding profiles by binding to closely related DNA sites [7]. BATF is known as AP-1 inhibitor [2, 8] forming heterodimers with proteins of the Jun family (c-Jun, JunD, and JunB) [1]. It has been shown that these heterodimers interact with TFs of the interferon regulatory factor [9] family, specifically IRF4 and IRF8. These BATF-IRF complexes bind to AP-1-IRF composite elements (AICEs) of their target genes and are thereby transcriptional regulators in different immune cell types. This mechanism is especially important in dendritic cell (DC) development, T helper (T_H) cell function and in antibody production [3, 10, 11].

Thus, BATF has a fundamental role in the functionality of the adaptive immune response by its influence on cells of the immune system.

1.1.2 The impact of BATF on cellular orchestrators of the immune system

The expression of *Batf* and *Batf3* is restricted to the haematopoietic system [2], while *Batf2* shows a broader expression profile [12]. BATF3 influences the development of CD8α$^+$ conventional dendritic cells (cDCs). Mice lacking *Batf3* are defective in antigen cross-presentation (ACP) and CD8$^+$ T cell response. These mice were unable to generate West Nile virus specific CD8$^+$ T cell responses and had an impaired tumour rejection ability [13]. Interestingly, various studies showed the generation of CD8α$^+$ cells in *Batf3*$^{-/-}$ mice during different infections indicating a *Batf3*-independent pathway for the development of these cells [11, 14]. The analysis of mice lacking *Batf3* has led to the discovery that BATF family members can partially compensate for each other. BATF and BATF2 can both compensate for BATF3 regarding CD8α$^+$ cell development through a shared specificity within the leucine zipper domain making interactions with IRF family members possible.

This compensation mechanism was also discovered for T_H cells with restriction to only BATF and BATF3 being functionally exchangeable [11]. T_H cells originate from CD4$^+$ T lymphocytes developing in the thymus. Once they become T_H cells, they can for example interact with B lymphocytes to initiate antibody production or develop into regulatory T cells themselves. With these functions in addition to interleukin (IL) production they play an important role in different infections and autoimmune diseases [15]. *Batf* is required for the differentiation of IL-17 producing T_H (T_H17) cells [16, 17] as well as T_H9 cells [18] partly via its interaction with IRF4. Thereby it contributes to chromatin accessibility by increasing the recruitment of the chromatin remodelling factor *Ctcf* [19, 20].

Since BATF is also known as B cell activating transcription factor due to its origin [1], it is not surprising that it also has an influence on B cell functions. A loss of T follicular helper (T_{FH}) cells was observed in mice lacking *Batf* concomitant with a reduction in certain enzymes and antibody production. These conditions lead to a defect in a process called class switch recombination (CSR) [17]. It describes the mechanism how a B cell can switch from producing one immunoglobulin isotype to another. The goal is to express different antibodies leading to variable effector functions [21]. CSR is disrupted by BATF absence on the T cell as well as the B cell level. Firstly, *Batf* is required for the expression of other transcription factors regulating T_{FH} development [22], namely B cell lymphoma 6 (*Bcl-6*) [23, 24] and *c-Maf* [25]. Secondly, *Batf* controls the expression of activation induced cytidine deaminase (AICDA), an enzyme expressed in B cells and

fundamentally required for CSR [17, 22] as well as the expression of other genes (*Nfil3*, *Wnt10a* and *miR155hg*) playing essential roles during CSR [26].

BATF not only influences CD4⁺ T cell development and functions, but it has also been demonstrated to act as a checkpoint within the transcriptional process of effector CD8⁺ T cells. BATF has been found to upregulate critical TFs as well as cytokine receptors to reinforce a proper differentiation of this cell group [27]. In addition, BATF deficiency was observed to result in CD8⁺ T cell intrinsic defects leading to an impairment of virus control and viral persistence after infection with lymphocytic choriomeningitis virus (LCMV) in a mouse model [28].

Recently, it was also shown that BATF deficient mice lack another cell type serving as early responders to mucosal barrier disruption: tissue resident group 2 innate lymphoid cells (ILC2s). ILC2s can be subdivided into two distinct populations according to their responsiveness to IL-25 and IL-33 [29, 30]. The IL-25 responsive subset, called iILC2, is the one found to be affected by BATF expression. Together with CD4⁺ T cells, iILC2s serve as major IL-4 and IL-13 producers [31], playing an important role especially during helminth infections [32-34].

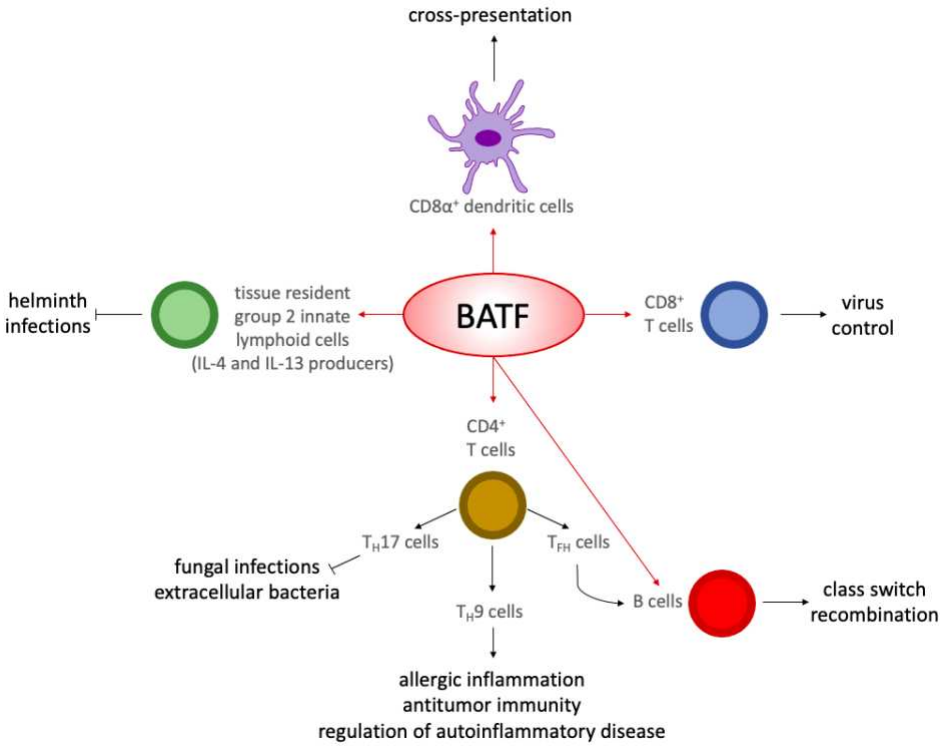

Fig. 1: Different cell types influenced by BATF-expression and their main fields of function (for illustration the servier medical art database was partly used, cartoons were adapted. Modified after Murphy, 2013). IL = interleukin, $T_{(F)H}$ = T (follicular) helper cell.

Regarding all this information, BATF has a major impact on different cell types executing diverse functions within several immune defence processes (see Fig. 1). This suggests a possible pivotal role of BATF in multiple diseases like autoimmune disorders, infections, and cancer.

1.1.3 *Batf* in the context of disease onset and course of action

As presented above, *Batf* has been identified to have an impact on a great deal of cells of the immune system and thereby influences the immune defence under various conditions (see section 1.1.2). In general, several bZIP proteins have been identified to play a role in cancer disease patterns concomitant with the fact that transcriptional deregulation is a basic mechanism of oncogenic transformation [5, 35, 36]. *Batf* has been suggested to include *c-Myb* as one of its target genes [37]. The *c-Myb* gene encodes a TF that regulates cell proliferation, differentiation and apoptosis and has been associated with various tumours including hematopoietic malignancies, breast cancers, colon cancers, pancreatic cancers, melanomas and several others [38]. Regarding these results it is not surprising that *Batf* itself was found to be associated with numerous malignant disease patterns. Only recently it was identified to be part of a prognostic 8-gene signature for acute myeloid leukaemia, representing a high-risk gene within this context. Patients with high expressions of BATF had a significantly lower survival rate in this study [39]. BATF expression was also found to be significantly upregulated in non-small cell lung cancer (NSCLC) tissue. Furthermore, *Batf* knockdown in the human NSCLC A549 cell line induced apoptosis while inhibiting cell proliferation. These results suggest that BATF may be a potential target for treatment of NSCLC as it potentially conducts an oncogenic role during the disease development [40]. As mentioned before, *Batf* is critical for the development and function of multiple cell subsets (see section 1.1.2). *Batf* dependent T_H17 cells were identified as crucial regulators of sporadic and inflammation induced colorectal cancer formation and progression. *Batf* expression correlated with IL-23 and IL-23 receptor (IL-23R) expression within cancerous tissue samples [41]. Predisposing for colorectal cancer is a condition referred to as inflammatory bowel diseases (IBDs), representing a group of chronic immune-mediated disorders, where *Batf* also seems to be a critical regulator of disease activity [42]. Targeting *Batf* and *Batf* dependent IL-23R$^+$ T cells emerges as a promising future therapeutic strategy for IBDs and colorectal cancer [41, 42].

In addition to autoimmune IBDs, *Batf* has also been reported to play a crucial role in allergic asthma mediating lymphocyte- and mast cell driven immune responses [43, 44]. Regarding allergic asthma, *Batf* deficiency seems to represent a protective condition resulting in defective IgE levels, mast cell development and cytokine production including interferon-gamma (IFNγ) production by $CD8^+$ T cells. In addition, the mRNA expression of *Batf* in peripheral blood mononuclear cells is increased in patients not treated with glucocorticoids [43]. Glucocorticoids represent one of the most effective and common treatments of asthma [45].

Finally, *Batf* has been associated with different chronic infections. Regarding chronic hepatitis (CH) B for example, BATF expression is significantly up regulated in the peripheral blood of CH B patients compared to healthy individuals. Also, an examination of infiltrating cells in the liver revealed an accumulation of BATF-positive cells in the livers of CH B patients as well as a correlation of high numbers of these cells with a higher grade of inflammation [46]. In general, $CD8^+$ T cells develop functional defects during chronic viral infections, collectively referred to as exhaustion [47, 48]. A phenomenon occurring due to T cell exhaustion is the increased expression of multiple inhibitory receptors. One of these is Programmed Death 1 (PD-1) [49, 50], which is known to contribute to the impairment of virus-specific T cell function [50, 51]. It has been demonstrated that PD-1 upregulates a program of genes including BATF in virus specific $CD8^+$ T cells in human immunodeficiency virus (HIV) patients. Antigen-specific T cells with the greatest degree of dysfunction were observed to show high BATF levels. Silencing BATF on the other hand led to the rescue of HIV-specific T cell function suggesting a key role of BATF mediating T cell responses during chronic viral infections like HIV [52].

As illustrated above, BATF decisively influences the development and immunological response actions to various diseases, especially by its influence on T cell function and regulation of other influencing variables. Despite the pivotal functions of T cells, DCs have key roles as well in this regard acting as central players during immune response plus being an attractive target for treatment options [53-55].

1.2 Dendritic cells

DCs were first discovered by Ralph Steinman and Zanvil Cohn in 1973. The researchers described a phagocytic dendrite-like cell with pseudopods [56] and subsequently

mapped out their functional role as potent stimulators of T cell response [57, 58]. Since then, the central role of DCs regarding immune defence mechanisms as well as maintenance of tolerance has been elaborated within the literature. When DCs encounter invading pathogens, they undergo a process referred to as DC maturation. This maturation process describes the induction of several changes within the cell, like the upregulation of costimulatory molecules and chemokine receptors, pro-inflammatory cytokine release and a complex mechanism called antigen presentation (AP) [59-61]. Especially regarding AP DCs act as key players which is discussed in detail within this thesis in the following chapter (see section 1.3). Today, DCs are distinguished based on different phenotypical and transcriptional markers. Thus, they can be separated into different functional subsets. They are often referred to as antigen presenting cells (APCs) comprising cDC types (cDCs1 and cDCs2), plasmacytoid dendritic cells (pDCs), monocyte-derived DCs and Langerhans cells [62-64]. This work sets the focus on the first two subsets, especially on pDCs.

DCs, like most immune cells, develop from a bone marrow resident hematopoietic stem cell [65]. Their differentiation process is tightly regulated by different transcription factors [66]. Hematopoietic stem cells give rise to multipotent progenitors [67-69], which subsequently develop into lymphoid-primed multipotent progenitors and further along become so-called common myeloid progenitors and common lymphoid progenitors [70]. The generation of actual cDCs and pDCs is dependent on a common DC progenitor [71, 72], which evolve from bipotent macrophage-DC progenitors [73]. cDCs have another precursor, the pre-DC, intercalated before terminally differentiating into cDCs within the blood vessels [70, 74]. pDCs, on the contrary, fully develop within the bone marrow and travel ready to act to targeted tissues and organs via the blood stream [75, 76].

Both, cDC and pDC development crucially depends on the Fms-like tyrosine kinase 3 (Flt3) and its ligand (Flt3-L) [77-79]. Flt3 is expressed by various precursor cells [80] as well as fully developed DC subpopulations [81]. Flt3 expression is controlled by the transcription factor PU.1 influencing cell-fate decisions [82]. *In vitro* cultures of murine bone marrow precursors generate pDC and cDC equivalents under the presence of Flt3 [74], and also *in vivo* an expansion of these cell types has been demonstrated under Flt3-L administration [83].

Fully developed DCs pursue unique effector functions and can be distinguished by their phenotypical characterization and functional specialization (see Fig. 2), which is presented in more detail in the following sections (see sections 1.2.1 and 1.2.2).

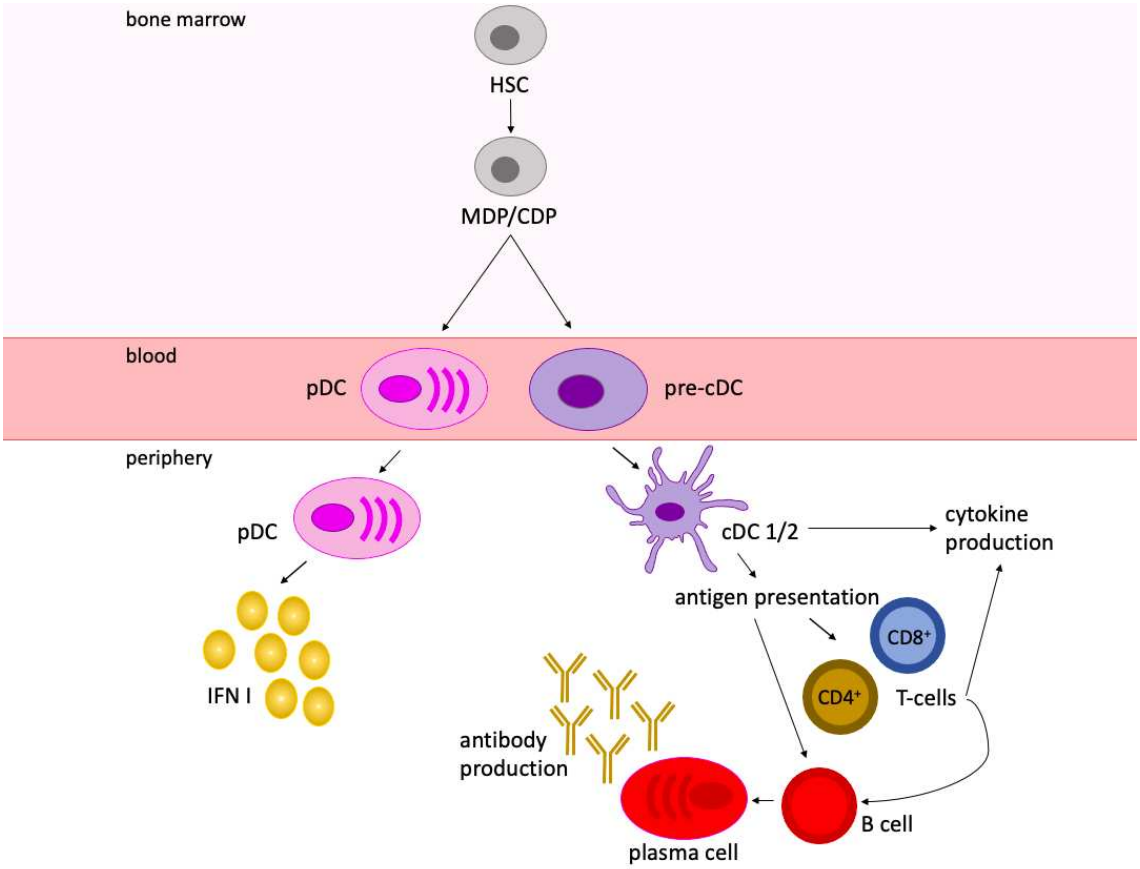

Fig. 2: Development of dendritic cell subsets and their main tasks
(for illustration the servier medical art database was partly used, cartoons were adapted. Modified after Ivashkiv, 2014; Merad, 2013; Schraml, 2015). HSC = hematopoietic stem cell, CDP = common dendritic cell progenitor, MDP = macrophage dendritic cell progenitor, cDC = classical dendritic cell, pDC = plasmacytoid dendritic cell

1.2.1 Conventional dendritic cells

cDCs are professional antigen presenting cells with pivotal functions assuring an appropriate immune response [59, 84]. DCs in general express the haematopoietic markers MHCII, CD45 and CD11c on their cell surface [59] and can be divided into further groups taking more surface markers into account [59, 62, 66].

The first subset, cDCs1, is depending on their migratory manner positive for the markers CD8α and CD103 [59, 62, 64, 85]. In addition, they express Xcr1 [86] and CD26 [63] as well as Clec9A [87]. cDCs1 have been shown to depend on several transcriptional regulators like *Batf3* [13], *Irf8* [88-90], *Bcl6* [91, 92], inhibitor of DNA binding (Id) 2 [93, 94], nuclear factor interleukin-3-regulated protein [95] and ETS variant 6 [96]. Due to their expression of surface markers and dependency on certain transcription factors,

cDCs1 are often referred to as *Irf8*- or *Batf3*-dependent as well as CD103$^+$ DCs in literature [66].

The most important function of cDCs1 is probably their ability to cross-present antigens leading to the cross-priming of CD8$^+$ T cell responses [13, 97, 98]. This mechanism is critical for tumour and virus response as further discussed in the following sections (see section 1.3.1). Besides its superior role in cross-presenting antigens to CD8$^+$ T cells, the cDC1 subset also induces CD4$^+$ helper T cell responses [99, 100]. These cells predominantly differentiate into T_H1 helper T cells, a mechanism mainly driven by IL-12 secretion upon stimulation [101]. Moreover, IFNλ production was observed within this subset after stimulation [102].

The second subset of cDCs, cDCs2, is a functionally more diverse subpopulation expressing the marker Sirpα (CD172a) [63, 86] and CD11b [59]. It is important to consider, that CD172a is not a unique marker for cDCs2 and must be combined with another DC marker, like major histocompatibility complex (MHC) class II or CD11c to exclusively identify this subset [64]. cDCs2 dependent on the transcription factors Notch2 [103, 104] and Klf4 [105].

They are specialized in presenting antigens via MHC II and therefore play a crucial role in the protection from extracellular pathogens [106]. Via this mechanism they facilitate the activation and proliferation of naïve CD4$^+$ T cells into CD4$^+$ T_H cells [59]. They have also been shown to act as a major source of IL-23 inducing protective responses against infections [103].

To distinguish these two subsets, the hallmark of CD172a or Xcr1 expression can be used since these two markers are selectively expressed and independent of activation status and location [86]. A third group of DCs, pDCs, is defined by own surface markers and is especially important during viral infections as described in the subsequent section (see section 1.2.2).

1.2.2 Plasmacytoid dendritic cells

pDCs are mostly famous for their major production of type I interferons (IFN I - IFNα and β) [64, 107-110]. The prompt induction of the secretion of massive amounts of IFN I is dependent on the adaptor myeloid differentiation primary response gene 88 (MyD88) [111] and the transcription factor IRF7, which is highly expressed by pDCs [112-114].

pDCs act as sensors for viral infections primarily via the two toll-like receptors (TLRs) 7 and 9 [109, 115, 116]. Stimulation of these TLRs by viral nucleic acids leads to the forming of a complex comprising MyD88, IRF7 and TRAF6 [117, 118] together with IRAK4 [118]. This process leads to the to the activation of IRF7 by phosphorylation and its translocation into the nucleus inducing IFN I production [119]. Even if pDCs are not directly infected themselves, they can respond with IFN I production causing a general reduction of viral titres [66, 120]. In addition, IFN I promote the expression of interferon-stimulated genes which are associated with the restriction of viral entry and replication [121, 122]. TLR triggering also activates the nuclear factor kappa B (NF-κB) pathway in pDCs achieving the production of other pro-inflammatory cytokines and the expression of costimulatory molecules [123].

Murine pDCs express the surface markers Siglec-H, CD317 (PDCA-1, BST2), Ly6C and B220 (CD45R) [64, 66, 124], while human pDCs can be characterized by CD123 (IL-3R), CD303 (BDCA2) and CD304 (BDCA4) [64, 124]. Their development is dependent on several transcription factors. As mentioned before, PU.1 controls dendritic cell development [82]. This regulation functions via an induction of the transcriptional regulator DC-SCRIPT. Since it represses pDC differentiation, pDC progenitors only show low levels of PU.1 [125]. In addition, the Ikaros family zinc finger protein 1 (IKZF1) has been suggested to contribute via a repression of transcriptional programs [126]. IKZF1 was recently found to play an important role in humans for pDC as well as cDC development [127]. Also, E2-2 seems to play a particularly pivotal role [128]. E2-2 belongs to the group of E proteins, which are together with Id proteins known to regulate various differentiation processes within the hematopoietic system [129]. Id2 overexpression has been demonstrated to inhibit pDC development *in vitro*. Especially at an early stage, the E2-2 and Id2 axis determines pDC versus cDC1 lineage decision [66, 130, 131]. E2-2 has also been found to directly activate genes encoding other transcription factors or genes associated with pDC functions [64, 128, 129, 131, 132], like *Spib* and *Bcl11a*. Both are involved in pDC development, partly by E2-2 and Id2 regulation [66, 133, 134]. E2-2 also regulates the expression of *Runx2*. Once fully developed, *Runx2* promotes pDC migration into the periphery from the bone marrow. This process is facilitated by the expression of chemokine receptors, like Ccr5 [135]. *Runx2*-deficiency also causes an impairment of IFNα response leading to higher viral titers [136]. Similar to cDCs, pDCs can travel to target organs from the periphery, also in a chemokine receptor-dependent manner, like CCR7 [137] and CCR9 [138].

Despite their unquestioned standing as IFN I producing cells, the efficiency of pDCs to present antigens within the different known pathways remains a debate in the literature, especially when compared to cDCs [66, 139, 140]. Nevertheless, pDCs have been demonstrated to be able to present antigens to activate both, $CD4^+$ T cells [141] as well as $CD8^+$ T cells [142-145]. Interestingly, regarding ACP there seems to be a general difference between mouse and human DC subsets. While in mice cDCs1 are the key cross-presenting cells leaving the role of pDCs in cross-presentation controversial [146], human DC subsets appear to be equally capable [147]. In humans, it is accepted that pDCs efficiently cross-present antigen and initiate an antigen-specific CD8 T cell response [148-150]. Mouse pDCs on the other hand have sometimes failed at attesting their efficacy to cross-present exogenous antigens [141, 144]. However, in other studies they proved to be capable of cross-presenting ovalbumin (OVA) to $CD8^+$ T cells [145]. As a matter of fact, they can capture, degrade antigen and cross-prime naïve $CD8^+$ T cells *in vitro* and *in vivo* [151, 152]. A recent study tried to understand the mechanism in more detail and suggested a DC dependency for the ACP process of pDCs [153].

Regardless of how the process works in detail, there is increasing evidence that pDCs play a role in cross-priming and it is becoming more likely that both, pDCs and cDCs, are necessary in order to achieve optimal $CD8^+$ T cell immunity [70, 154-157]. Moreover, focusing on pDCs in actual clinical pictures, immunotherapies including pDCs have shown promising results [158-161].

1.2.3 The role of pDCs during infections and possible immunotherapy targets

During infections of all sorts pDCs feature their specialization in producing IFN I, which is particularly important at early stages of systemic viral infections [162]. In addition, persistent or uncontrolled activation of pDCs is associated with several inflammatory and autoimmune diseases and cancer.

Already in previous studies regarding severe acute respiratory syndrome (SARS) and middle east respiratory syndrome (MERS) coronavirus, pDCs have been in the focus of research in coronavirus infections. In mouse models their contribution to defence against coronaviruses via IFN I production is an essential factor determining the course of infection [163, 164]. During the early phase of infection pDCs migrate to the lung which matches with a high IFNα production [164, 165]. Regarding coronavirus disease 19

(COVID-19) patients, their pDC number was reduced in blood samples. This may be due to a prior response resulting in a diminution of circulating pDCs and/or their mobilization to the infected site [166].

Despite that, pDCs have been most intensively studied for their role during chronic viral infections, especially HIV [55, 167-180] and CH [181-189]. In hepatitis B and C infections pDCs act as IFN I producing cells [184] but display reduced numbers and deficiencies at chronic disease state [182, 183]. Differing from other viral infections, pDCs were observed not to depend on primary contact with virus particles upon hepatitis C infection. Direct exposure to an infected cell with active viral replication is enough to set their IFN I production in motion [184]. Regarding HIV, the contribution of pDCs in pathogenesis has not been fully understood [178, 190]. Here, pDCs were found to express high levels of the major receptor of HIV-1 (CD4) in addition to the co-receptors (CCR5 and CXCR4) [108, 173] enabling them to be rapidly activated and produce high levels of IFNα mainly via TLR7 [172]. Making use of pDC depletion mouse models, they were even identified as the major source of IFN I production during HIV-1 infection contributing to the suppression of viral replication [190]. This coincides with the finding in HIV-infected patients, where a decrease in IFNα production is correlating with numerical and functional deficiencies in circulating pDCs [191]. In general, HIV-1 patients display a reduced number of DCs through several subsets [192]. In chronic HIV infections pDC levels also inversely correlate with the viral load measured in plasma samples [171] and their depletion is associated with disease progression as well as opportunistic infections [193]. Notably, this early IFN I response in HIV-1 infections seems to be distinct from the early changes during HIV-2 infections, where pDCs rather perform the task of antigen presentation [194]. However, one hallmark of HIV-1 infection correlating with disease progression to developing an acquired immunodeficiency syndrome is an aberrant immune activation [195, 196]. Concomitant with that, permanently activated pDCs have also been linked to disease progression [197, 198] and their activation level was observed to correlate with $CD4^+$ T cell depletion [22] representing one of the most important clinical markers for disease progression [199]. Therefore, new approaches targeting pDC depletion or IFNAR blockade might provide new insights [55]. To sum up, pDCs respond with robust IFN I secretion to HIV infection but further research is needed to understand whether this contribution is primarily offering benefits for the host or may also bring harmful aspects, especially when remaining in an activated status.

Infiltrating pDCs and evidence of IFN I responses have also been associated with multiple autoimmune disorders including systemic lupus erythematosus, Sjögren's

syndrome, systemic sclerosis, psoriasis, IBDs and multiple sclerosis. In addition, different types of neoplastic formations involving pDCs have been identified: the blastic pDC neoplasm [200-204] and a condition referred to as mature pDC proliferation associated with myeloid neoplasms including chronic myelomonocytic leukaemia [205], myelodysplastic syndrome [206, 207] and acute myeloid leukaemia [208-211]. Therefore, numerous therapeutic approaches targeting either pDCs themselves or the IFN pathway including nucleic acid sensors are currently being explored during these conditions [55, 212].

Besides the ability of pDCs to crucially support the innate immune defence with their IFN I production, IFN I is also known to contribute to antigen cross-presentation [213, 214].

1.3 Antigen presentation

AP is a fundamental requirement to achieve an appropriate immune response. Regarding the immune response to invading pathogens there are two main defence systems acting synergistically together: the innate and the adaptive immune response. Each comprising both cellular and humoral components accomplishing different effector functions. The innate immune response represents the rapid unspecific first line defence. While the adaptive immune response acts pathogen-specific and induces the development of an immune memory making the hosts response considerably more effective when being encountered a second time with the same specific pathogen [215].

Physical barriers like intact skin or mucosa are part of the innate immune defence. Once these barriers are broken and pathogens can penetrate, the first step is the recognition of these pathogens. So-called pathogen-associated molecular patterns (PAMPs) are recognized by pattern recognition receptors (PRR), like TLRs. TLRs are among other cells particularly found on macrophages and dendritic cells [215, 216]. Macrophages start phagocytosing the invading pathogens while releasing different cytokines like chemokines, IL-1β and IL-6 and tumour necrosis factor leading to a recruitment of further immune cells and causing an inflammatory reaction. In addition, a local coagulation cascade prevents further blood-stream dissemination and acute-phase proteins are produced. This leads to the activation of the complement system which can opsonize pathogens directing them into elimination processes [217].

An important key player within this process are DCs acting as professional APCs after phagocytosing pathogens. They travel to the lymph nodes presenting parts of the internalized material on their surface to T cells and are thereby linking the innate sensing of pathogens to the adaptive immune response [215, 217]. DCs have the crucial capacity of activating T cells. Following internalization and several processing steps the antigens are loaded onto MHC molecules. These are essential for the display of the processed intake on the cell surface to interact with T cells and thereby activating them to empower their helper function or cytotoxic capacities [218].

How this antigen presentation process takes place in detail is dependent on the origin of the presented antigen. Endogenously synthesized antigens within the cell cytosol, for example of viral or tumour origin, are degraded in the proteasome and further trimmed in the endoplasmic reticulum (ER) before being finally bound to MHC I. These MHC I/peptide complexes travel to the cell surface where they are presented to $CD8^+$ cytotoxic T lymphocytes (CTLs). This mechanism enables the T lymphocytes to identify and eliminate infected or cancerous cells. On the contrary, extracellular antigens are taken up into the cell by endocytosis are bound to MHC II molecules and presented to $CD4^+$ T_H cells. They undergo processing steps which mainly function via lysosomal proteases and cathepsins within the endosome/phagosome and the MHC II compartment organelle [219-221].

These two described antigen presentation mechanisms are referred to as classical or direct antigen presentation. An interesting mechanism, termed ACP, is linking the two classical routes by presenting exogenous antigens via MHC I molecules. Cross-presentation has been shown to play an important role regarding the immune response against tumours and viral infections [222-224].

1.3.1 The process of antigen cross-presentation

ACP was first described in 1976 by Bevan et. al. It was observed that mice receiving allogeneic cells, a donor specific $CD8^+$ T cell response is induced [97]. Until then, it was believed that MHC I molecules could only present endogenous peptides [225] like described above as one of the classical ways of antigen presentation.

The detailed course of events during cross-presentation remains a matter of debate. However, two main intracellular cross-presentation pathways have been described: the endosome-to-cytosol or cytosolic pathway and the vacuolar pathway [226-228] (see Fig.

3), which can be further distinguished according to their dependency on different proteins (see Fig. 5). The cytosolic route is sensitive to proteasome inhibitors [229], indicating that ingested proteins are degraded in the proteasome after accessing the cytosol [226, 230]. Derived peptides are subsequently fed into the classical MHC I presentation pathway. This involves a transport in the ER via a transporter associated with antigen processing (TAP) and a further trimming by ER associated aminopeptidase (ERAP) 1 before loading the peptides on MHC I molecules [229, 231, 232]. Whereas the idea of the vacuolar pathway is based on the fact, that there is evidence for ACP to take place in a proteasome-inhibitor resistant and TAP independent way [233-235]. This mechanism on the other hand is sensitive to endosomal proteases, especially cathepsin S inhibitors [233]. In addition, the ACP capacity of soluble ovalbumin is not affected by ERAP1 deficiency, suggesting that the processing may take place in an environment which does not contain ERAP1 [232]. The insulin-responsive aminopeptidase (IRAP) was identified to localize in endosomes [236], suggesting that both antigen degradation, including final processing and loading onto MHC I molecules, could take place within the endocytic compartments within this pathway [226]. This is often referred to as TAP independent ACP pathway [237, 238]. A third approach, cross-linking the two pathways, is a TAP dependent but ER circumventing pathway. This is based on the idea that cytoplasmatic processing is indeed necessary, but derived peptides might be reimported from the cytoplasm into phagosomes where MHC I loading then occurs [239].

Overall, it is difficult to determine how much the different pathways contribute *in vitro* and *in vivo*. There is evidence, pointing to the proteasome dependent cytosolic pathway as the predominant mode of operation. This evidence is mainly based on the observation, that DCs deficient in a subunit of the immunoproteasome, namely LMP7, are impaired in ACP [230]. There are always three crucial steps, which are tightly regulated by numerous proteins: antigen internalization, processing and presenting via MHC I molecules including the generation of MHC I/peptide complexes and their trafficking towards the cell surface [227].

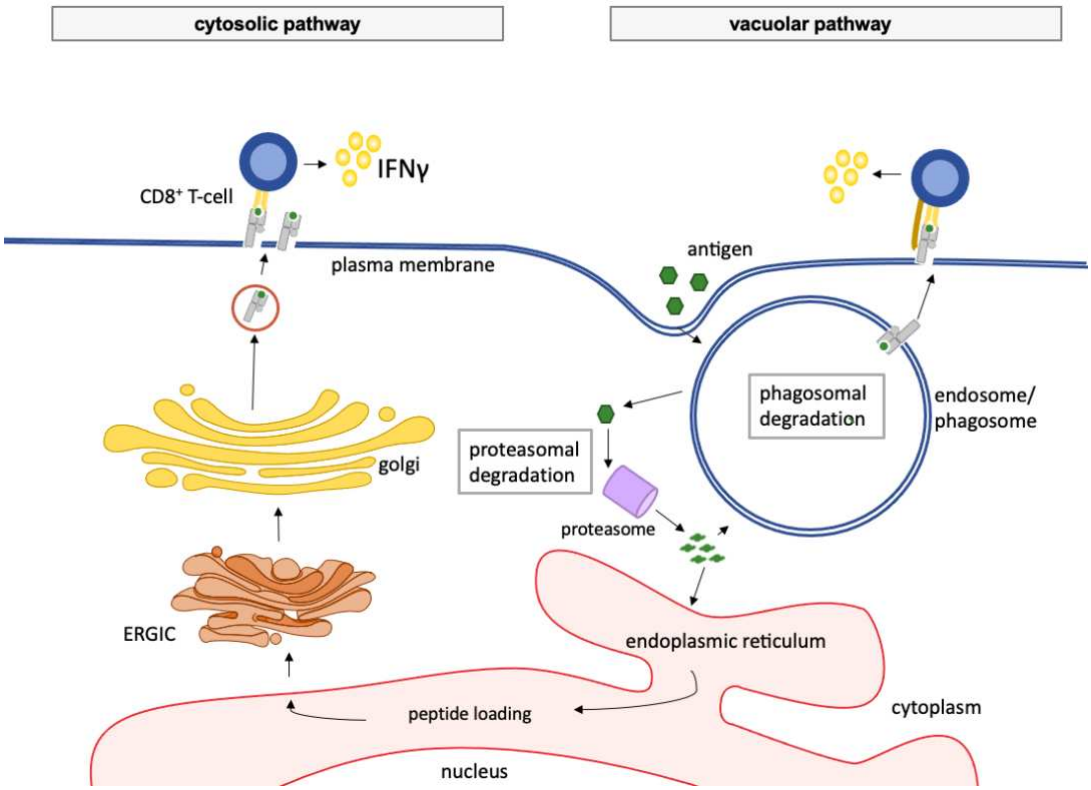

Fig. 3: The different pathways of cross-presentation.
One possibility is that antigens need to enter the endoplasmic reticulum to be fully processed and loaded onto MHC I molecules. This way is referred to as the cytosolic pathway. Another way, named vacuolar pathway, describes the option of antigen processing and loading solely within the phagosomal compartment. In both cases the result is that peptide loaded MHC I molecules travel to the cell surface and interact with $CD8^+$ T cells (for illustration the servier medical art database was partly used, cartoons were adapted. Modified after Blander, 2018). ERGIC = endoplasmic reticulum golgi intermediate compartment, IFNγ = interferon-gamma

1.3.1.1 Uptake and first stages of intracellular transport

The term endocytosis describes two different types of mechanisms by which cells can take up extracellular materials: phagocytosis and pinocytosis. Phagocytosis is the process responsible for engulfing larger particles. Pinocytosis involves the uptake of fluids and small molecules and can be further divided into different processes. The term comprises micropinocytosis as well as mechanisms depending on certain proteins within the cell membrane [240, 241]. It is known that antigens that are taken up via fluid-phase pinocytosis are cross-presented very poorly [242]. Particulate antigens that were internalized by actin-dependent processes like phagocytosis or micropinocytosis [240, 243, 244] on the other hand are cross-presented much more efficiently [242].

Furthermore, the uptake of antigens targeted for ACP is subject to cell surface receptors. Receptor-mediated impact on cross-presentation seems to involve intracellular targeting

of exogenous antigens to subcellular compartments most facilitating cross-presentation [245]. It has been demonstrated that internalized antigens do not simply enter one common early endosome compartment [246].They are targeted into different pools influencing their further presentation pathway regarding their presentation capacity to $CD4^+$ or $CD8^+$ T cells (see Fig. 4). Antigens that are cross-presented need an only mildly acidic intraphagosomal pH value. For particulate antigens this requirement results in a time dependency, as MHC I and MHC II presentation take place one after another. Early phagosomes showing higher pH levels over time perform MHC I presentation followed by a loading onto MHC II molecules when more acidic pH values occur. The receptor-mediated predetermination of the targeted endosome is mainly affecting soluble antigens as their presentation is localization dependent correlating with the required pH. Soluble antigen taken up via the mannose receptor for example enter a stable early endosome which is an exclusive compartment for MHC I presentation [245].

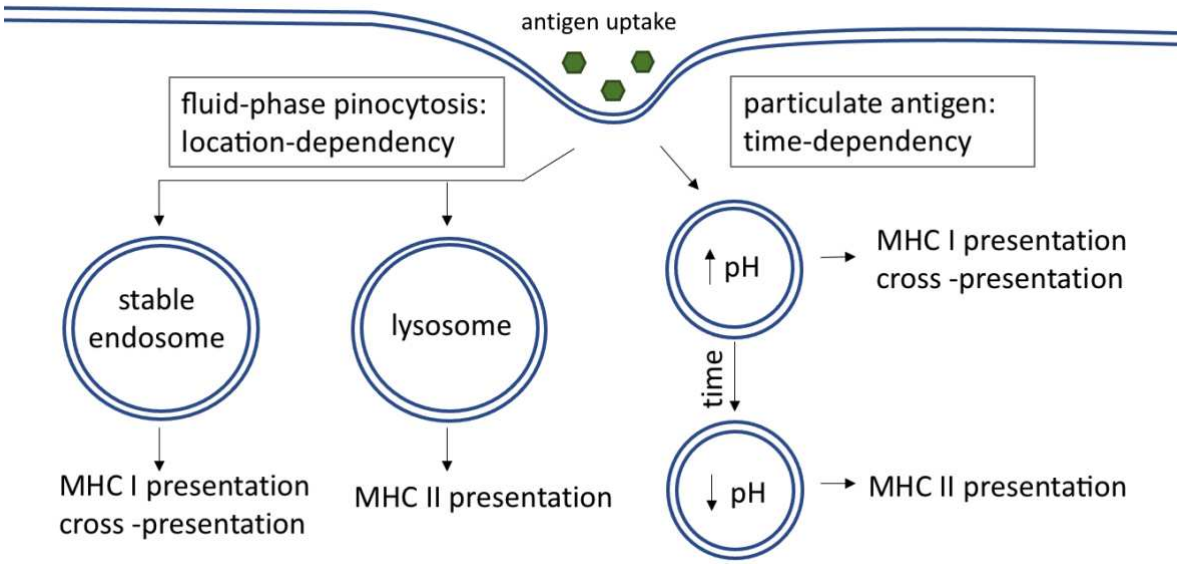

Fig. 4: Different mechanisms of antigen uptake deciding antigen fate regarding subsequent intracellular routes
(modified after Burgdorf, 2008). MHC I/II = major histocompatibility complex class I/II

Especially C-type lectin receptors have been shown to have an impact on ACP. Enhanced specific $CD8^+$ T cell responses were observed when antigen was delivered to the DCs via the C-type lectin domain family (CLEC) member 4A (CLEC4A) [247]. Also CLEC9A enhances cross-presentation by human blood DC antigen 3 $(BDCA3)^+$ cells [248] which are considered as the main cross-presenting human myeloid cells and therefore resembling mouse $CD8^+$ DCs [249-251]. In mice CLEC9A has been demonstrated to play a crucial role in cross-presenting dying infected cells and thereby

protecting from viral infections [252, 253]. Targeting human dendritic cells via the DC associated surface receptor DEC-205 increased both, internalization and cross-presentation capacity [254]. Regarding ACP efficiency the same results were observed for antigens targeted to DC-specific ICAM-3-grabbing non-integrin (DC-SIGN) using a human skin explant model [255]. Another CLEC-family member, CLEC12A, which is broadly expressed by all human DC subsets as well as mouse $CD8a^+$ and pDCs, also showed an increasement of cross-presentation in human DCs [256, 257].

These results could explain why certain receptors, for example the mannose receptor or DEC-205, are selectively expressed by APCs that can cross-present. These receptors may be a superior tool to identify cross-presenting APCs compared to the marker CD8 [258]. After the antigens have been internalized and pre-sorted into suiting endocytic compartments, the actual processing of the antigens takes place to prepare them for MHC molecule loading.

1.3.1.2 Processing

As discussed before, ACP is a process regulated by intra-endosomal antigen stability. The velocity of antigen degradation depends on the localization within the cell (see section 1.3.1.1). It is generally assumed that rapid antigen degradation inhibits efficient cross-presentation [259-261]. This behaves contrary to the MHC II pathway, where intense degradation leads to an upregulation of antigen presentation. Therefore, the first step after internalization is the regulation of lysosomal maturation and activation of lysosomal proteases. This process has been demonstrated to be fine-tuned by the transcription factor TFEB [262]. Generally, DCs as the most efficient cross-presenters display a reduced velocity of endosome maturation [263] as well as lower levels of lysosomal proteases [264]. In addition, an active alkalization of the antigen containing endosomes prevents pH-dependent activation of lysosomal proteases in DCs. This is achieved by the recruitment of NADPH oxidase (NOX) 2 toward the endosome membrane, where it has an influence on reactive oxygen species (ROS) generation. This on the other hand leads to proton trapping which causes an alkalization [265, 266]. The recruitment of NOX2 is controlled by Rab27a, a member of the rat sarcoma (Ras) super family of small GTPases [267] and VAMP8, a soluble N-ethylmaleimide-sensitive factor attachment receptor (SNARE) [268]. Another team player regarding this mechanism is the Ras-related C3 botulinum toxin substrate (Rac) 2, which is also responsible for the assembly and activation of NOX2 [269]. In addition, required for NOX2 activation via an immunoreceptor tyrosine-based activation motif (ITAM) pathway is the Vav family of

guanine nucleotide exchange factors [270], which has also been demonstrated to play a critical role in phagocytosis together with Rac family members [271]. Another mechanism that cells use to degrade their endogenous proteins is autophagy [272]. The loss of several components of the autophagy pathway leads to impaired cross-presentation under conditions where autophagy is induced [273].

After the stopover in a non-degradative endosomal compartment antigens entering the cytosolic pathway need to be transported across the endosomal membrane into the cytosol. This is where proteasomal degradation commences [228]. This process has not yet been understood in detail with multiple possibilities discussed in the literature. Members of the ER-associated degradation (ERAD) machinery may contribute to the dislocation of antigens, as several of them were found associated with or in phagosomes [274, 275]. In the ERAD pathway, proteins are tagged with ubiquitin and are transferred across the ER membrane with the aid of the cytosolic ATPase p97 [276], whose activity has also been shown to be essential for cross-presentation [277, 278]. Also, the heat shock protein (HSP) 90 is known to contribute the translocation of endosomal antigens [279]. Which protein channel is actually involved in this translocation is a debate based on controverse findings [228]. Sec61 has been suggested to be recruited towards antigen containing endosomes, as well as facilitating antigen endosome-to-cytosol translocation and cross-presentation in general [280], but also seems to have an influence on cross-presentation independently of endosome-to-cytosol export [281]. Disruption of the phagosome is another potential mechanism for the translocation of the antigens into the cytosol [282].

Once transferred into the cytosol, degradation into oligopeptides is performed by the proteasome. These antigen-derived peptides then need to be transported into the next compartment for further trimming and MHC I loading [229]. This process requires the TAP transporter. The peptides can either be transported back into the phagosome [239, 283] or like in the classical MHC I pathway into the ER [284, 285]. Since many derived peptides are too long to be bound stably to MHC I molecules they need to be trimmed by aminopeptidases [286]. Within the ER, this process is performed by ERAP1 [287, 288] and within the endosome by IRAP [236, 289].

After these long precursor peptides have been trimmed into MHC I presentable epitopes (see Fig. 5), they need to be bound to MHC I molecules and transported to the cell surface to interact with T cells.

1.3.1.3 MHC I traffic and peptide loading

The final site for peptide loading is either the ER or the phagosomal compartment. Here, the presence of MHC I molecules as well as the peptide loading complex (PLC) is required [227]. The PLC comprises TAP, the proteins ERp57, tapasin, calnexin and calreticulin [221]. In general, most nucleated cells express MHC I molecules ensuring that they can signal viral infection. The classical MHC class I molecule is encoded genes differing between mice (H2-D, H2-K and H2-L) and human beings (HLA-A, HLA-B and HLA-C) [290]. The heavy chain of MHC I is cotranslationally translocated into the ER through the Sec61 complex [291]. Its first interaction is with the chaperones calnexin and immunoglobulin-binding protein (Bip), which both support the folding process of the heavy chain polypeptide [292]. Next, it assembles with β-microglobulin (β_2m) to form an at this stage unstable heterodimer, which is recruited to the peptide loading complex by calreticulin. Further interactions with ERp57 and tapasin stabilizes the empty MHC I molecule and enabling it to bind high-affinity peptides [220, 227]. The loaded MHC I molecules then travel supported by the ER protein Bap31 via coat protein complex (COP) II-export vesicles to the ER-golgi intermediate compartment (ERGIC) [293, 294], a subcompartment of the ER [295]. Here, a quality control process is initiated. Only optimally loaded dimers that have passed this control travel to the surface for recognition by $CD8^+$ T cells [227]. The trafficking between the ER and the golgi is facilitated by Ras-GTPases, like Rab43 [296] or Rab22, which has also been demonstrated to play key roles in ACP [297].

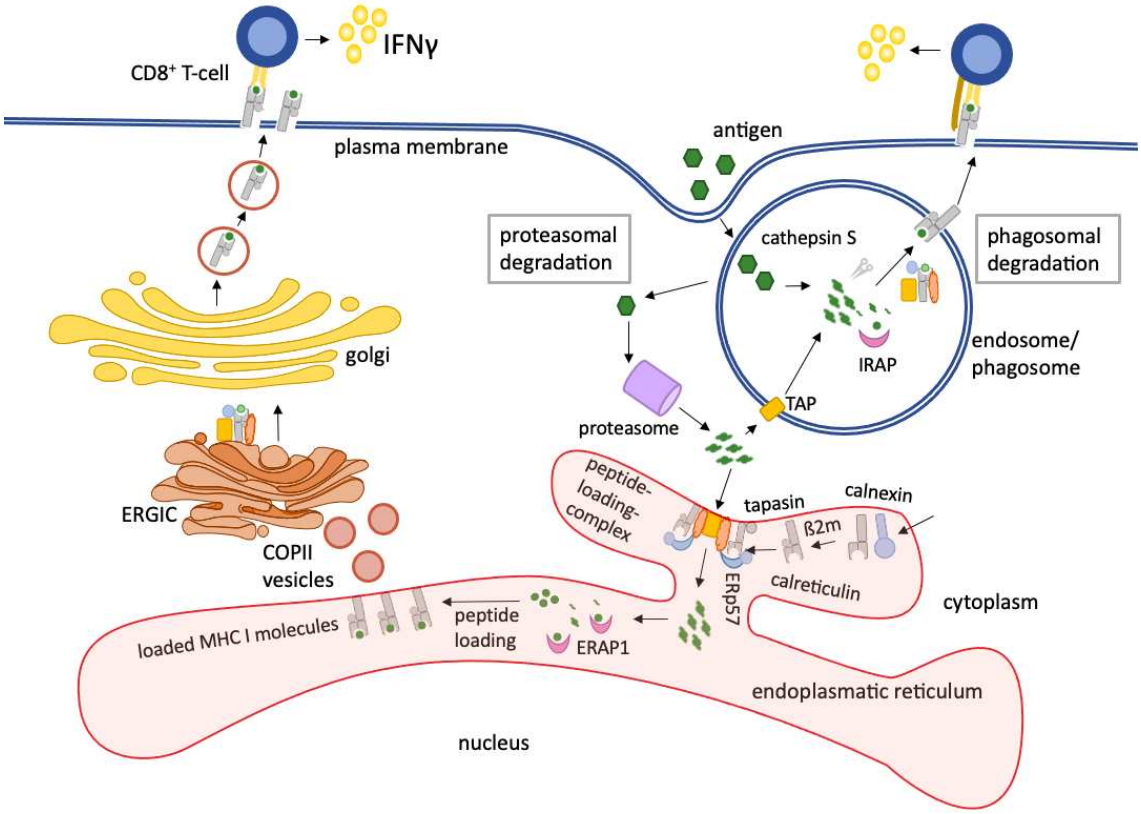

Fig. 5: Detailed depiction of the different processing ways during antigen cross-presentation and the MHC I secretory pathway
(for illustration the servier medical art database was partly used, cartoons were adapted. Modified after Blander, 2018). ERGIC = endoplasmic reticulum golgi intermediate compartment, IFNγ = interferon-gamma, COP = coat protein complex, ERAP = ER-associated aminopeptidase, IRAP = insulin-responsive aminopeptidase, TAP = transporter associated with antigen processing, β2m = β-microglobulin

Since many of the components of the peptide loading complex are originally located within the ER, they need to be transported to the phagosome for peptide loading together with MHC I molecules. This is accomplished by vesicular traffic from the ERGIC by pairing of the ER soluble SNARE Sec22b and the plasma membrane SNARE syntaxin 4 of the phagosome [298, 299]. Another mechanism to get MHC I molecules to the endosomal compartments is directly from the ER or from the plasma membrane via CD74 [300].

Besides this described classical secretory pathway within the ER and being present at the plasma membrane, MHC I molecules are also found within the endocytic network. They assemble at a defined perinuclear region, referred to as the endocytic recycling compartment (ERC) [227]. Their journey from the cell surface is dependent on the ADP ribosylation factor 6 (ARF6) [301, 302]. Subsequently they are delivered into early sorting endosomes [227, 303]. From there they are either routed for degradation or for recycling

[227]. These processes are amongst other variables tightly controlled by small GTPases, like Rab11a, Rab4 and Rab35 [304-306].

By presenting these processed antigen-derived peptides on the cell surface, the mechanism of ACP is greatly contributing to the adaptive immune response, playing a pivotal role in various infectious and autoimmune diseases as well as cancer.

1.3.2 Towards the clinic: cross-priming during infections, immune-mediated diseases, cancer and its therapeutic potential

Regarding intracellular pathogens and tumours, the immune defence against them lies in the field of action of specific $CD8^+$ CTLs. They are able destroy cells when presenting suitable antigens on their surface. To avoid the elimination of healthy bystander cells which have ingested viral or tumour fragments, this endocytosed material does in general not enter the MHC I pathway. This pathway is reserved for intracellular synthesized peptides. Nevertheless, these CTLs need to be activated and their activation depends on the AP of APCs. So if a pathogen does not directly infect APCs or a tumour does not arise from APCs, ACP comes into play [214].

In general, MHC I presentation of antigens must be regarded from two points of view: for the host it is clearly a benefit as it represents the key mechanism to fight infections or tumour proliferation. But for the invaders themselves it is a restricting factor regarding survival and further dissemination [284]. Thus, numerous viruses have evolved mechanisms disabling the MHC I pathway to escape from elimination, termed immune evasion. Especially viruses causing lifelong infections, such as cytomegalovirus (CMV), herpes simplex virus (HSV) and HIV, are able to inactivate different key components of the MHC I pathway [307] using the following mechanisms: inhibition of cytokine synthesis [308], impairment of TAP functions [309-314], promotion of MHC I degradation [315-317] as well as down-modulation of the expression of MHC I molecules [317-319]. And again, this is the point where cross-presentation becomes particularly important, since DCs can take up and cross-present-present viral antigens without being infected themselves. Within this context the molecules conducting immune evasion are insufficient so that $CD8^+$ T cell responses can be achieved [320-322]. It may seem like these effector cells would be completely unresponsive since the infected cells are impaired in antigen presentation and must therefore be invisible. However, viral immune evasion strategies appear to only diminish antigen presentation without entirely eliminating it. Hence, the

remaining presentation capacity is sufficient to be detected by cross-primed $CD8^+$ T cells and allows at least some control over the infection [284]. Intracellular parasites, e.g., are also able to impair T cell priming [323]. They have proteases enabling VAMP8 and therefore disrupting the proteolytic activity in phagosomes [268] (see section 1.3.1.2).

Regarding the development of autoimmune diseases, a mechanism referred to as central tolerance plays a key role. It describes the negative selection of maturing thymocytes that strongly recognize self-antigen ridding self-reactive and potentially autoimmune lymphocytes out of the T-cell repertoire [324-326]. However, some CTLs usually escape this mechanism and enter the circulation. Therefore, cross-tolerance serves as a second checkpoint within the secondary lymphoid organs. It describes the peripheral deletion of autoreactive $CD8^+$ T cells following the ACP of self-antigens [327-329]. Whether a T cell faces deletion or is suppressed depends on their avidity manner regarding antigen-binding. Low-avidity T cells managing to escape both, central and peripheral tolerance in turn cause autoimmunity [329]. CTLs and ACP have been shown to be relevant for the development of various autoimmune diseases [214] comprising amongst others diabetes [330, 331], glomerulonephritis [332], multiple sclerosis [333-335], autoimmune hepatitis [336, 337], thyroiditis [338] and is associated with transplantation tolerance [339, 340] and tumours [341].

Like viruses, also tumours are able to impair ACP [342, 343] probably attempting to escape from immune surveillance, too [284]. Even when efficiently cross-presented, tumour antigens usually fail to induce a strong antitumour CTL response without further manipulation [214, 344]. One of the main mechanisms whereby chemotherapy works is via the stimulation of antitumour immunity based on increased cross-priming of CTLs [342]. Chemotherapy induces apoptosis and in this in turn increases the amount of tumour antigen fed into the ACP pathway [345]. But also multiple other adjuvants have proven their potential of enhancing cross-priming of CTLs to tumour antigens, for example ISCOMATRIX [346], HSPs [347] and monoclonal antibodies [348]. At present, a frequently applied immunotherapy is the administration of so-called checkpoint inhibitors. These monoclonal antibodies are directed against regulatory immune checkpoint molecules that in turn impair T cell activation. Another relatively new but very promising concept is adoptive T cell transfer. It is based on the genetic modification of either naturally occurring tumour specific T cells from existing tumour masses or blood-derived T cells *ex vivo* followed by an expansion reinfusion assuring a proper T cell response [349]. In contrast to enhancing T cell responses, there are also therapeutics inhibiting ACP [350, 351]. Selective blocking of the ACP pathway by targeting its unique

components, segregating it from the classical MHC I and MHC II pathway, could proof helpful regarding other clinical situation, such as transplantation [284].

1.4 Aim of this thesis

The process of ACP has a major impact on the immune response under various conditions, especially regarding the hosts defence against viral infections and tumours. Identifying factors controlling ACP in different antigen presenting cell types and developing methods to manipulate their functions in a controlled fashion will provide new targets for therapeutic approaches. Considering that mostly DCs are the cells conducting efficient ACP emphasizes the requirement of characterizing the factors determining the functional range of the different DC subsets. Especially pDCs are an interesting target since they have not been well studied for their capacity to cross-present antigen. Therefore, we lack extensive research aiming to explore their actual potential in ACP. In particular, the identification of factors that may boost or dampen their antigen cross-presentation ability is needed.

Our research group is focused on identifying the factors regulating the development and functions of pDCs. During this research BATF was found to be expressed high in activated pDCs [4, 352] and to contribute to controlling the pDC development and their capacity to produce IFN I (Ali et al., unpublished data). Further unpublished results showed an increase of pDCs at the expense of the cDC1 subset in *Batf*-deficiency within bone marrow derived DC cultures. This raises the question of a concomitant function shift between these subsets. Especially since *Batf* can compensate for *Batf3* (which is required for the development of the highly ACP efficient cDC1 subset) the hypothesis that BATF has an impact on the functions usually conducted by the cDC1 subset, namely ACP was formed. This thesis is aimed to characterize the role of the transcription factor BATF in ACP ability of pDCs. Following listed are the key hypotheses formed for this study:

- The expression levels of factors steering ACP are influenced by BATF
- pDCs are antigen cross-presenting cells (ACPCs) with a BATF-dependent ACP performance level
- BATF acts as a manipulating factor in antigen uptake of pDCs
- BATF determines MHC I molecule expression of pDCs

2. Materials and methods

2.1 Materials

2.1.1 Antibodies and viability stains

2.1.1.1 Antibodies

All antibodies were used diluted in FACS-buffer.

Antibody	Clone	Dilution	Supplier	Catalog-no.
Anti-mouse CD16/32	93	1:50	Thermo Fisher Scientific, Waltham, USA	14-0161-82
Anti-mouse CD317 (PDCA1, BST-2)	Ebio927	1:50	Thermo Fisher Scientific, Waltham, USA	12-3172-81
APC anti-mouse CD11b	M1/70	1:100	BD Biosciences, Heidelberg	553312
APC anti-mouse CD45R/B220	RA3-6B2	1:50	BD Biosciences, Heidelberg	563092
APC anti-mouse IFN gamma	XMG1.2	1:400	Thermo Fisher Scientific, Waltham, USA	17-7311-82
APC anti-mouse SiglecH	551	1:50	BioLegend, London, United Kingdom	129612
APC-Cy7 anti-mouse CD11b	M1/70	1:100	BD Biosciences, Heidelberg	557657
APC-Cy7 anti-mouse CD11c	N418	1:100	BioLegend, London, United Kingdom	117324
BV 421 anti-mouse CD86	GL1	1:100	BD Biosciences, Heidelberg	564198
BV 421 anti-mouse SiglecH	551	1:50	BD Biosciences, Heidelberg	566581
BV 421 anti-mouse XCR1	ZET	1:50	BioLegend, London, United Kingdom	148216
BV 510 anti-mouse MHCII	M5/114.15.2	1:100	BioLegend, London, United Kingdom	107635

BV 510 anti-mouse Siglec H	440c	1:50	BD Biosciences, Heidelberg	747674
eFluor® 450 anti-mouse CD8a	53-6.7	1:300	Thermo Fisher Scientific, Weltham, USA	48-0081-82
FITC anti-mouse CD172alpha	P84	1:50	BioLegend, London, United Kingdom	144005
FITC anti-mouse CD45R/B220	RA-6B2	1:50	BD Biosciences, Heidelberg	553088
FITC anti-mouse CD8alpha	53-6.7	1:100	BD Biosciences, Heidelberg	553031
FITC anti-mouse H-2kb	AF6-88.5	1:50	BioLegend, London, United Kingdom	116505
PE anti-mouse CD172alpha	P84	1:50	BioLegend, London, United Kingdom	144012
PE anti-mouse H-2kb/H-2Db	28-8-6	1:75	BioLegend, London, United Kingdom	114608
PE-Cy7 anti-mouse CD11c	N418	1:100	BioLegend, London, United Kingdome	117317
PE-Cy7 anti-mouse CD86	GL1	1:100	BioLegend, London, United Kingdom	105014
PerCP-Cy 5.5 anti-mouse CD3e	145-2C11	1:100	BD Biosciences, Heidelberg	551163
PerCP-Cy5.5 anti-mouse CD19	1D3	1:100	BD Biosciences, Heidelberg	551001

Table 1: Antibodies.

2.1.1.2 Viability stains

All viability dyes were used diluted in FACS buffer.

Dye	Dilution	Supplier	Catalog-no.
7-AAD	1:200	BD Biosciences, Heidelberg	559925
eFluor™ 780	1:5000	Thermo Fisher Scientific, Weltham, USA	65-0865-14
eFluor™ 506	1:600	Thermo Fisher Scientific, Weltham, USA	65-0866-14

Table 2: Viability dyes.

2.1.2 Primers

All primers were custom synthesized by Metabion international AG (Planegg/Steinkirchen). All probes were purchased from Roche (Mannheim). The primers were designed according to the following criteria: primer length preferably between 18-24 bp, product size of the amplicon preferably between 80-150 bp, GC-content preferably between 40-60%, avoidance of runs (repeated nucleotides) and repeats (repetitive nucleotide sequences), a primer melting temperature close to 64°C and an annealing temperature close to 5°C below the melting temperature was set as a target.

Gene	Probe library number	Direction	Sequenz (5'-3')
CD8alpha	45	forward	CCTCACCTGTGCACCCTAC
		reverse	ATCCGGTCCCCTTCACTG
Clec9a	85	forward	TCCTTGGTTCCAAAGACTGC
		reverse	AAGGAGAAACACGGGCTTG
Eif2ak4	76	forward	GACTTCAGACTACACTTGCC
		reverse	TGTAAGATTGTTTCCTTGGGTAGG
H2-D1	107	forward	CAAGTGGGAGCAGAGTGGT
		reverse	TGATGTCAGCAGGGTAGAAGC
H2-K1	107	forward	ACCAAACACAAGTGGGAGCA
		reverse	TGATGTCAGCAGGGTAGAAGC
Herpud1	93	forward	ACCTGAGCCGAGTCTACCC
		reverse	GAGACACTGGTGATCCAACA
Hip1r	97	forward	TGGCACGGGTAAAGGAAC
		reverse	CAACTGGTCGCTCTGCTCTTC
Hsp90aa1	25	forward	TGAGGAAACCCAGACCCAAGA
		reverse	CATTAACTGGGCAATTTCTG
Hsp90ab1	55	forward	GTCAAGATGCCTGAGGAAGTG
		reverse	GAAGCATTAGAGATCAACTCGC
Rab30	3	forward	AACAGTATGCTAGCAATAAAGTCATCA
		reverse	CCTGAGCCTCTGAGAACTCTTC
Rab43	98	forward	TCGTGCAGCTGCTGATTG
		reverse	CTCGATGGCACAGAGGATG

Rac2	102	forward	ACGCCTTCCCTGGAGAATACA
		reverse	AGGTTCACCGGCTTACTGTC
Serpinb9	38	forward	GGGTGTGGACCTCAGCAAG
		reverse	AACCTCAACATCAGTGCTCTTC
ß-Actin	106	forward	TGACAGGATGCAGAAGGA
		reverse	CGCTCAGGAGCAATG
Vav3	22	forward	AAGGAGACATGGTGAAGATTTAC
		reverse	GGTCAACACTGGATAGGACTTTA

Table 3: Primers.

2.1.3 Cell lines

Cell line	Origin
Murine $CD8^+$ T Cell lines	Kindly provided by Professor Ingo Drexler, Institute of Virology, Heinrich Heine University Düsseldorf. Generation and maintenance are published elsewhere. Briefly, LPS blasts were produced by incubating splenocytes derived from naïve C57BL/6 mice with LPS and dextran-SO_4 (both Sigma-Aldrich) followed by irradiation. The cells were incubated with β-microglobulin and the appropriate peptide ($B8_{20-27}$ (TSYKFESV), $OVA_{257-264}$ (SIINFEKL), both H2-K^b-restricted; purchased from Biosynthan). All peptides were purchased from Biosynthan (Germany). LPS-blasts were co-cultivated with splenocytes from MVA-PK1L-OVA vaccinated C57BL/6 mice. $CD8^+$ T cells were maintained by weekly restimulation using peptide loaded EL.4 cells (ATCC® TIB-39™), naïve splenocytes and M2 medium containing 5% TCGF (supernatant from rat splenocytes stimulated with 5µg/ml Concanavalin A). Cells were irradiated prior to peptide-loading and/or incubation with $CD8^+$ T cells [353].
Murine Cloudman S91 melanoma cells	Kindly provided by Professor Ingo Drexler, Institute of Virology, Heinrich Heine University Düsseldorf. They were originally obtained from ATCC (ATCC® CCL-53.1™). The cells were cultured in M2-Medium containing 10% FCS at 5% CO_2 in a humified incubator at 37°C. The cells were passaged 2-3 times/week.
Murine RAW 264.7 macrophage cells	RAW 264.7 (ATCC® TIB-71™) cells were purchased from ATCC. The cells were cultured in Iscove's Modified Dulbecco's Medium (IMDM) containing 10% FCS at 10% CO_2 in a humified incubator at 37°C. The cells were passaged every 2-3 days.

Table 4: Cell lines and their origins.

2.1.4 Growth factor Flt3-L

The supernatant of Chinese hamster ovary (CHO) cells was prepared and tested against the recombinant Flt3-L in the Laboratory of Professor Scheu by Sonja Schavier (Scheu Lab, Institute of Medical Microbiology and Hospital Hygiene, Heinrich Heine University Düsseldorf). The optimal concentration for application in the experiments is indicated in the respective method section.

2.1.5 Virus

The recombinant modified vaccina virus Ankara (MVA) was kindly provided by Professor Ingo Drexler, Institute of Virology, Heinrich Heine University Düsseldorf. The virus generation and properties are published elsewhere [353]. The used multiplicity of infection (MOI) was 1, indicating that the amount of virus to the infection target (in our case feeder cells) was evenly balanced.

2.1.6 Media and buffers

2.1.6.1 Media

Name	**Field of application**	**Constituents**
Flt3-L medium	preparation BMDCs	VLE RPMI 1640 medium 10% FCS 5-10% Flt3-L
IMDM medium	Raw-cells	IMDM medium 10% FCS 1% glutamine
M2 medium	Cross-presentation-assay, Cloudman (feeder) cells, T-cells	RPMI 1640 glutaMAX 10% FCS 28 µl β-mercaptoethanol (80%)

Table 5: Media and their constituents.

2.1.6.2 Buffers

Name	Field of application	Constituents
Borate buffer	FITC-OVA coated beads	PBS
		0.1 M boric acid
		NaOH until pH of 8.5
FACS buffer 1	Flow cytometry	PBS
		2% FCS
		2 mM EDTA
FACS buffer 2	Flow cytometry: only cross-presentation-assay	PBS
		1% BSA
		500 µl NaN_3 (20%)
Storage buffer	FITC-OVA coated beads	80 ml PBS
		20 ml of 0.1M phosphate buffer pH 7.4
		0.88g NaCl
		1 g BSA
		5 ml glycerol
		0.1 g NaN_3

Table 6: Buffers and their constituents.

2.1.7 Kits and beads

Name	Supplier	Catalog-no.
BD Compensation Beads	BD Biosciences, Heidelberg	552845
BD Cytofix/Cytoperm Fixation/Permeabilization Solution Kit	BD Biosciences, Heidelberg	554714
NucleoSpin®RNA	Macherey-Nagel, Düren	740955.250
Polybead® carboxylate microspheres 3.00µm	Polysciences, Hirschberg an der Bergstrasse	09850-5
DNA isolation kit	Genekam, Duisburg	SB0072
SuperScript™ III Reverse Transcriptase	Thermo Fisher Scientific, Weltham USA	18080093

Table 7: Kits and beads.

2.1.8 Chemical agents

Name	Supplier
2-Mercaptoethanol ≥ 99.0%	Sigma-Aldrich, Taufkirchen – now Merck, Darmstadt
2-Mercaptoethanol 50mM	Thermo Fisher Scientific, Weltham, USA
Agarose	Biozym, Hessisch Oldendorf
Bovine serum albumin	Sigma-Aldrich, Taufkirchen – now Merck, Darmstadt
Brefeldin A	Merck, Darmstadt
CpG 2216	TIB Molbiol, Berlin
Cytochalasin D	Sigma-Aldrich, Taufkirchen – now Merck, Darmstadt
Dimethyl Sulphoxide (DMSO) D2650	Sigma-Aldrich Taufkirchen – now Merck, Darmstadt
dNTP-set	Thermo Fisher Scientific, Weltham, USA
DOTAP (1,2-Dioleoyl-3-Trimethylammonium-Propan)	Roche, Mannheim
DPBS, Dulbecco's phosphate buffered saline	Thermo Fisher Scientific, Weltham, USA
Dulbecco's phosphate buffered saline (1X)	Thermo Fisher Scientific, Weltham, USA
Erylysis buffer pH 7.2-7.4	Morphisto, Offenbach am Main
Ethanol	VWR chemicals, Darmstadt
Ethidiumbromid	Merck, Darmstadt
Fetal calf serum	Sigma-Aldrich, Taufkirchen – now Merck, Darmstadt
FITC-ovalbumin	Thermo Fisher Scientific, Weltham, USA
Glycerol	VWR chemicals, Darmstadt
Hank´s Balanced Salt Solution (HBSS)	Thermo Fisher Scientific, Weltham, USA
IMDM medium	Thermo Fisher Scientific, Weltham, USA
Immersol™ 518 F immersion oil	ZEISS, Oberkochen
Oligo-(dT)-primer	Thermo Fisher Scientific, Weltham, USA
Paraformaldehyde (PFA)	Sigma-Aldrich, Taufkirchen – now Merck, Darmstadt
Penicillin/Streptomycin	Biochrom GmbH, Berlin

RNaseZap®	Thermo Fisher Scientific, Weltham, USA
RPMI Medium 1640 (1X) + GlutaMAX™-I	Thermo Fisher Scientific, Weltham, USA
Sodium azide	Sigma, Taufkirchen – now Merck, Darmstadt
Takyon MasterMix blue dTTP	Eurogentec, Seraing, Belgium
Trypan blue (0.4%)	Thermo Fisher Scientific, Weltham, USA
Trypsin	Thermo Fisher Scientific, Weltham, USA
UltraPure 0.5 M EDTA	Thermo Fisher Scientific, Weltham, USA
VLE RPMI 1640 Medium	Biochrom GmbH, Berlin

Table 8: Chemical agents.

2.1.9 Consumables

Name	Supplier
Cell culture flaks	Corning, Amsterdam, Netherlands
Cell scraper	Greiner bio-one/CytoOne, Frickenhausen
Cell strainers	Corning, Amsterdam, Netherlands
Combitips advanced	Eppendorf, Hamburg
Filter tips	Starlab group, Hamburg
Micro tubes	Sarsted, Nümbrecht
Omnifix syringes and needles	B. Braun, Melsungen
Petri dishes untreated	Greiner bio-one, Frickenhausen
Plastic Falcons 15/50ml	Sarstedt, Nümbrecht
Polystrene round bottom tube	BD Falcon, Heidelberg
Safe-Lock Tubes	Eppendorf, Hamburg
Stripettes 1-50ml	Corning, Amsterdam, Netherlands
Well plates	Corning, Amsterdam, Netherlands
µ-Slide 4 Well $^{Ph+}$	Ibidi, Gräfelfing

Table 9: Consumables.

2.1.9.1 Instruments and softwares

2.1.9.2 Instruments

Name	Supplier
BD Facs Aria III	BD Biosciences, Heidelberg
BD FACS Canto II	BD Biosciences, heidelberg
Confocal microscope	ZEISS, Oberkochen
Gel Doc™ XR+ Imaging System	Bio-Rad, Feldkirchen
Hera Cell 240 (incubator)	Heraeus, Hanau
iQ™5 iCycler	Bio-Rad, Feldkirchen
Microscope Axiovert 100	ZEISS, Oberkochen
Mini Spin (benchtop centrifuge)	Eppendorf. Hamburg
NanoDrop 1000 (photometer)	Peqlab, Erlangen
Neubauer-improved counting chamber	Paul Marienfeld Gmbh & co.KG, Königshofen
Rotanta 96HC centrifuge	Hettich, Tuttlingen
Surgical instruments	Fine science tools, Heidelberg, Uetze
Thermocycler	Biometra, Göttingen
Thermomixer-Mixer HC	Starlab group, Hamburg
Vortex shaker	VWR chemicals, Darmstadt
Water bath	Koettermann Labortechnik, Uetze

Table 10: Instruments.

2.1.9.3 Software for visualization of the data

Name	Field of application
Adobe illustrator, Microsoft Powerpoint	Final editing of illustrations
CFX Maestro Software	Bio-Rad CFX rtPCR analysis
FLOWJO	Analysis and depiction of flow cytometry data
GraphPad PRISM	Statistical analysis of data and graph design
Smart SERVIER MEDICAL ART	Image designing
ZEISS ZEN	Confocal microscopic pictures
BioVenn	Making of Venn-diagrams

Table 11: Softwares.

Graphics were partly generated using Servier Medical Art, provided by Servier, licensed under a Creative Commons Attribution 3.0 unported license

(https://creativecommons.org/licenses/by/3.0/). Changes were made to the original cartoons. Venn diagrams were produced as published elsewhere [354].

2.2 Methods

2.2.1 Laboratory animals

No animal experiments were performed for this thesis. All mice from which organs were used in experiments performed for this thesis are assigned to the file numbers O44/17 and O83/18 (Killing of animals (without pre-treatment) for scientific purposes according to §4 para.3 of the Animal Welfare Act). All mice were derived from in-house breeding of the animal research facility "Zentrale Einrichtung für Tierforschung und wissenschaftliche Tierschutzaufgaben" (ZETT) of the Heinrich Heine University Düsseldorf. The animals were kept under specific pathogen-free conditions. All mouse lines were genetically backcrossed to C57BL/6 background.

Name	**Description**
$BATF^{+/+}$	Wildtype mouse
$BATF^{-/-}$	*Batf* knockout mouse

Table 12: Mouse lines.

2.2.2 Organ removal and cell cultivation

2.2.2.1 Bone marrow preparation

Mice at 8-20 weeks of age were used for bone marrow preparation. After killing mice with cervical dislocation the animals were disinfected with 70% EtOH. Tail tips were cut and kept at -20°C for the upcoming re-genotyping of the mice (see section 2.2.3.1). Tibia and femur were isolated and cleared of muscle and tissue. After cleaning the bones were kept in PBS, followed by 3 min disinfection in 70% ethanol and subsequent washing with PBS. To get access to the bone marrow canal the very proximal and distal parts of the bones were cut off. The bone marrow was flushed out into a petri dish with RPMI-VLE 1640 medium using a syringe with a 26-gauge needle. Single cell suspension was generated by multiple pipetting steps after transferring the bone marrow into a 50ml falcon tube. The cells were centrifuged for 5 min at 4°C and 1200 rpm. The supernatant

was discarded. To clear the cell fraction from erythrocytes a red blood cell lysis was performed. Therefore, the cell pellet was resuspended in 3 ml red blood cell lysis buffer. After an incubation time of 3min at room temperature the reaction was stopped by adding 10 ml medium or PBS. Before further centrifugation (5 min, 4°C, 1200 rpm) the cell suspension was filtered through a 70 µm cell strainer to remove left over bone parts. The supernatant was discarded, and the cells were resuspended in fresh medium.

2.2.2.2 Development of BMDCs in Flt3-L cultures

Cell culture work was performed under sterile conditions under a clean bench. 2 x 10^7 cells/10 ml were resuspended in medium containing Flt3-L (see section 2.1.6.1) and seeded in 10 cm cell culture untreated petri dishes. Cells were incubated at 37°C in a humified incubator containing 10% CO_2. The cells were fed on day 5. For this purpose, 5 ml medium of each petri dish were removed and transferred into a falcon tube. After centrifugation (5 min, 4°C, 1200 rpm) the supernatants were discarded, and the cell pellets were resuspended in 5 ml fresh warm medium. These cell suspensions were pipetted back into the according petri dishes. On day seven cells were fully differentiated and ready to be harvested. They were either left untreated or stimulated with a TLR agonist (see section 2.2.2.3).

2.2.2.3 Stimulation

Stimulation of Flt3-L cultures of BMDCs (see section 2.2.2.2) was conducted using the TLR9 agonist CpG-ODN 2216/A (1µM) complexed to DOTAP. DOTAP is a liposomal transfection reagent which allows an increase of the effect of stimulation. The following volumes were used for the stimulation of 10ml volume:

CpG 2216 + DOTAP		
Solution A:	20 µl (0.5 nM/µl) CpG	+ 80 µl HBSS
Solution B:	30 µl DOTAP	+ 70 µl HBSS

Table 13: Content of stimulation solutions.

Both solutions were mixed (=solution C). After an incubation period of 15 min at room temperature, solution C was applied accordingly (20 µl/ml).

After the stimulation period (2h/6h/12h) the cell culture plates were incubated at 4°C to achieve a detachment of the cells from the plastic surface. After 30min the plates were

scraped with a cell scraper and washed twice with cold PBS. The cell suspension was transferred into a flacon tube and centrifuged (5 min, 4°C, 1200 rpm). The washed pellet was used for further procedures.

2.2.2.4 Cultivation of raw cells

Raw cells (see section 0) were used for the endocytosis-assays as controls. They were cultivated in 25 cm^2 culture flasks in IMDM-medium (see section 2.1.6.1). For cultivation, cells were incubated at 37°C and 10% CO_2. Cells were split three times a week at 80-90% cell confluency or two days before the flow cytometry experiments. For this, the cells in the culture flasks were scraped with a cell scraper and washed with warm PBS. Cells were centrifuge at room temperature (5 min, 1200 rpm) and resuspended in fresh IMDM-medium. Subsequently, they were transferred into new culture flasks.

2.2.2.5 Trypan blue cell exclusion

The cell number was always determined using a hemocytometer (Neubauer). The cell suspension was diluted 1:10 with 0.4% trypan blue to differentiate between dead and live cells. Since dead cells are permeable for the dye, they appear dark blue under the microscope. Only vital cells were counted and plated accordingly using the following formula [355]:

Cell number = $\frac{counted\ cells\ x\ dilution\ factor\ x\ 10.000}{counted\ squares}$.

2.2.3 Molecular biological methods

2.2.3.1 Mouse genotyping

For all experiments the stated genotype of the used mice was verified for each animal separately. Briefly summarized, the first step was the DNA isolation of the cut tail tips. This was achieved using the DNA isolation kit from Genekam according to the manufacturer's instructions. Briefly summarized, solution A:C were prepared at a 1:10 ratio and 100µl of this mixture was added to 1.5 ml micro tubes each containing one tail tip. Next, the tubes were kept at 88°C for 20 min in a heating block with gentle mixing. After removing the tubes from the heating block 100 µl of solution B was added to each

sample followed by 100µl of solution C. The tubes were centrifuged for 5 min at 13400 rpm. 250 µl of the supernatant were transferred into a fresh tube. The rest was discarded. Using this supernatant PCR products were generated and further processed using gel electrophoresis.

For gel electrophoresis 1-2% agarose-gel was prepared by heating up agarose in TAE-buffer and adding 2 µl/100 ml ethidium bromide. The gel was poured into a gel casting tray, left for cooling and solidifying and put into the electrophoresis chamber. The pockets were filled accordingly. After 45 min at 100V the gel was taken out of the chamber and put into the Gel Doc™ XR+ Imaging System for visualization and recording of the results.

2.2.3.2 RNA-isolation of sorted BMDCs

Before working with RNA the entire work space was extensively cleaned to prevent any contamination with RNases. To win purified RNA the exact steps of the NucleoSpin®RNA Kit manufacturer's protocol were followed. The basic principle is based on a cell lysis buffer which inactivates RNases. Additionally, it facilitates the binding of the RNA to the silica membrane. To eliminate DNA a DNase solution is applied. In further washing steps salts, metabolites and other macromolecular cellular components are removed to finally gain pure RNA which is eluted in RNase-free H_2O. Isolated RNA samples were stored at -80°C until further usage.

Quantity and quality assessment was performed before storage via NanoDrop, a spectrophotometer. This method is based on measuring the absorbance of the RNA sample at different wave lengths. On basis of the absorbance at 260nm (A_{260}) the concentration can be verified. An A_{260} value of 1 indicates that the sample contains 40µg/ml RNA. The purity of the sample can be determined by taking the ratio of absorbance at 260nm versus 280nm (A_{260}/A_{280}) wavelength into account. Ideally, samples have an A_{260}/A_{280} close to 2.0. Far lower values indicate a significant level of protein contamination within the measured sample [356].

2.2.3.3 cDNA-synthesis

The eluted RNA (see section 2.2.3.2) was further used for cDNA-Synthesis. In order to get the same final concentration for all samples, the least concentrated sample was taken into account and the higher concentrated samples were adjusted accordingly by

diluting them with dH_2O. First, the RNA samples were pipetted following the depicted scheme:

substance		volume
dH_2O	(RNase-free)	2 µl
dNTPs	(10 µM)	1 µl
Oligo dT-primer	(50 µM)	1 µl
RNA		10 µl

Table 14: Pipet scheme of used substances for cDNA-synthesis.

Next the samples were undertaken two subsequent incubation periods: 5 min at 65°C in a thermomixer, followed by 1 min on ice. In the next step, the following material was added:

Substance		volume
DTT	0.1 M	1 µl
First strand buffer	5x	4 µl
SuperSript® III	200 U/l	1 µl

Table 15: Pipet scheme of used substances for cDNA-synthesis after incubation periods.

After cautious mixture, the solution was incubated at room temperature for 5 min before entering the thermocycler and running through the following programme:

Temperature	time	effect
50°C	90 min	transcription into cDNA by reverse transcriptase
70°C	15 min	inactivation step
4°C	until further dilution	cool-down and safe-keeping

Table 16: Thermocycler-programme for cDNA-synthesis.

It was heated up to 50°C for 90 min to be transcribed into cDNA by the reverse transcriptase. The cooled-down newly synthesized cDNA was diluted to 5 ng/µl and stored at -20°C until further processing.

2.2.3.4 Quantitative real-time PCR

For analysing gene expression, real-time (RT)-PCR was conducted. The previously synthesized cDNA (see section 2.2.3.3) was further diluted to 1 ng/µl. The reaction was performed using a 96-well plate, each well was filled as follows:

substance		volume
mastermix		12.5 µl
primer fwd	(20 µM)	0.3 µl
primer rev	(20 µM)	0.3 µl
probe		0.5 µl
water		6.4 µl
cDNA (1 ng/µl)		5 µl
Total/well		25 µl

Table 17: Pipet scheme for real-time PCR.

The well-plate was incubated in an iQ5-cycler under the following conditions:

steps	temperature	duration	repetitions
1. DNA denaturation	95°C	10 min	1x
2. DNA denaturation	95°C	15 sec	Steps 2-3 in series:
3. Hybridisation and elongation	60°C	1 min	40x
4. hold	4°C	until switch off	

Table 18: Thermocycler-programme for RT-PCR.

For every primer pair three cDNA-free wells served as negative controls within the reaction. The reference gene used for normalization and quantification was ß-actin. Every sample was run as triplicate. Gene expression was calculated with the $2^{-\Delta CT}$ method [357].

2.2.4 Functional assays

FACS purified BDMCs were used for the cross-presentation assay (see section 0). For this purpose, the BMDCs were generated in Flt3-L cultures (see section 2.2.2.2). BMDCs were stained (see section 2.2.6.2), FACS-sorted (see section 2.2.6.1) and used untreated or after stimulation (see section 2.2.2.3). The following BMDC groups were used as described below in the experimental setups (see sections 0, 2.2.4.2):

Genotype	Cell type	Stimulation	Labeling
$BATF^{+/+}$	pDCs	12 h CpG	WT pDCs +
		unstimulated	WT pDCs
	cDCs	12 h CpG	WT cDCs +
		unstimulated	WT cDCs

BATF$^{-/-}$	pDCs	12 h CpG	KO pDCs +
		unstimulated	KO pDCs
	cDCs	12 h CpG	KO cDCs +
		unstimulated	KO cDCs

Table 19: BMDC groups for ACP assay.

2.2.4.1 Antigen cross-presentation assay

Day 1: first step was the infection of the feeder cells. Murine Cloudman S91 melanoma cells (see section 0) were seeded the day before infection, aiming for ~80% cell confluency on day 1. Major contamination was ruled out by controlling the culture flasks microscopically. The supernatant was discarded and the cells were detached by adding 3 ml trypsin per flask followed by a 2 min incubation at 37°C. The trypsin was inhibited by adding the double amount of FCS containing M2-medium. The cells were collected in 50ml falcons and counted using trypan blue and a hemocytometer as described before (see section 2.2.2.5). Two million cells were transferred into 15 ml tubes and centrifuged (5 min, room temperature, 1500 rpm). Cell pellets resuspended in 200 µl of medium and infected with virus. The amount of virus needed was calculated aiming at a MOI 1. The MOI describes the ratio of the number of virus particles to the number of target cells within the falcon. In addition, mock controls without virus were prepared. The samples were incubated at 37°C and 5% CO_2 for 2 h. Within this time, the falcons were gently shaken every 10min during the first hour, and every 20min during the second hour of infection. Afterwards, the cells were washed twice with medium. One million cells/ml were seeded in 6-well plates followed by another 8 h of incubation at 37°C and 5% CO_2. Infected feeder cells and mock controls underwent PUVA (psoralen and ultraviolet A)-treatment: 0.3 µg/ml psoralen were added to the wells and the samples were kept in the incubator for 15 min prior to UVA irradiation for another 15 min. Cells were detached using a cell scraper, put in falcons, centrifuged as described above and washed twice before $1x10^6$ cells/ml were cocultured at a ratio of 1:1 with BMDCs in 6 cm petri-dishes. These cocultures were incubated at the conditions described before for 12 h. The cells were later analysed for their ability to reactivate antigen specific $CD8^+$ cell lines (see section 2.2.4.2). The protocol of this assay conducted with other cell groups has been published [353].

2.2.4.2 $CD8^+$ T cell activation assay

Day 2: The antigen cross presenting capacity of the investigated cells was determined with the aid of peptide specific $CD8^+$ cell lines. The overnight incubated cells were scraped, centrifuged and transferred into falcons as described before. The samples were co-cultured in a 96-well plate according to the following scheme: 100 µl of BMDCs (4 x 10^6/ml) plus 100 µl of T cells (2 x 10^6/ml) (ratio of DCs:T cells = 2:1) in the presence of 50 µl (1 µg/ml) brefeldin A per well. Each group of BMDCs mentioned above (see section 2.2.4) is being co-cultured separately with the two different $CD8^+$ T cell lines. Co-culturing takes places for 4 h at 37°C and 5% CO_2. IFNγ production was used as a read out for T cell activation of CD8+ T cells. It was analysed by performing an intracellular cytokine staining (see section2.2.6.3). The protocol of this assay conducted with other cell groups has been published [353].

2.2.5 Endocytosis assays

2.2.5.1 Fluid phase pinocytosis assay

1.5x10^6 cells were suspended in 500 µl of complete medium in polystyrene round bottom tubes after being partially stimulated (see section 2.2.2.3) and harvested after Flt3-L culture (see section2.2.2.3). Prior to an incubation period at 37°C, fluorescein isothiocynate FITC)-OVA was added at a final concentration of 100 µg/ml. Initially, the following incubation periods were tested: 15 min, 20 min, 30 min, 1 h. Subsequent experiments were all conducted with an incubation duration of 1 h. Samples kept on ice during the incubation period served as negative controls. After incubation, the cells were washed three times with cold PBS containing 1% of FCS to stop the uptake of OVA. Prior to flow-cytometry analysis the samples were stained as described before (see section 2.2.6.2).

2.2.5.2 Latex bead protein coupling

The coupling of FITC-OVA to the beads was done according to the manufacturer's instruction of the Polybead® carboxylate microspheres (see section 0). First, 0.5ml of the bead solution was pipetted in a 1.5ml micro tube. A washing step was performed by filling up the tube with 1 ml of borate buffer (see section0), swirling and centrifuging it in a mini-spin (5 min, room temperature, 13.000 rpm). The supernatant was discarded and

the washing step was repeated for two more times as described. After the last centrifugation step, 1 ml of borate buffer was added and mixed thoroughly with the washed beads. The mixture was transferred into a lightproof micro tube. A total of 400 µl of FITC-OVA solution (1mg FITC-OVA/ml PBS) were added and the tube was sealed with parafilm. The mixture was incubated at room temperature for 12 h with continuous end-to-end mixing overnight. The next day, it was centrifuged (10 min, 13.000 rpm) and the bead pellet was resuspended in 1 ml of borate buffer containing 10 ng/ml BSA., followed by an incubation period of 30 min at room temperature while being continuously shaken in a vortex mixer. These centrifugation and incubation steps were repeated for three runs in total. After the last centrifugation step, the bead pellet was resuspended in 1 ml of storage buffer and kept at 4°C protected from light.

2.2.5.3 Phagocytosis assay

A total of 3 x 10^5/200µl FACS sorted (see section 2.2.6.1), untreated or stimulated (see section 2.2.2.3) pDCs and cDCs were suspended in complete medium. The cells were incubated with FITC-OVA coated latex beads (see section2.2.5.2) at a ratio of 1:10 (cells:beads) for 1 h at 37°C. Pre-treated samples with 2.5 µl/ml cytochalasin D for 20 min served as controls. Cyt D inhibits actin polymerization, which plays an essential part of the uptake process via phagocytosis. To stop the uptake-process, the samples were rapidly cooled down with ice-cold PBS containing 1% FCS followed by three washing steps. After the last centrifugation, the pellets were resuspended in 100 µl FACS-buffer containing 7-AAD. The uptake capacity of the cells was determined by flow cytometry. The measurement of the samples was performed in the presence of 0.4% trypan blue (10 µl/sample) achieving the quenching of extracellular florescence. This technique clears adulterant extracellular fluorescence resulting from beads remaining outside of the cells.

2.2.6 Flow cytometry

2.2.6.1 Cell analysis and fluorescent activated cell sorting

With flow cytometry it is possible to measure different characteristics of a single cell or particle while passing through a light source. The basic operation principle can be traced back to light scattering and fluorescence emission. A laser beam acts as excitation source striking particles in motion within a fluid stream [358]. Fluorescent features can

be added by treating the cells with antibodies and can be used together with size and granularity to further differentiate cells. This operation method can be used for two different types of flow cytometry with variable outcomes: non-sorting analysis or sorting of particles with identical characteristics within a sample [359]. For cell sorting cells of Flt3-L culture (see section 2.2.2.2) were used. Cells were prepared as described with antibody-stainings (see sections 2.2.6.2, 2.2.6.3). The sorting process was conducted by Dr. Shafaqat Ali (Scheu Lab, Institute of Medical Microbiology and Hospital Hygiene, Heinrich Heine University Düsseldorf) using the FACSAria™ III. The compensation process was performed with compensation beads according to the manufacturer's protocol. To get pure cultures of pDCs and cDCs the cell-like particles were pre-sorted using the forward and side scatter. Alive cells were further differentiated due to their expressed surface markers.

2.2.6.2 Extracellular staining

Cells suspensions were centrifuged (5 min, 4°C, 1200 rpm) and the supernatant was decanted. Fc receptors were blocked to prevent unspecific binding of antibodies. 100 µl of a CD16/CD32 antibody dilution (1:50 in FACS buffer) were added to each sample, mixed well and incubated in the dark for 10 min at 4°C. The antibodies were used as described (see sections 2.1.1.1).

Respectively, 100 µl of the prepared staining solution (selected antibodies in FACS buffer) were added and incubated in the dark for another 30min at 4°C. After washing the cells with 2 ml FACS buffer, they were centrifuges as described before and the supernatant was discarded. The cells were resuspended in FACS buffer or viability dyes were applied as described before (see section 0).

2.2.6.3 Intracellular staining

Intracellular staining was performed on ice after completing the last washing step of the surface antibody staining (see section2.2.6.2). After discarding the supernatant 100 µl of cytofix were added to each sample and incubated for 15 min in darkness. Cytoperm was used 1:10 in Milli Q water. The samples were washed 1.5 times with 150 µl of diluted cytoperm. Prior to an incubation period of 30 min in the dark, 50 µl staining solution (antibodies diluted in cytoperm) were added. After additional 2 times of washing with

180µl of cytoperm, samples were fixed in 1% PFA and stored at 4°C in the dark until flow cytometry.

2.2.7 Confocal microscopy

The samples were treated as described before in the phagocytosis assay (see section 2.2.5.3) before being analyzed via confocal microscopy. A cell-bead mixture (cells:beads = 1:10) containing $1.5x10^4$ cells were suspended in 700 µl of PBS containing 1% PFA and filled in U-slide 4 well chambers. Of each sample pictures of cells with ingested beads were taken with additional Z-stack image recording.

2.2.8 Genomics and transcriptomics

2.2.8.1 Next-generation sequencing (NGS)

NGS, also called massive parallel sequencing, is a high-output approach to DNA sequencing. It allows the sequencing of a whole genome within a relatively short time [360]. For NGS BM-derived pDCs ($CD3^-$, $CD19^-$, $CD11c^+$, $CD11^{blow}$, $B220^+$, $SiglecH^+$ and $mPDCA1^+$) were FACS purified using FACS Aria III [12]. The pDCs were left untreated or stimulated with 1 µM CpG 2216 (Tib Molbiol, Nr. 930507l) complexed to transfection reagent DOTAP (roche) for 2, 6 or 12 h. RNA was isolated by using NucleoSpin RNA mini kit (macherey-Nagel) and subjected to RNA-Seq. NGS-data shown in this thesis were generated in close collaboration with the biological-medical research center (BMFZ) Düsseldorf. Data analysis was performed by Ritu Mann-Nüttel.

2.2.9 Statistical analysis

If not explicitly stated otherwise GraphPad prism was used for all statistical analyses. For all performed statistical analyses GraphPad Prism was used. For the statistical comparison of two groups the unpaired, two-tailed Student's t-test was used. Statistical significance (P) is represented as: $*P \leq 0.05$; $**P \leq 0.01$; $***P \leq 0.001$.

3. Results

3.1 Gene expression profiling

Plasmacytoid dendritic cells are professional IFN I producers [162, 352, 361] and can present antigens to T cells during viral infection [142, 144]. However, only a small subpopulation of pDCs actively produce IFN I after TLR7/9 activation [352]. Our lab published that activated IFNβ producing pDCs also express high amounts of BATF. To better understand the molecular functions of BATF in pDCs, the Scheu lab (the research group of the supervisor of this work) performed a transcriptome profiling of resting and CpG stimulated bone marrow-derived pDCs. For this purpose, FACS purified BM-pDCs from *Batf*$^{+/+}$ and *Batf*$^{-/-}$ mice were stimulated with CpG in a time course study (untreated, 6 h, 12 h – each condition including three biological replicates). NGS of these cells was performed in collaboration with Professor Karl Köhrer (Biologisch-Medizinisches Forschungszentrum, Heinrich-Heine University, Duesseldorf). The RNA-Seq data was kindly analysed by Ritu Mann-Nüttel, a PhD candidate of the Scheu lab (Institute of Medical Microbiology and Hospital Hygiene, Heinrich Heine University Düsseldorf). A part of this profiling data illustrating the transcription reservoir in wild type pDCs has been published elsewhere [4]. A Kyoto Encyclopedia of Genes and Genomes (KEGG)-pathway analysis was performed aiming at identifying the most affected cellular pathways in sense of differential gene expression comparing cells derived from BATF WT vs KO (data from Ritu Mann-Nüttel, not shown). This analysis revealed the process of antigen presentation to be the 5th most affected one in terms of gene expression in dependency of BATF presence. More precisely assigned, most of these genes appeared to rather be of importance within the antigen cross-presentation pathway than within the direct antigen presentation pathways. To generate a validated overview of this observation literature research was conducted. A list of variables (n = 74) that have been published to play a role specifically within the antigen cross-presentation pathway was assorted. Each factor was matched accordingly to its official gene symbol using the gene data base of the National Center for Biotechnology Information (NCBI) for the organism *Mus musculus* (house mouse). These symbols were further used to extract the genes encoding the selected factors from the NGS data set. To evaluate patterns of expression changes regarding the time course of stimulation (modelling early events after virus infection) a hierarchical clustering of all selected genes based on the normalized expression in naïve and stimulated pDCs was carried out. Different clusters according to the expression pattern emerged: genes, that were upregulated by stimulation (either

after 6 h or 12 h of stimulation or in both conditions, depicted in the upper part of the heatmap) and genes that were generally being downregulated by stimulation (either after 6 h or 12 h of stimulation or in both conditions, depicted in the bottom part of the heatmap) (Fig. 6A). Verifying the observation of the KEGG-pathway analysis, multiple genes showed a diverse expression in dependency of *Batf* presence. Strikingly, this diversity became more distinct, both in number of affected genes and in degree of their expression level, after CpG exposure. Assuming that the effects of CpG stimulation are equivalent to the early events of an infection, this data can be summarized by stating that BATF influences the ACP pathway by regulating the expression of crucial factors within this pathway.

3.1.1 BATF deficiency leads to a dysregulation of gene expression in the antigen cross-presentation pathway

To find out how decisive the influence of BATF on ACP is, I first investigated the significance of expression level differences regarding ACP relevant factors (*Batf*$^{+/+}$ or *Batf*$^{-/-}$ pDCs at steady state and after CpG stimulation at 6 h, 12 h). Genes with a *p*-value of <0.05 corrected for the false discovery rate (pFDR) were considered significantly differentially expressed. Out of the 74 genes studied, a total of 24 genes showed a significant difference in expression level depending on *Batf*-presence. This number increased to 39 genes after 6 h of stimulation and slightly decreased to 33 genes after 12 h of stimulation. The biggest overlap of genes (n = 25) is found between 6 h vs 12 h stimulated pDCs. A total of 8 genes showed a significant differential expression under all conditions (naïve vs 6 h vs 12 h). Furthermore, it was noticed that the genes with altered expression pattern were mostly downregulated in BATF KO in comparison to the WT after stimulation. At steady state, only 41.7% (10 of the 24 differentially expressed genes) showed a lower expression level, after 6 h of stimulation it was 74.4% (29 of 39) and after 12 h 69.7% (23 of 33). Upregulation was seen in 58.3% (14 of 24) without stimulation, 25.6% (10 of 39) after 6 h and 30.3% (10 of 22) after 12 h of stimulation (Fig. 6B).

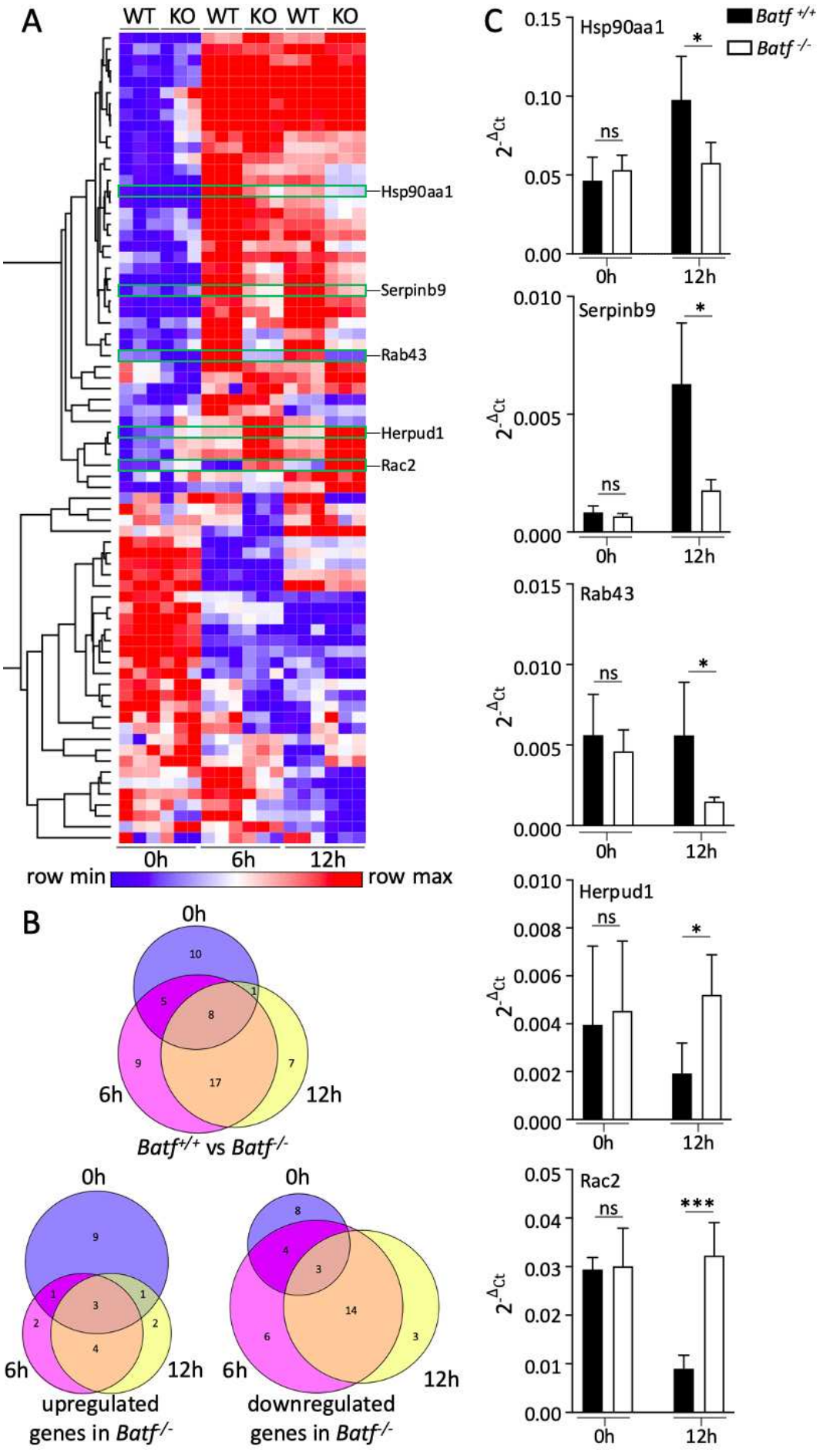
A
WT KO WT KO WT KO
Hsp90aa1
Serpinb9
Rab43
Herpud1
Rac2
0h 6h 12h
row min
row max
B
0h
10
5
1
8
9
7
17
6h
12h
Batf+/+ vs Batf-/-
0h
9
1
3
1
2
2
4
6h
12h
upregulated genes in Batf-/-
0h
8
4
3
14
6
3
6h
12h
downregulated genes in Batf-/-
C
Batf +/+
Batf -/-
Hsp90aa1
Serpinb9
Rab43
Herpud1
Rac2
2-ΔCt
ns
*
***
0h
12h

Fig. 6: RNA-Seq reveals significant gene expression differences in BATF WT and KO. Heatmap showing the normalized expression values (cpm, count per million) of the enlisted genes (involved in antigen cross-presentation) in pDCs at steady state and after 6 h and 12 h of CpG stimulation. Hierarchical clustering on rows with average linkage and the ONE minus Pearson correlation metric was performed (A). Venn diagrams displaying significantly ($p \leq 0.05$) differentially expressed (upper diagram), up-regulated (bottom, left), or down-regulated (bottom, right) genes between *Batf*$^{+/+}$ and *Batf*$^{-/-}$ (B). Bar charts depicting the RT-PCR results of significantly up- or down-regulated genes in *Batf*$^{+/+}$ vs *Batf*$^{-/-}$. Shown is the $2^{-\Delta Ct}$ of the mean ± the standard deviation (SD) of two pooled independent experiments of four biological replicates (n=8) in each experiment (naïve and stimulated) of the gene in focus and ß-actin (serving as a reference gene). The mean value of three technical replicates of each biological replicate was used for calculations. Statistical significance (P) is represented as: *$P \leq 0.05$; **$P \leq 0.01$; ***$P \leq 0.001$ (C). pDCs = plasmacytoid dendritic cells, cDCs = classical dendritic cells, RT-PCR = real-time PCR

In addition, the expression differences of selected genes were retested by RT-PCR. RT-PCR is the method of choice downstream of NGS for result verification to ensure data integrity. For this purpose, Flt3-L-cultures of BMDCs of BATF WT and BATF deficient mice were generated. After FACS purification, the cells were stimulated, RNA was isolated and cDNA synthesized accordingly followed by RT-PCR quantification. I could verify the expression pattern of selected genes as observed in the NGS data (pFDR of NGS data <0.05; p-value of RT-PCR analysis <0.05: Hsp90aa: 0 h, 12 h; Serpinb9: 0 h, 12 h; Rab43: 12 h; Herpud1: 12 h; Rac2: 12 h). However, in some cases the statistical significance levels were varying (pFDR of NGS data <0.05 but no significant correlation in RT-PCR: Rab43: 0 h; Herpud1: 0 h; Rac2: 0 h) (Fig. 6C).

In summary, during TLR9 activation (mimicking the prevailing conditions of early infection) *Batf* deficiency leads to a dysregulation of certain factors involved in the process of ACP.

3.2 BATF significantly influences the antigen cross-presentation capacity of pDCs

The main hypothesis, that BATF has an impact on ACP in pDCs, implies the assumption that pDCs can cross-present antigen at all. Therefore, an ACP assay was performed to investigate the in general controversially discussed ACP ability of pDCs. The analysis was performed under various stimulation modes. cDCs as commonly known very efficient ACPCs were used as comparison to better classify the results. After establishing the conditions, I was able to characterize BATF for the first time as a critical factor determining the ACP fate in pDCs.

3.2.1 Establishing stimulation conditions for antigen-cross-presentation in pDCs

Fig. 7A shows an overview of the experimental steps of the ACP assay. Infected feeder cells underwent washing-steps and PUVA treatment preventing false-positive results caused by directly presenting cells accidentally infected with input virus. Two T cell lines with different epitope specificities were used achieving an intra-experimental verification of the collected data. A $CD8^+$ T cell activation assay led to the final read-out of IFNγ production. The gating strategy is depicted in Fig. 7B.

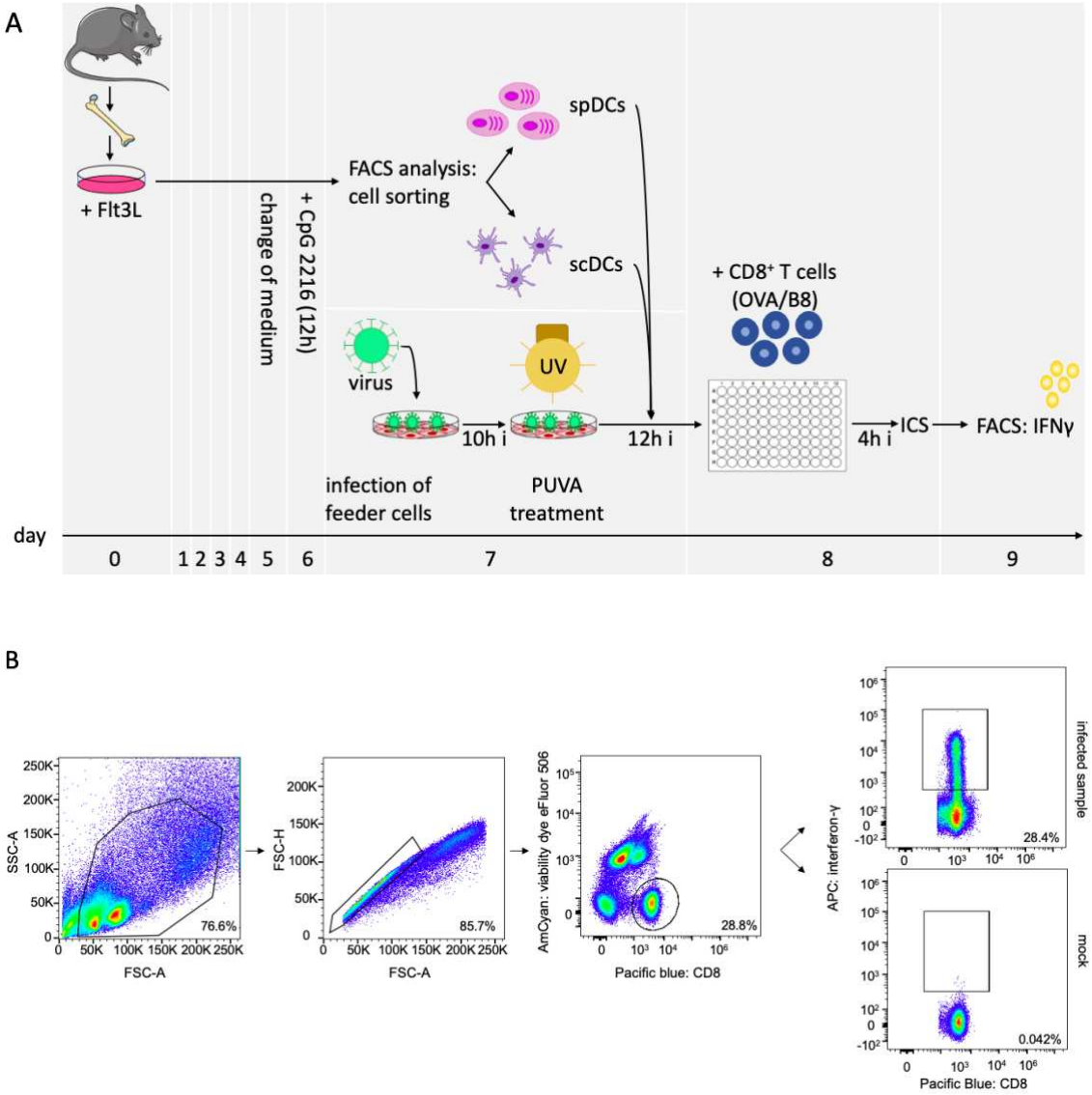

Fig. 7: Experimental setup and gating strategy for the antigen cross-presentation assay. For the ACP assay BMDCs were cultivated as Flt3-L-cultures and either left untreated or stimulated with CpG. The cells were harvested and distinguished in a sorted pDC subset ($CD3^-$ $CD19^-$ $CD11c^+$ $CD11b^{low}$ $B220^+$ $SiglecH^+$ $CD317^+$) (spDCs) and a sorted cDC subset ($CD3^-$ $CD19^-$ $CD11c^+$ $CD11b^+$ $B220^-$) (scDCs) according to their surface markers. Feeder-cells were infected

with virus particles for an incubation time (i) of 10 h. Mock-controls (samples sparing viral infection) were generated for each sample individually. After PUVA treatment the infected feeder cells were co-cultivated with the spDCs/scDCs. After $CD8^+$ T cell activation assay and ICS, FACS analysis led to IFNγ readout (for illustration the servier medical art database was used, cartoons have been adapted) (A). Depicted is the gating strategy for the cross-presentation assay. Samples were measured using a BD FACS Canto II and subsequently analysed by FlowJo 10.5.3. Samples were initially gated for cell sized particles and single cells. Next, live $CD8^+$ cells were gated. The final read-out for the assay was the measurement of IFNγ within this group. Displayed is the read-out of a virus-infected sample (upper right picture) and the matching mock-control that had no contact to the virus (lower right picture). Percentages indicate the frequencies of the parental populations (B). FSC = forward scatter, SSC = side scatter, pDC = plasmacytoid dendritic cell, cDC = classical dendritic cell, ICS = intracellular staining, s = sorted

The ACP ability of pDCs is often bound to the condition of additional TLR stimulation [144, 151]. Hence, the first pilot ACP assay run included the testing of the impact of different stimulation conditions. The ACP assay was performed as previously described (Fig. 7A, B) integrating an additional stimulation condition which led to the following studied groups: naïve pDCs, pDCs pre-treated with CpG once (for a duration of 12 h before the sorting process) and pDCs stimulated twice (once for 12 h before the sorting process and once more when being co-cultured with the infected feeder cells after PUVA treatment). In addition, the IFNγ production of T cells after coculture with non-stimulated cDCs was analysed (Fig. 8C, D). The $CD8^+$ T cell activation assay was conducted with two different T cell lines on the above mentioned sample groups: one OVA specific T cell line (Fig. 8A, C) and one B8-specific T cell line (Fig. 8B, D).

The data show, that a one-time CpG stimulation (12 h) of pDCs led to a higher IFNγ expression by T cells in comparison to non-stimulated pDCs (OVA-specific T cell line: 10.2% vs 31.3% - increase of 206.9%; B8-specific T cell line: 13.3% vs 32.1% - increase of 141.4%) (Fig. 8A, B), respectively to a higher ACP capacity of pDCs. The additional amount that could be obtained by double-stimulation showed a much smaller percentage gain in comparison to the one-time stimulated pDCs (OVA-specific T cell line: 31.3% vs 43.5% - increase of 39%; B8-specific T cell line: 32.1% vs 46.1% - increase of 43.6%) (Fig. 8A,B). Another independent observation was the slight presence of background noise in the uninfected mock-controls in the stimulated samples. According to the achieved stimulation dependent relative enhancement of ACP capacity, I decided against continuing with a dual stimulation concept for the following ACP assays, since the percentage gain turned out to be much lower in comparison with the one-time stimulation method.

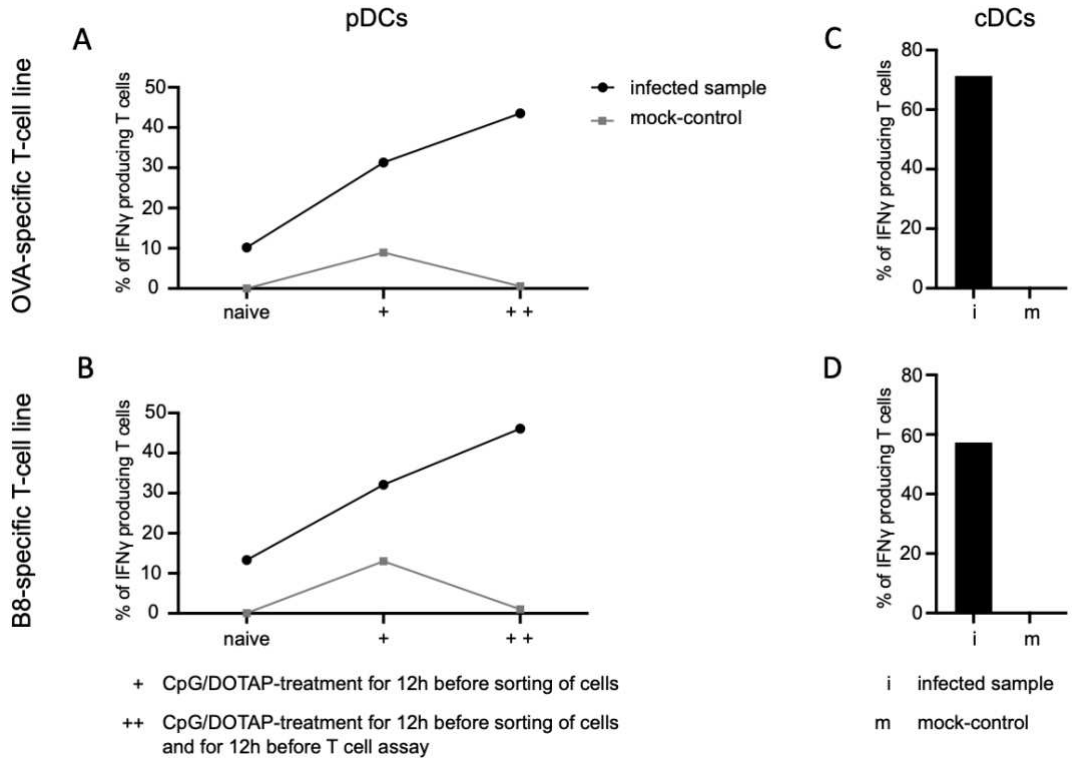

Fig. 8: Optimal stimulation conditions for pDCs in the ACP assay.
To evaluate the optimal stimulation time point and period the cells subsequently underwent a trial ACP assay followed by the $CD8^+$ T cell activation assay. Compared were the following groups: untreated (naïve) pDCs, pDCs stimulated once (for a duration of 12 hours before the sorting process) and pDCs that were stimulated twice (for 12 hours before the sorting process as well as once again for 12 hours before entering the $CD8^+$ T cell activation assay). Stimulation was performed with CpG and DOTAP. Displayed are the results of one pilot experiment showing one biological sample from each of the described groups with a concomitant mock-control (A, B); cDCs were left untreated (C, D). The assay was performed with two different T cell lines: one specific for OVA (A, C), the other one specific for B8 (B, D). Significance calculations were dispensed due to sample size. pDCs = plasmacytoid dendritic cells, cDCs = classical dencritic cells

3.2.2 pDCs are generally capable of antigen cross-presentation

The data presented above (Fig. 8) indicates (to a very limited extent) that pDCs after all are ACPCs. Therefore, the first fundamental question I wanted to answer was if pDCs can cross-present antigen at all. To investigate the ACP capability of pDCs, MVA-infected MHC I-mismatched feeder cells unable to directly present antigen to T cells were used in the ACP assay. $CD8^+$ $IFN\gamma^+$ T cells could be identified after co-culturing them with pDCs that had run through the ACP assay before. This was true for pDCs prepared from *Batf*$^{+/+}$ and *Batf*$^{-/-}$ mice as well as for both tested T cell lines (one specific for the recombinant antigen OVA and the other specific for the viral antigen B8). A distinct IFNγ expression could be measured regardless of whether the cells had experienced an additional TLR9 activation in advance (Figure 9A, C). These results characterize pDCs

as ACPCs. The experimental setup was designed to closely mimic physiological conditions by infecting feeder cells with actual viral particles instead of simply exposing the pDCs to protein. Thus, I could demonstrate that the ACP ability of pDCs in a true-to-life setting is not determined by additional stimulation. These observations could be made independent of BATF expression.

3.2.3 TLR9 activation enhances the antigen cross-presentation capacity of pDCs

Secondly, we wanted to investigate whether an additional TLR-stimulation of pDCs before conducting the cross-presentation has an impact on the effector T cell activation *in vitro*. The cells were treated with CpG to induce activation. Again, the experiment was conducted with two separate T cell lines (B8, OVA). In both cases, a significant upregulation of the IFNγ expression could be registered after a stimulation with CpG for 12 h on pDCs prior to their contact with the infected feeder-cells. This observation applied to both tested genotypes (OVA-specific T cell line (naïve vs stimulated): 10.2% vs 49.2% in *Batf*$^{+/+}$ pDCs, 20.8% vs 49.1% in *Batf*$^{-/-}$ pDCs; B8-specific T cell line (naïve vs stimulated): 6.3% vs 39.3% in *Batf*$^{+/+}$ pDCs, 10.7% vs 44.3% in *Batf*$^{-/-}$ pDCs). TLR9 activation in pDCs leads to a significant increase of their ACP capacity. This observation could be made independently of BATF expression in pDCs (Figure 9A, C).

3.2.4 cDCs remain the unsurpassed antigen cross-presenting cells, but do they really no matter what?

Finally, I was interested in how these two groups (naïve pDCs, stimulated pDCs) perform in comparison to the masters of ACP, the cDCs. I analysed T cell responses to naïve and stimulated pDCs as well as to naïve cDCs after the ACP assay. In both T cell lines, the two groups of pDCs produced a significantly lower IFNγ expression in the T cells in comparison to the cDCs in BATF WT BMDCs (OVA-specific T cell line: 10.2% and 49.2% vs 77.7%; B8-specific T cell line: 6.3% and 39.3% vs 54%). This was also true comparing stimulated *Batf*$^{-/-}$ pDCs to naïve *Batf*$^{+/+}$ cDCs (OVA-specific T cell line: 59.1% vs 77.7%; B8-specific T cell line: 44.3% vs 54%) (Figure 9A, C). In BMDCs from BATF KO mice a significant difference could only be seen comparing naïve pDCs to naïve cDCs (OVA-specific T cell line: 20.8% vs 70%; B8-specific T cell line: 10.7% vs 31.3%). Interestingly, in *Batf*$^{-/-}$ pDCs we saw no significant difference in CD8^{+} T cell activation between the stimulated pDCs in comparison to the cDCs (OVA-specific T cell line: 59.1% vs 70%;

B8-specific T cell line: 44.3% vs 31.3%) (Figure 9A, C). Summing up, pDCs exposed to the same conditions as cDCs cannot trigger an equally strong T cell answer as cDCs. However, it is striking that with an additive TLR9 activation as well as in BATF deficiency the difference to the ACP capacity of cDCs is no longer significant. This indicates a decisive effect of BATF expression on pDC and/or cDC ACP performance.

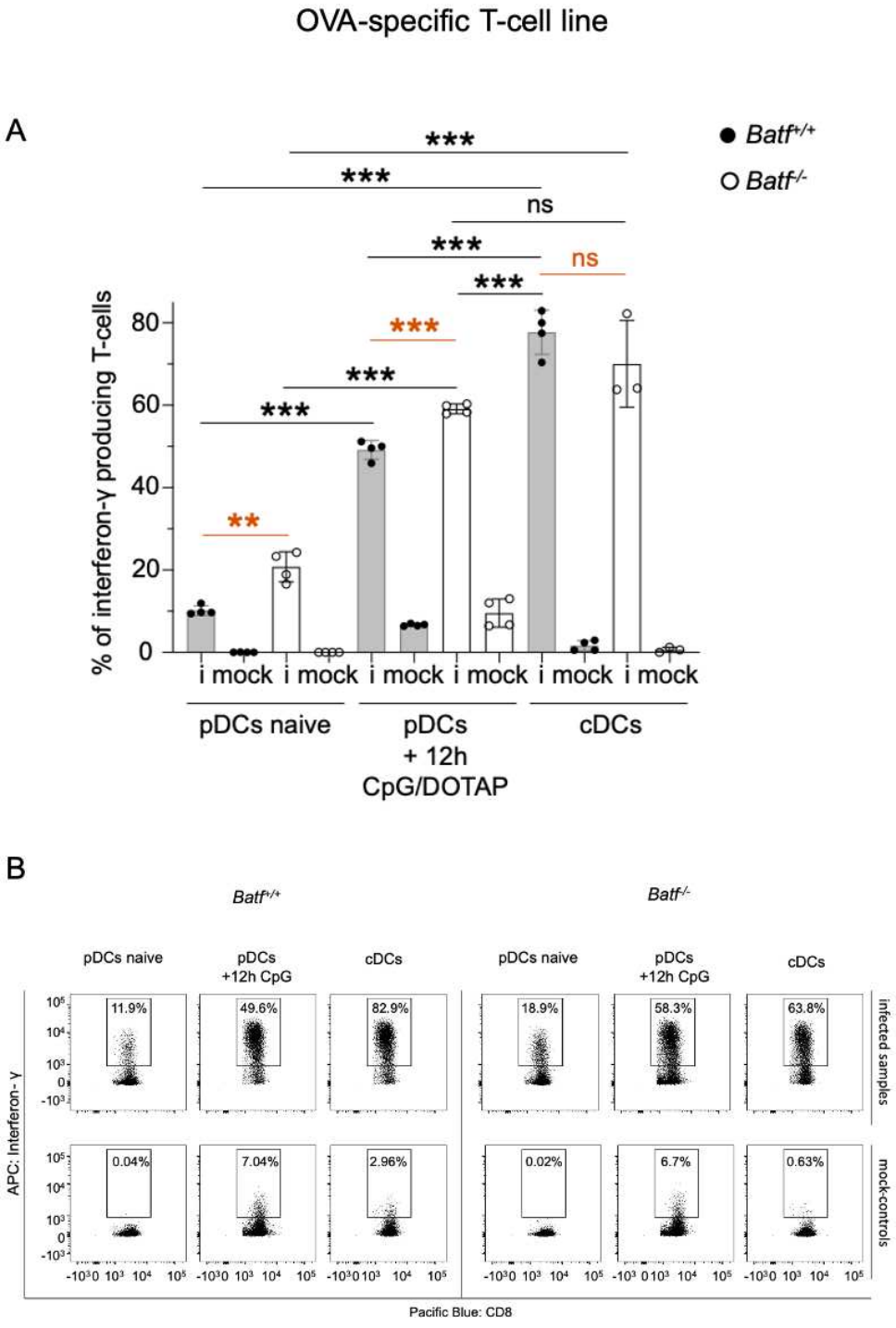

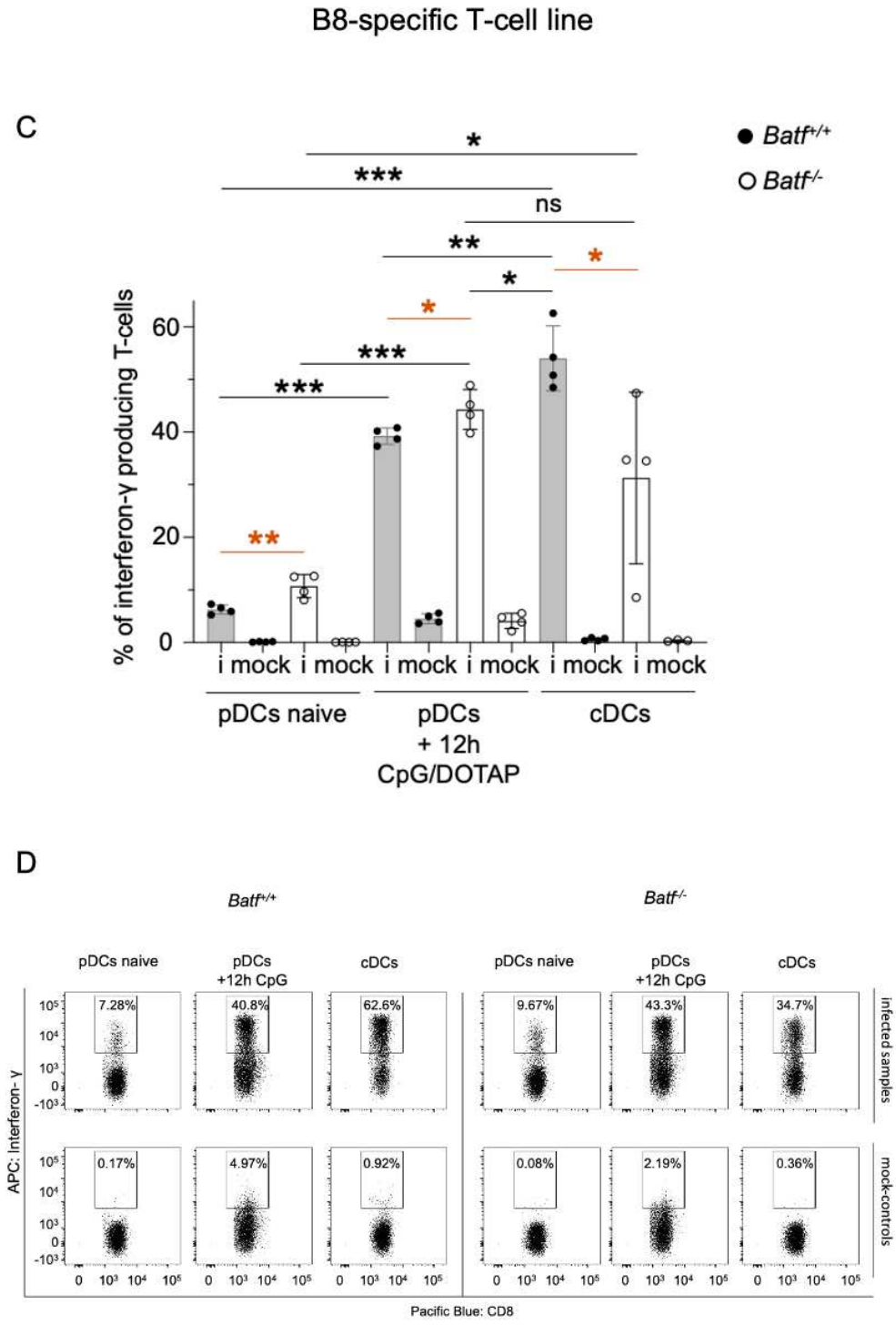

Figure 9: Impact of BATF on the antigen cross-presentation capacity of pDCs (naïve, stimulated) and cDCs.
Flt3-L cultured BMDCs generated from BATF KO mice or WT littermates were sorted for pDCs ($CD3^-$ $CD19^-$ $CD11c^+$ $CD11b^{low}$ $B220^+$ $SiglecH^+$ $CD317^+$) and cDCs ($CD3^-$ $CD19^-$ $CD11c^+$ $CD11b^+$ $B220^-$). BMDCs were either left untreated or stimulated with CpG for 12h. Cross-presentation assay followed by T cell activation assay were conducted. Samples were analysed via flow cytometry for interferon-γ^+ cells pre-gated on single, live, $CD8^+$ cells. The T cell activation assay was conducted with two different T cell lines, one specific for the recombinant antigen OVA (A, B), the other one specific for the MVA-derived viral antigen B8 (C, D). The results are depicted as mean ± SD of n = 4 biological replicates (mice) per group. Shown is one out of two independent

experiments. Statistical significance (P) is represented as: *P ≤ 0.05; **P ≤ 0.01; ***P ≤ 0.001. Depicted is the final read-out (interferon-γ$^+$ cells) for each group (naïve pDCs, stimulated pDCs, cDCs) of one representative sample. For each sample (upper row) the matching mock-control (lower row) is shown. Graphs map the results of both tested epitopes individually, (C) measurements of the OVA-specific T-cell line and (D) for the B8-specific T-cell line. Percentages indicate the frequencies of the parental cell population (single, live, CD8$^+$). pDCs = plasmacytoid dendritic cells, cDCs = classical dendritic cells

3.2.5 BATF deficiency significantly increases the antigen cross-presentation capacity of pDCs

After verifying that pDCs are capable of ACP (see section 3.2.2) and establishing the optimal investigation conditions for ACP of pDCs I aimed at confirming my main hypothesis. The assumed impact of BATF on ACP in pDCs was so far solely based on the presented NGS-data (see section 3.1.1). For this purpose, IFNγ production of CD8$^+$ T cells was analysed comparing T cells after co-culturing them with BMDCs generated from BATF WT or KO mice that were exposed to the infected feeder-cells before. BATF deficiency led to a significant increase of T cell activation in pDCs (Figure 9). This result could be verified for both epitope specificities tested via the two different T cell lines, OVA (Figure 9A, B) and B8 (Figure 9C, D). The significantly increased T cell response revealed by the lack of *Batf* was independent of the pDC stimulation status (OVA-specific T cell line (WT vs KO): 10.2% vs 20.8% in naïve pDCs, 49.2% vs 59.1% in stimulated pDCs; B8-specific T cell line (WT vs KO): 6.3% vs 10.7% in naïve pDCs, 39.3% vs 44.3% in stimulated pDCs) (Figure 9). Hereby, BATF is identified as a negative regulator in ACP in pDCs.

3.2.6 BATF deficiency diminishes T cell response to antigen cross-presentation of cDCs

Interestingly, the absence of *Batf* showed a different outcome in cDCs than in pDCs. In cDCs *Batf*-deficiency lead to a significant lower ACP capacity in the B8-specific T cell line (WT vs KO: 54% vs 31.3%) (Figure 9C, D). The same trend could be seen in the OVA-speficic T cell line (WT vs KO: 77.7% vs 70%) (Figure 9A, B).

I could characterize BATF as a suppressing factor in ACP in pDCs and at the same time observe a BATF dependent downsize in T cell response after ACP of cDCs. Thus, BATF plays a unique role in different groups of BMDCs regarding its influence on ACP. Identification of the affected processes and a detailed understanding of them may lead to a use of BATF expression in a targeted manner.

3.3 Endocytosis

After confirming a crucial impact of BATF on ACP in pDCs, I wanted to understand the underlying mechanisms behind this effect. As mentioned before, the contribution of pDCs in cross-presentation of antigens is diversely discussed [146]. However, the fact that they can ingest antigen has been studied and confirmed multiple times [151, 152]. Since exogenous antigen uptake is one of the requirements for ACP, I went on to investigate this process closer, especially in *Batf* deficiency. Based on the findings regarding the impact of BATF on ACP I hypothesized, that BATF expression leads to a decrease of uptake rate in pDCs. Phagocytosis seems to be the crucial mechanism for antigen uptake in terms of efficient ACP [362]. To detect potential differences of BATF influence on the processes, the uptake capacity of soluble as well as of particulate antigen were studied separately.

3.3.1 Establishing conditions for fluid-phase pinocytosis of pDCs

BMDCs were generated as described before and fluid phase pinocytosis was enabled by co-culturing with soluble FITC-OVA. Cells were subsequently analysed by flow cytometry by further differentiating the cells into pDCs ($CD3^-$ $CD19^-$ $CD11b^{low}$ $B220^+$ $SiglecH^+$) and cDCs ($CD3^-$ $CD19^-$ $CD11c^+$ $CD11b^+$ $B220^-$), cDC1 subset ($XCR1^+$) and cDC2 subset ($CD172\alpha^+$) respectively, according to their surface markers. The percentage of $FITC^+$ cells of the parental frequencies served as a final read-out. Fig. 10 depicts the gating strategy.

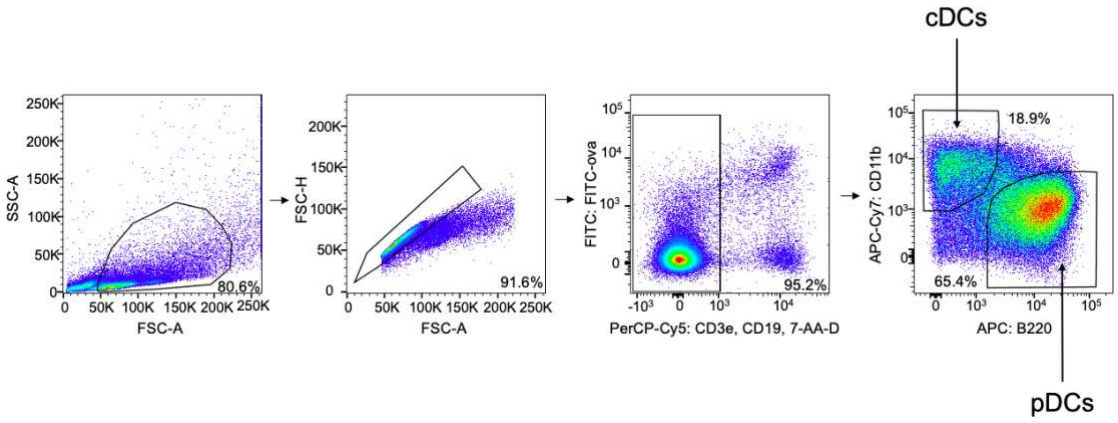

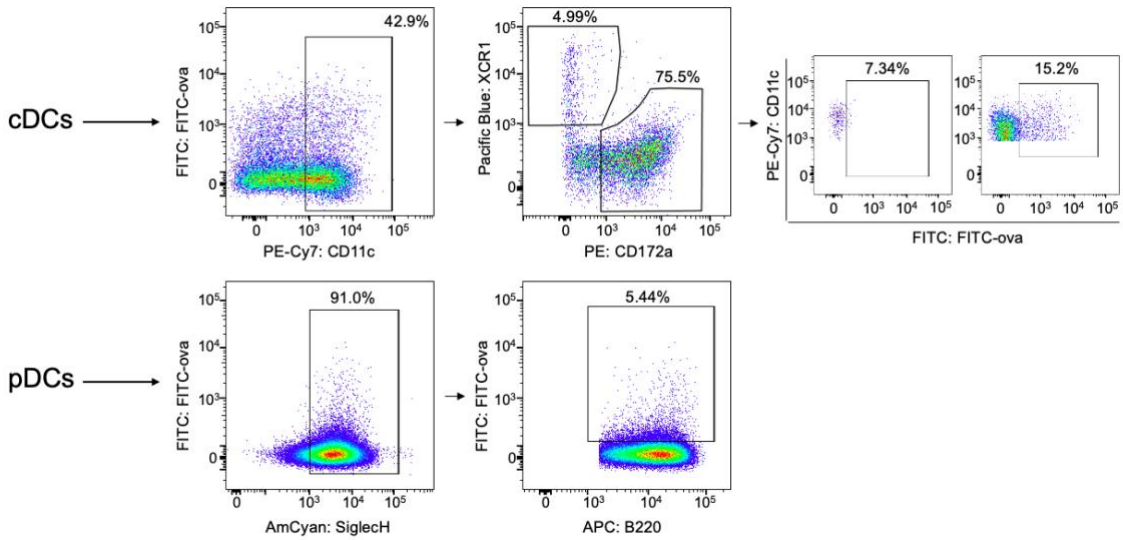

Fig. 10: Gating strategy for fluid phase pinocytosis assay.
Samples were measured using a BD FACS Canto II and subsequently analysed by FlowJo 10.5.3. Samples were initially gated for cells and single, alive cells. Next, CD11b^{high} cells were gated and thereby identified as cDCs, B220^{+} cells were identified as pDCs. For cDCs, CD11c^{+} cells were further differentiated into a cDC1 subset (XCR1^{+}) and a cDC2 subset (CD172α^{+}). For pDCs, SiglecH was considered as a second marker identifying this population. The final read-out were FITC-positive cells from the pre-gated groups described (pDCs, cDC1subset, cDC2 subset). Displayed is one representative sample. Percentages indicate the frequencies of the parental populations. pDC = plasmacytoid dendritic cell, cDC = classical dendritic cell, FSC = forward scatter, SSC = side scatter

Firstly, the required duration of co-culture with soluble FITC-ova was evaluated. Therefore, we tested four different periods of time (10 min, 20 min, 30 min and 1 h) of incubating the BMDCs with the FITC-Ova. BDMCs were stimulated with CpG for 12 h before entering the assay. Co-culturing took place at 37°C. The further uptake was stopped by washing the samples with ice-cold PBS. Ice-controls served as negative controls and were prepared simultaneously under the same conditions, except for being kept on ice during the entire incubation time. The cDC2 subset contained the highest percentage of FITC^{+} cells (Fig. 11C), indicating that these cells were the most efficient regarding pinocytosis. Looking at the duration of the incubation time, all subsets showed the same trend. A slow constant increase could be registered within the first 30 min (mean of FITC-positive cells of two samples 10 min vs 30 min: 0.56% vs 1.33% in pDCs (Fig. 11A), 0.25% vs 0.84% in the cDC1 subset (Fig. 11B), 7.48% vs 24.1% in the cDC2 subset (Fig. 11C)). This was followed by another distinct increase within another 30 min (1 h in total) of co-culturing with soluble FITC-ova (mean of FITC-positive cells of two samples 30 min vs 1h: 1.33% vs 4.14% in pDCs (Fig. 11A), 0.84% vs 1.24% in the cDC1 subset (Fig. 11B), 24.1% vs 41.8% in the cDC2 subset (Fig. 11C)). In summary, a persistent increase of the antigen uptake rate could be registered in correlation with the

incubation time. The biggest leap was achieved within 30-60 min. Subsequently, the following pinocytosis assays were performed with an incubation duration of 1 h.

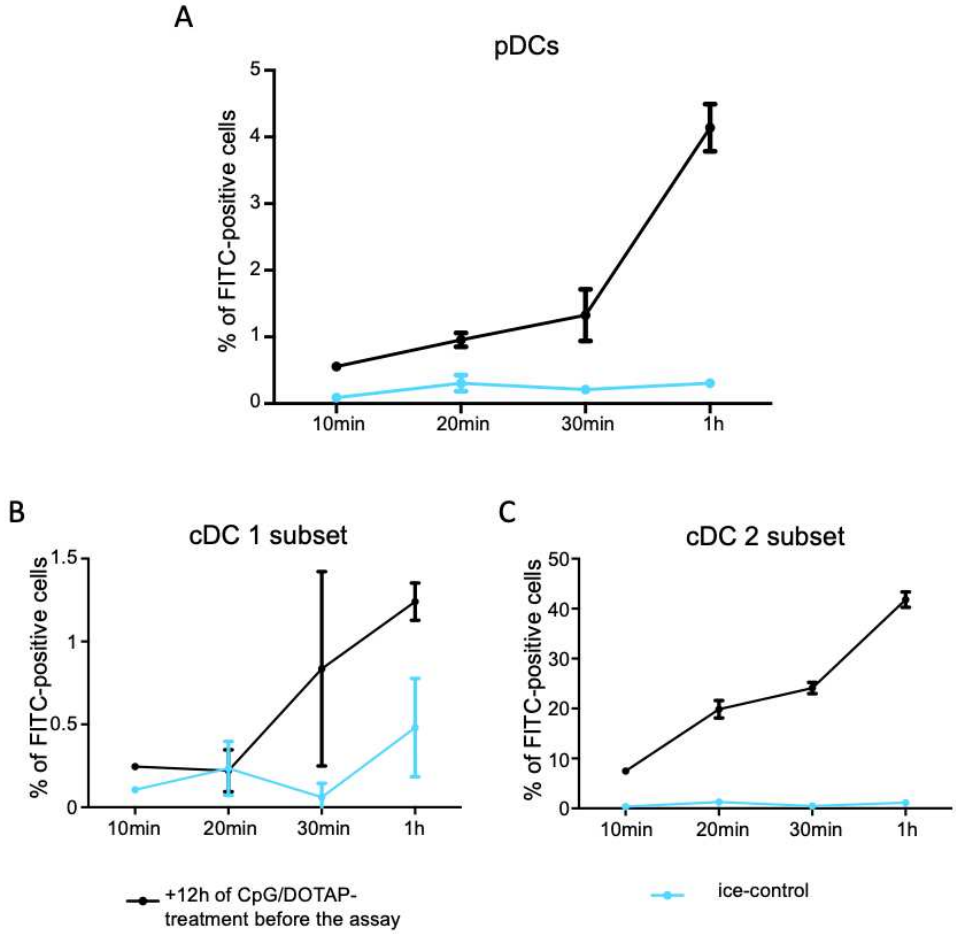

Fig. 11: Optimal duration of co-culturing for fluid-phase pinocytosis of soluble material in pDCs.
Stimulated BMDCs (CpG for 12h) were co-cultured with soluble FITC-ova for different periods of time at 37°C and 10% CO_2 with corresponding ice-controls. Samples were analysed via flow cytometry for FITC$^+$ cells pre-gated on single and live cells and further distinguished into pDCs (CD3$^-$ CD19$^-$ CD11c$^+$ CD11b^{low} B220$^+$ SiglecH$^+$ CD317$^+$) and cDCs (CD3$^-$ CD19$^-$ CD11c$^+$ CD11b$^+$); cDCs were further divided into a cDC1 subset (XCR1$^+$) and a cDC2 subset (CD172α$^+$). Displayed is the uptake capacity of pDCs (A), the cDC1 subset (B) and the cDC2 subset (C) after 10 min, 20 min, 30 min and 1 h of incubation time. Shown is one pilot experiment. The results are depicted as mean ± SD of n = 2 technical replicates per group and stimulation duration. pDC = plasmacytoid dendritic cell, cDC = classical dendritic cell

3.3.1.1 BATF has no significant influence on pinocytosis in activated pDCs

Regarding the uptake capacity of soluble material (macrophages served as a control, Fig. 12A), no significant difference could be detected between the cDC1 and cDC2 subset comparing cells derived from BATF KO vs. BATF WT mice independent of their stimulation status (KO vs WT: 10.42% vs 12.28% in naïve cells (cDC1 subset), 5.43%

vs 5.08% in stimulated cells (cDC1 subset); 16.68% vs 17.1% in naïve cells (cDC2 subset), 31.35% vs 23.58% in stimulated cells (cDC2 subset)) (Fig. 12C, D). In pDCs, naïve and stimulated pDCs showed a diverse result. Like in cDCs, the percentage of FITC-positive cells was not significantly different comparing *Batf*$^{+/+}$ with *Batf*$^{-/-}$ pDCs that underwent stimulation treatment (KO vs WT: 5.43% vs 5.47%) (Fig. 12B). Naïve pDCs in contrast showed a significantly lower rate of FITC-ova uptake in the cells in *Batf* deficiency (KO vs WT: 5.61% vs 9.32%) (Fig. 12B).

For pinocytosis it can be stated that BATF presence facilitates a significantly higher uptake amount of soluble antigen. This observation could only be made pDCs, However, the effect vanished after TLR9 activation.

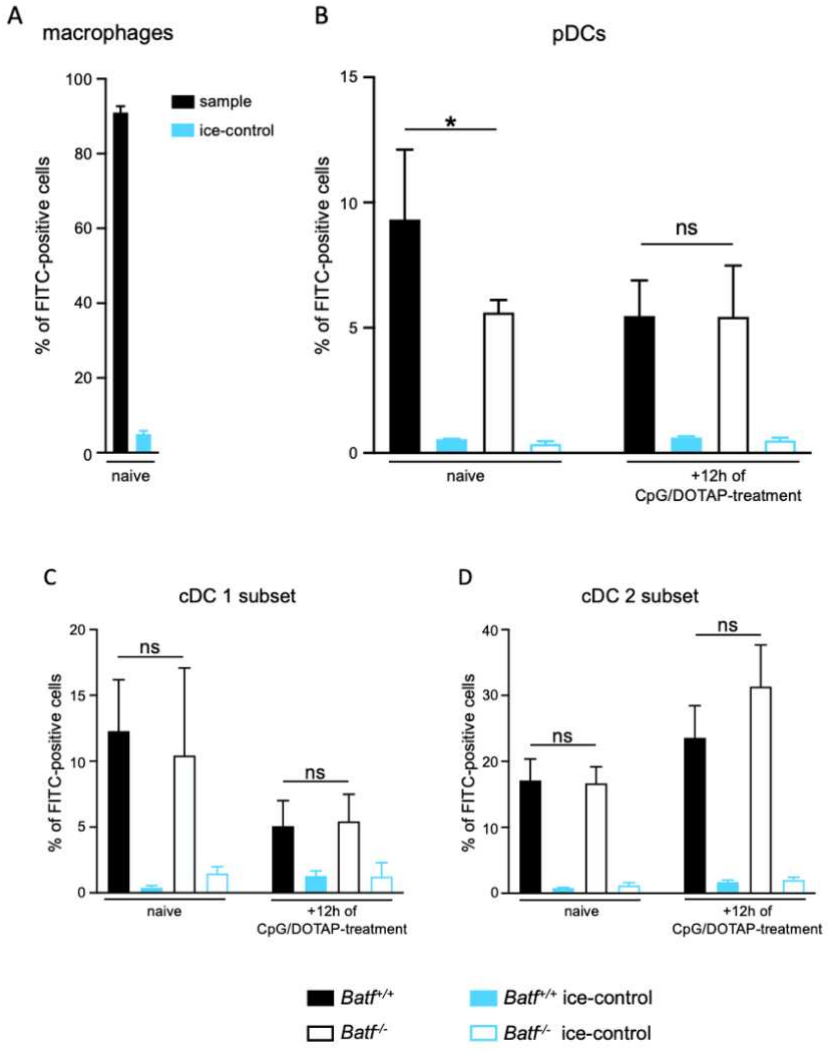

Fig. 12: Uptake capacity of fluid-phase pinocytosis of soluble material in pDCs and cDC-subsets.

Cells were co-cultured with soluble FITC-ova for 1 h at 37C° and 10% CO_2 with corresponding ice-controls. Samples were analysed via flow cytometry for $FITC^+$ cells pre-gated on single and live cells and further distinguished into pDCs ($CD3^-$ $CD19^-$ $CD11c^+$ $CD11b^{low}$ $B220^+$ $SiglecH^+$ $CD317^+$) and cDCs ($CD3^-$ $CD19^-$ $CD11c^+$ $CD11b^+$); cDCs were further divided into a cDC1 subset ($XCR1^+$) and a cDC2 subset ($CD172\alpha^+$). Macrophages were used as controls, here displayed with their matching ice-control (A). Shown is the uptake capacity of naïve and stimulated (12h of CpG/DOTAP-treatment) pDCs (B). Uptake capacity of naïve and stimulated cDC-subsets (C, D). The results are depicted as mean ± SD of n = 4 technical replicates per group. Shown is one out of two independent experiments. Statistical significance (P) is represented as: *P ≤ 0.05; **P ≤ 0.01; ***P ≤ 0.001. pDC = plasmacytoid dendritic cell, cDC = classical dendritic cell

3.3.2 Establishing conditions for phagocytosis of particulate antigens in pDCs

In activated pDCs no significant difference in the fluid-phase uptake rate of antigen was observed, which could have explained the effect of BATF on ACP. Next, I investigated whether a potential influence of BATF on phagocytosis may provide an explanatory approach for the BATF dependent ACP capacity in pDCs. For this assay, spDCs and scDCs were either left untreated or stimulated with CpG for 12 h before being co-cultured with FITC-ova coupled beads. The prepared beads mimicked particulate antigen and their uptake was later measured gating on FITC-positive cells via flow cytometry. Whether the process of coupling of FITC-ova onto the beads has been successful was verified by screening them for their FITC-positivity before using them (Fig. 13).

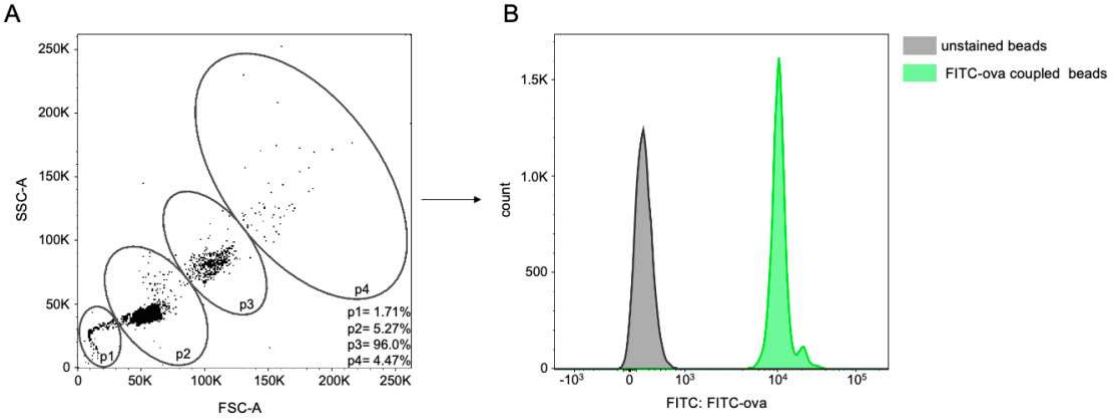

Fig. 13: Verification of successful FITC-ova coupling to latex beads used for the phagocytosis assay.
Samples were measured using a BD FACS Canto II and subsequently analysed by FlowJo 10.5.3. Displayed is one sample of beads in forward and sideward scatter, indicating different bead-populations (p1-4). Percentages indicate the frequencies contained in the gated areas, with one major population (p3) containing 96% of the beads (A). Shown is a histogram overlay of one exemplary sample consisting of beads before (FITC-negative grey graph) and after (FITC-positive green graph) the coupling process (B). FSC = forward scatter, SSC = side scatter, FITC = fluorescein isothiocyanate, ova = ovalbumin

Successful phagocytosis was approved by measuring the percentage of FITC$^+$ cells as an indirect sign of bead uptake. FITC-positivity of the cells due to beads sticking on the cell surface was prevented by quenching the fluorescent background. This was achieved by splitting of the samples and adding trypan blue into every half of each sample directly before the measurement with the FACS machine was conducted. Fig. 14A shows the gating strategy of the pre-sorted BMDCs for cells, live and single cells as well as FITC-positivity. Fig. 14B depicts the effect of the quenching with trypan blue. A sample with solely FITC-ova coupled beads without BMDCs works as a control. Initially, 99.9% of the particles within this probe are confirmed as FITC$^+$, after the add-on of trypan blue the detection aof FITC$^+$ particles has vanished almost completely.

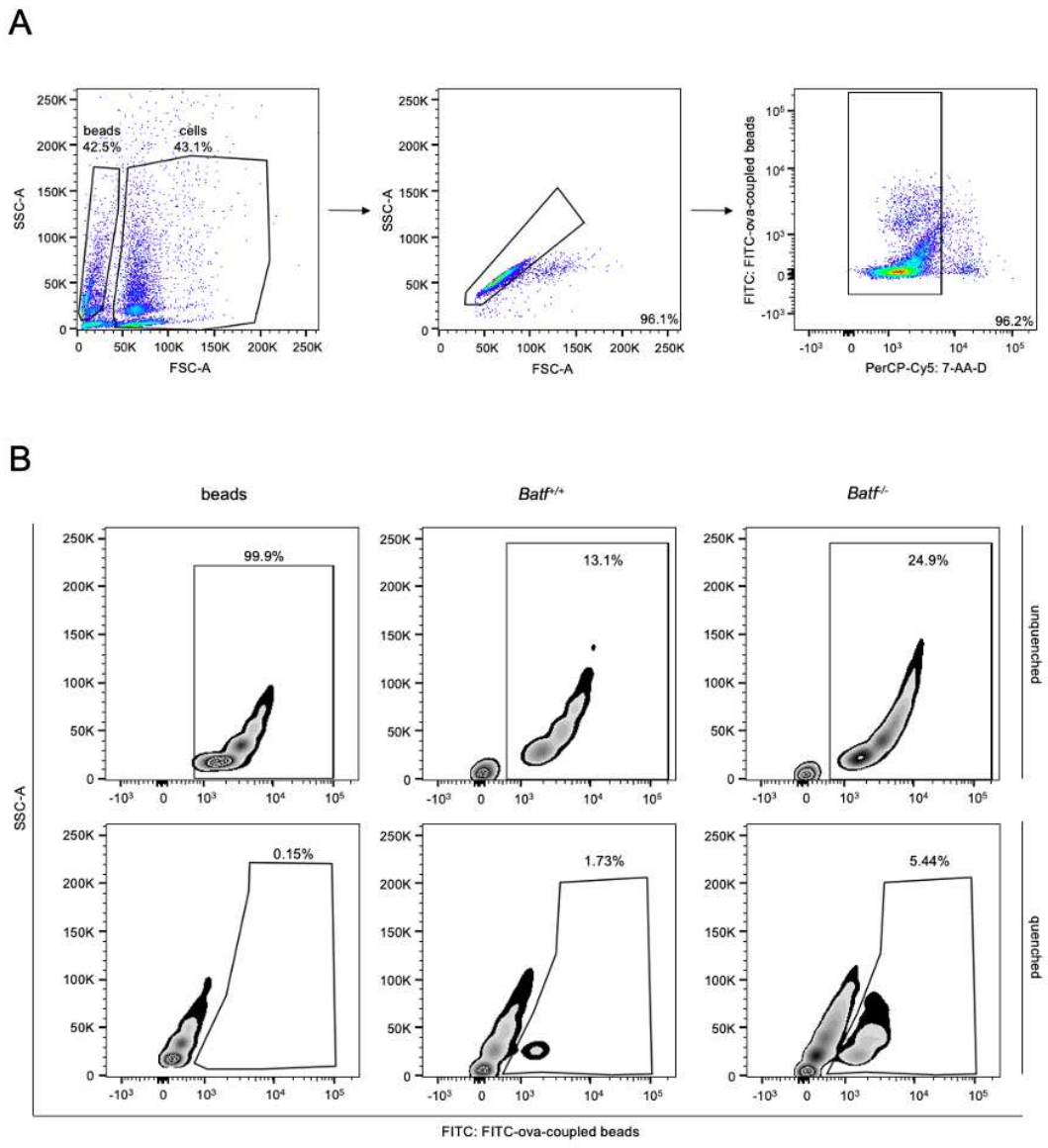

Fig. 14: Gating strategy for the phagocytosis assay.

Samples were measured using a BD FACS Canto II and subsequently analyzed by FlowJo 10.5.3. Pre-sorted pDCs ($CD3^-$ $CD19^-$ $CD11c^+$ $CD11b^{low}$ $B220^+$ $SiglecH^+$ $CD317^+$) and cDCs ($CD3^-$ $CD19^-$ $CD11c^+$ $CD11b^+$ $B220^-$) were co-cultured with FITC-ova coupled beads. Subsequently the samples were divided: one half was measured without further add-on, the other half analysed after trypan blue was added. The initial gating differentiated cells from beads (A). Next, single cells and live cells were identified. The final read-out for the assay were FITC-positive cells within this pre-gated group as displayed (B). The upper alignment shows the final read-out of an exemplary sample before quenching for a WT and a KO sample as well as a control sample consisting of only beads without BMDCs. The lower alignment shows the matching quenched samples. FITC-measurement of the bead-sample served as a control of the quenching process (left two pictures). Percentages indicate the frequencies of the parental populations. FSC = forward scatter, SSC = side scatter, FITC = fluorescein isothiocyanate, ova = ovalbumin

3.3.2.1 BATF acts as a negative regulator in phagocytosis of pDCs

The impact of BATF on phagocytosis was tested by co-culturing pre-sorted pDCs and cDCs with FITC-ova coated latex beads at a ratio of 1:10 for 1 h at 37°C. The uptake process was stopped by adding ice-cold PBS after the incubation period. Samples exposed to cytochalasin D, an actin polymerization inhibitor, served as negatives controls. A significant higher capacity of particulate antigen uptake was detected for both, naïve and stimulated pDCs, in *Batf*-deficiency ($FITC^+$ cells KO vs WT: 4.48% vs 1.14% in naïve pDCs, 4.14% vs 1.73% in stimulated pDCs) (Fig. 15A). This outcome was also presented by stimulated cDCs ($FITC^+$ cells KO vs WT: 6.42% vs 3.51%) (Fig. 15B). In naïve cDCs *Batf*-deficiency did not show a significant difference in antigen uptake ($FITC^+$ cells KO vs WT: 17.11% vs 15.04%) (Fig. 15B). Strikingly, CpG stimulation had a significantly inhibitory effect in cDCs ($FITC^+$ cells naïve vs stimulated: 15.04% vs 3.51% in WT, 17.11% vs 6.42% in KO) and BATF WT pDCs ($FITC^+$ cells naïve vs stimulated: 1.14% vs 1.73% in WT) in phagocytosis (Fig. 15A, B). Only BATF KO pDCs did not show a relevant decrease of their uptake capacity due to stimulation ($FITC^+$ cells naïve vs stimulated: 4.48% vs 4.14%) (Fig. 15A). These results identify BATF as a suppressor of phagocytosis.

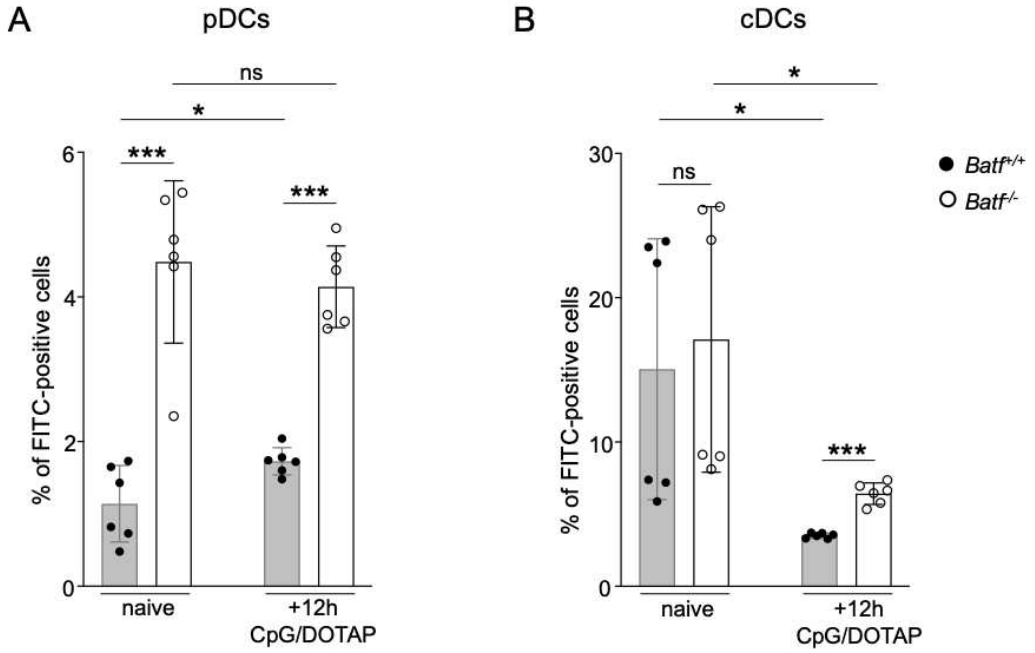

Fig. 15: Uptake-capacity particulate antigens (FITC-ova coated beads) in pDCs.
Flt3-L cultured cells were pre-sorted in pDCs ($CD3^-$ $CD19^-$ $CD11c^+$ $CD11b^{low}$ $B220^+$ $SiglecH^+$ $CD317^+$) and cDCs ($CD3^-$ $CD19^-$ $CD11c^+$ $CD11b^+$ $B220^-$). Cells were either left untreated or stimulated with CpG and DOTAP for 12h before the assay. They were subsequently co-cultured with the prepared beads for 1h at 37°C and 10 % CO2. Corresponding controls treated with cytochalasin D were prepared under the same conditions. Samples were analysed via flow cytometry for FITC-positive cells. Half of the samples were completed with trypan blue for quenching of extracellular fluorescence of beads. Displayed is the uptake capacity of (A) pDCs and (B) cDCs (naïve and stimulated). Macrophages served as a control. The results are depicted as mean ± SD of n = 6 biological replicates per group pooled out of two independent experiments. Statistical significance (P) is represented as: *P ≤ 0.05; **P ≤ 0.01; ***P ≤ 0.001. pDCs = plasmacytoid dendritic cells, cDCs = classical dendritic cells

3.3.2.2 Phagocytosis of particulate antigen by pDCs can be verified by confocal microscopy

To confirm the presence of the beads inside the cells instead of the cell surface, confocal microscopy for z-stack recording was conducted. For this purpose, small subsets of the samples used for the phagocytosis assay (see sections 2.2.5.3, 3.3.2.1) were suspended in PBS (1% PFA) and filled into U-slides for microscopy. Microscopy data (Fig. 16) reinforces that the beads were not simply sticking onto the cell surface but were completely ingested into the cells.

The microscopic verification of the actual bead ingestion together with the significantly higher antigen uptake rate (see section 3.3.2.1) in a *Batf*-dependent manner may provide an explanatory approach to BATF being a negative regulator of ACP in pDCs. This

suggests BATF as relevant factor determining the internalization of antigen which paves the way for efficient ACP.

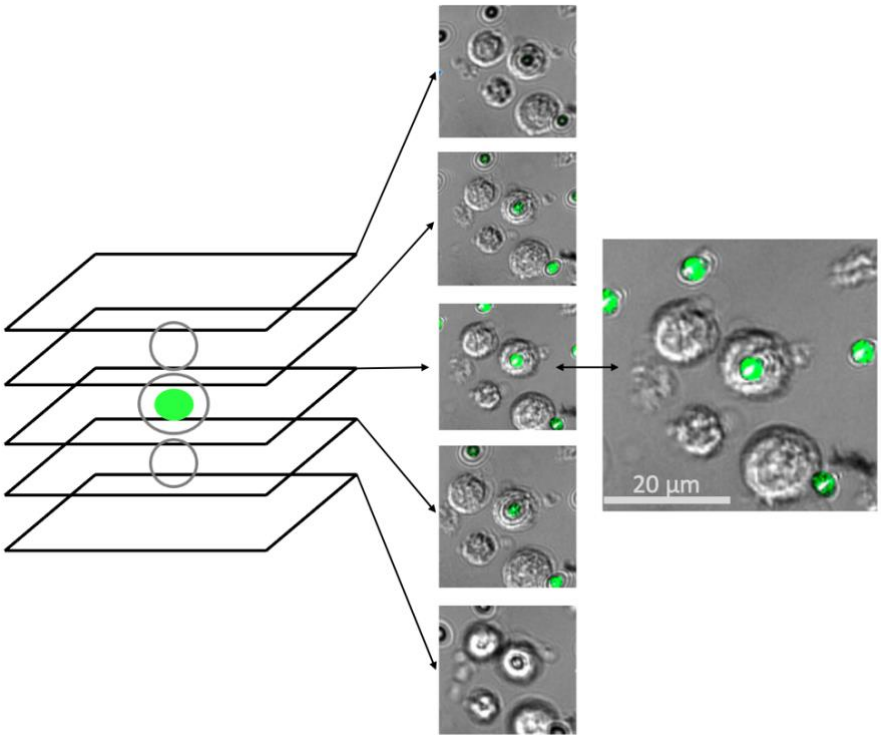

Fig. 16: Z-stack imaging.
Depicted is an image series of a stimulated (12h CpG) pDC after 1h of co-culture with FITC-ova coated latex bedas (ratio cells:beads = 1:10). Displayed is a successful ingestion of one single bead into a pDC. Z-stack images were collected at 1.6µm steps (not all slices shown) by confocal laser scanning microscopy. Green colour corresponds to the FITC-emitted fluorescence measured in the eGFP-channel (490-553nm).

3.4 Influence of BATF on MHC I expression of pDCs at steady state and after activation

Regarding our main finding, that *Batf*-deficiency leads to an increased cross-presentation capacity in pDCs, we wanted to further investigate the underlying mechanism behind this effect. Firstly, we looked at antigen uptake. Here, a significant higher rate of exogenous antigen was ingested by *Batf*-deficient pDCs. Next, we wanted to explore the presentation-step of these processed antigen of pDCs to $CD8^+$ T cells. Therefore, again the significance of expression level differences (see section 3.1) this time of mouse MHC class I genes were investigated ($Batf^{+/+}$ and $Batf^{-/-}$ pDCs at steady state or after CpG stimulation at 6 h, 12 h). Genes with a *p*-value of <0.05 corrected for the false discovery rate (FDR) were considered significantly differentially expressed.

Once more, the expression differences of selected genes were verified by RT-PCR as described before. In addition, the expression of MHC I molecules on *Batf*$^{+/+}$ or *Batf*$^{-/-}$ pDCs at steady state or after CpG stimulation was studied by antibody staining and subsequent FACS-analysis. Interestingly, we documented different results at gene level and at protein level.

3.4.1 BATF is a downregulating factor of MHC I gene expression while upregulating MCH I molecule expression at protein level in pDCs

First, a list of all genes encoding MHC I molecules in Mus musculus (house mouse) were extracted from KEGG genes GenomeNet. The genes expressed in our NGS data set (n = 20) were further analysed. A total of 13 genes showed a significant difference in expression level depending on *Batf*-presence. This number decreased to one single gene after 6h of stimulation and slightly increased again to 4 genes after 12h of stimulation. At steady state, all 13 significantly differentially expressed genes are upregulated in the BATF KO in comparison to the WT, after 6h the one gene shows a downregulation in BATF KO, and after 12h 1 out of 4 genes is downregulated in KO whilst the other 3 genes are upregulated (Fig. 17A).

To study cross-presentation H2-D1 and H2-K1 restricted peptides are commonly used [353]. Therefore, we decided to take a closer look at H2-D1 and H2-K1. The $OVA_{257-264}$ (SINFEKL) peptide derived from ovalbumin used for our cross-presentation assay was H2-K1 ($H2\text{-}K^b$) restricted. In the NGS-analysis both (H2-D1 and H2-K1) showed a significantly higher expression at steady state, the same expression trend was seen under both stimulation conditions (6 h, 12 h). In addition, the expression differences were investigated by RT-PCR. For this purpose, cells were sorted from Flt3-L cultures as described. RNA of these cells was isolated, and cDNA synthesized accordingly followed by RT-PCR. In each gene tested we could see at least the same expression trend as in the NGS dataset, but we were not able to verify a significance between the expression levels between *Batf*-presence and deficiency at steady state ($2^{-\Delta CT}$ WT vs KO H2-D1: 0.15 vs 0.17, H2-K1: 0.17 vs 0.21) (Fig. 17B). After 12 h of stimulation with CpG, H2-D1 showed a significant higher expression in *Batf*-deficiency in the rtPCR ($2^{-\Delta CT}$ WT vs KO H2-D1: 0.10 vs 0.15, H2-K1: 0.13 vs 0.19) (Fig. 17B).

Next, we investigated the expression of MHC I molecules on the cell surface of pDCs. For this purpose, Flt3-L cultures of BMDCs were generated and stimulated as described

before. Stimulation with CpG was performed on day 6 for 12h overnight. On day 7, the cells were harvested and stained accordingly and further distinguished into pDCs and cDCs according to their surface markers (see section 3.3.1 without subdividing cDCs into cDC1/cDC2 subsets) with the addition of a MHC I antibody staining. The mean fluorescent intensities (MFI) of the MHC I stainings were analysed by FACS. At protein level, we initially saw the same trend as in the NGS data and the RT-PCR with a higher MHC I expression at steady state in pDCs (MHC I MFI WT vs KO: 2668.75 vs 2890.12) (Fig. 17C). After 12h of CpG-stimulation, supposed to mimic the physiological processes of viral infection, we made a whole new observation. Strikingly, a significant higher MHC I expression could be recorded in the presence of BATF (MHC I MFI WT vs KO: 5234.5 vs 3179.38) (Fig. 17C). This significant difference is predominantly achieved by a significant upregulation of MHC I molecules on the cell surface in WT pDCs due to stimulation (MHC I MFI WT vs stimulated WT: 2668.75 vs 5234.5). Since one reason might have been that the MHC I molecules simply had not yet reached the cell surface after the 12-hour stimulation period and were still intracellular, we generated preliminary data for intracellular MHC I staining (data not shown). This showed the same expression pattern as the cell surface staining with a higher MHC I expression in the WT after stimulation. The same trend was also seen in cDCs (not shown). This indicates, that in *Batf*-presence the MHC I expression at protein level is upregulated compared to *Batf*-deficency. This upregulation is independent of the cell population (pDCs, cDCs).

In summary, *Batf*-deficiency leads to a higher gene expression of genes encoding the MHC I molecule, especially at steady state in pDCs. After initiation of processes of TLR9 activation this upregulation fades and even turns around at protein level to a significantly diminished MHC I molecule quantity on the cell surface (and most likely also a diminished intracellular MHC I supply) in *Batf*-deficiency.

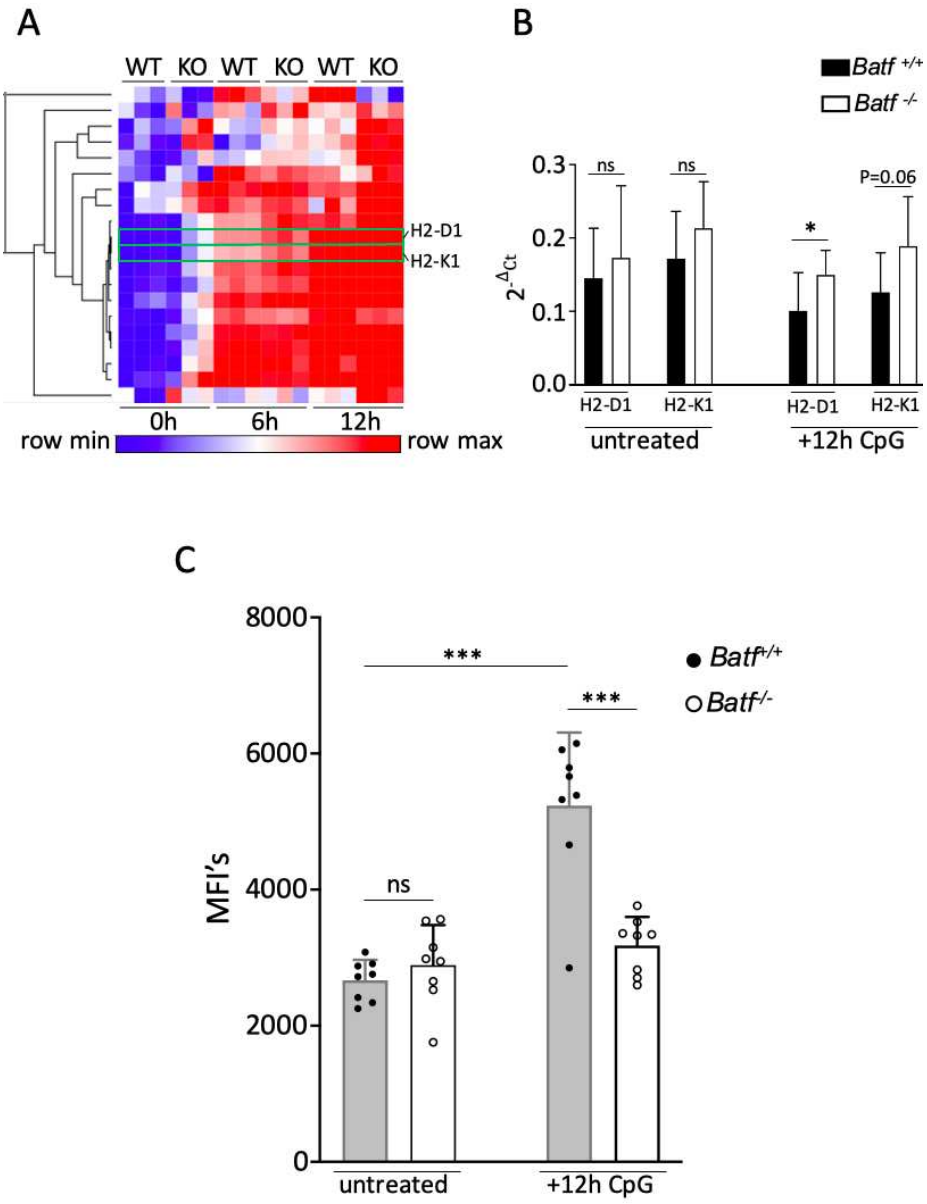

Fig. 17: RNA-Seq reveals significant gene expression differences in BATF WT in comparison to KO.
Heatmap showing the normalized expression values (cpm, count per million) of the selected genes in pDCs at steady state and after 6 h and 12 h of CpG stimulation. Hierarchical clustering on rows with average linkage and the ONE minus Pearson correlation metric was performed (A). Bar charts depicting RT-PCR results of H2-D1 and H2-K1 expression in *Batf*$^{+/+}$ and *Batf*$^{-/-}$. Shown is the $2^{-\Delta Ct}$ of the mean ±SD of two pooled independent experiments of four biological replicates (n=8) in each experiment (naïve and stimulated) of the gene in focus and ß-actin (serving as a reference gene). The mean value of three technical replicates of each biological replicate was used for calculations (B). Data are representative for two pooled independent experiments and are represented as MFI and represent the mean ± SD of *n* = 4 biological replicates per experiment (C). Bar charts depicting Statistical significance (P) is represented as: *P ≤ 0.05; **P ≤ 0.01; ***P ≤ 0.001. MFI = mean fluorescent intensity

4. Discussion

The identification of factors steering ACP and an understanding of how these factors control the process in detail is needed as it may provide promising targets for the use of immunotherapies in cancer and other autoimmune diseases. In this thesis the yet unknown impact of BATF on the process of ACP in pDCs was characterized. With the data of gene expression (RNA-Seq) in naïve and (TLR9) activated murine BATF WT vs BATF KO pDCs in a time course study the expression pattern of a specific set of genes known to be relevant in ACP was analysed. ACP, antigen uptake and MHC I expression in pDCs were investigated in detail to reveal the actual impact of a detected BATF-dependent expression dysregulation in this gene set. Hereby, I was able to identify BATF as a critical factor deciding over ACP ability in pDCs. The respective results are discussed in the following sections.

4.1 The standing of pDCs regarding antigen cross-presentation

ACP describes the process, where exogenous antigen is routed for presentation on MHC I molecules. It lays the foundation for cytotoxic $CD8^+$ T cell responses against tumours and infections, where APCs are not directly infected themselves. Although many cells can present extracellular antigen on MHC I, DCs are known as the most relevant ACPCs. However, we do know that within the population of DCs there are distinct differences between the subpopulations (cDC1, cDC2 and pDCs) regarding their efficiency in ACP. While cDCs1 are known as the masters of cross-presentation [228], it is generally accepted that cDCs2 can cross-present antigen as well [151, 363]. Only pDCs take on the role of the underdog since their ACP capacity and even their ability to do so at all are under debate to this day [364]. Against this background, the key question that must be asked once more at the beginning is the actual capability of pDCs to conduct ACP. In the conducted experiments, a distinct IFNγ expression was measured in $CD8^+$ T cells after co-culture with pDCs that previously were exposed to infected feeder cells. The results were additionally strengthened by an intraexperimental verification by using two different T cell lines. Thereby, I could show, that pDCs attain the ability to successfully conduct ACP.

In vitro both, murine and human pDCs, have been reported to be able to cross-present antigen [147-149, 365]. However, *in vivo* multiple studies have suggested that pDCs are not involved in cross-priming [141, 144, 366] while others showed the opposite [151,

367]. The relevance of forming a deeper understanding on ACP in pDCs is becoming more and more important as pDCs are further identified with crucial roles among others in different malignancies [368, 369] and are an emerging focus as therapy target [370]. Nevertheless, extensive research on ACP in pDCs is lacking. Taking a closer look to common experimental setups investigating ACP, pDCs are oftentimes externally stimulated with a TLR agonist and co-cultured with polystyrene microspheres mimicking exogenous antigen to investigate cross-presentation [365]. However, this is a very artificial attempt reconstructing the environment in which ACP actually takes place. Here, we show an *in vitro* but as close to life as possible designed assay. This was achieved by using MVA-infected MHC I mismatched feeder cells unable to directly present antigen to T cells. It provides a much more physiological context than simply adding beads to additionally activated pDCs. Moreover, PUVA treatment of infected feeder cells prevented false-positive results caused by directly antigen presenting pDCs accidentally infected with input virus. Finally, by pre-sorting the DCs the assay was run specifically testing pDCs ruling out a potential bias due to interactions with other cells.

In vitro the ability of pDCs to conduct ACP is strictly dependent on their activation status and is reserved to activated pDCs. Resting (splenic) mouse pDCs are unable to cross-present. The activation of pDCs can be induced by exposing them to TLR9 agonists, but also an activation brought about by viral contact leads to cross-priming of naïve CD8+ T cells [151]. In this thesis the ACP assay was generally conducted with virus. I was able confirm that viral activation licenses pDCs to conduct ACP. However, no statement regarding the ACP ability of pDCs at steady state can be made. How decisive the fact is that pDCs are only enabled to conduct ACP after activation remains to be seen, since ACP is not an isolated process and is subject to other influences. Nevertheless, sparing out pDCs at steady state came with the advantage that the amplification of a further stimulation could be objectified. A significant enhancement of ACP capacity could be measured in both T cell lines. This suggests, that pDCs which are already empowered to conduct ACP in any way, can be significantly enhanced in their performance level. Finding ways to regulate ACP in pDCs in a controlled manner will contribute to finding new therapy strategies using pDCs as target.

Another fact, that should not go unnoticed regarding pDCs as professional IFN I producing cells, is that IFN I is also known to contribute to ACP [213, 214]. Multiple cells of the immune system (B cells, cDCs, natural killer cells and T cells) are activated and recruited by pDCs and indirectly regulate $CD8^+$ T cell priming by IFN I production [371]. Whether the results attained in the context of pDCs and $CD8^+$ T cell activation are due

to antigen presentation by pDCs or for example due to IFN I mediated activation of cDCs remains unclear in some experimental setups [372]. In the presented ACP assay, we tried to rule this fact out by pre-sorting the pDCs and entering the assay isolated. Still, there is ambiguity as to what constitutes the capability of pDCs to cross-present antigen and what is simply adulteration of the results due to other activated pathways.

4.2 BATF as a game changer in antigen cross-presenting pDCs

Since we observed an increase in numbers of pDCs at the expense of the cDC1 subset in *Batf*-deficiency we raised the question of a function shift to other DC subsets under *Batf*$^{-/-}$ conditions. *Batf* has been demonstrated to be able to compensate for *Batf3* (the factor that is required for the development of the cDC1 subset) [11]. Based on these data we hypothesized that *Batf* may also have an impact on the functions (cross-presentation in the focus of our report here) usually conducted by the cDC1 subset. For this purpose, IFNγ production of CD8$^+$ T cells was analysed comparing pDCs from BATF WT vs KO mice. In BATF deficiency we registered 10.2% vs 20.8% (WT vs KO) of IFNγ$^+$CD8$^+$ T cells in the ovalbumin specific T cell line. After CpG stimulation the overall amount of IFNγ$^+$CD8$^+$ T cells increased, maintaining a significant difference between those exposed to pDCs originating from WT mice (49.2%) in comparison to those exposed to pDCs originating from KO mice (59.1%). Congruent trends were measured in the B8-specific T cell line, where 6.3% vs 10.7% (WT vs KO) T cells could be distinguished as IFNγ$^+$. After stimulation of pDCs, 39.3% of the T cells who were in contact with pDCs collected from WT mice were IFNγ$^+$ vs 44.3% when the pDCs were collected from KO mice. Hereby, the formed hypothesis was confirmed by identifying BATF as a negative regulator in cross-presentation in pDCs.

One reason for this could be the BATF dependent regulation of the expression of different genes encoding for cross-presentation relevant factors. NGS data adequately supports this hypothesis. A well-studied mechanism controlling the process of cross-presentation is the fine tuning of antigen degradation controlled by the phagosomal pH. cDCs have been reported to steer this via a ROS dependent consumption of protons, which is stimulated by a Rab27a dependent recruitment of NOX2 to the phagosomes [265]. In line with this, *Batf*-deficient pDCs presented a significant upregulation for the gene encoding for NOX2 (*Cybb*) at steady state. After stimulation (6 h) we observed a significant downregulation within the BATF KO pDCs. Another critical factor determining subcellular NOX2 assembly is *Rac2* [269]. *Rac2* showed a significant higher gene

expression in pDCs derived from BATF KO mice independent of their activation status and could additionally be confirmed after stimulation with rtPCR. Another TF, namely TFEB, has also been identified to play a crucial role in the presentation of exogenous antigens. TFEB promotes antigen degradation by phagosomal acidification [262]. *Tfeb* stood out by a significant downregulation in Batf-deficiency in pDCs at steady state and a significant upregulation after stimulation. In conclusion, BATF seems to act as a molecular switch regarding phagosomal pH regulation in pDCs. This potentially explains its impact on the cross-presentation process since it has just recently been shown that the mechanism of antigen protection through alkalization of the phagosomal pH is a crucial in pDCs [365]. Other players who received a lot of attention in the context of cross-presentation are HSPs. HSP transcription is a stress induced process in cells, and they are especially studied for their role of cytosolic translocation of internalized antigens. HSP90, one of the most thoroughly investigated candidates, has been demonstrated to play a crucial role within this process among others by un- and refolding of antigen. Immunization with Hsp90-complexes even induced Ag-specific $CD8^+$ T cell responses as well as strong antitumor immunity in vivo [237, 279, 373]. Structurally this protein is a dimer with monomer subunits. The two isoforms present in the cytoplasm are HSP90α and HSP90β [374]. Both are encoded by different genes, HSP90α by *Hsp90aa1* and HSP90β by *Hsp90ab1* respectively. Strikingly, both showed a significant lower expression after pDC activation in *Batf*-deficiency. The same result could be observed for HSP70. HSP70 has been reported to show different characteristics in the context of cross-presentation. On the one hand it was reported as a down regulator of antigen translocation [375], on the other hand it strongly enhanced cross-presentation in multiple antigen presenting cells [347]. In summary, BATF influences multiple factors determining antigen processing. Rapid antigen degradation is considered to be inhibiting in the process of ACP [259-261], possibly explaining a downregulation in BATF KO of some genes (for example Hsp90aa1, Hsp90ab1, Hspa1b) that are rather encoding for factors enhancing ACP. This suggests BATF as determining factor in the fine-tuning of antigen degradation.

Together with the previously discussed results regarding phagosomal pH regulation this might suggest that BATF influences rather the vacuolar than in the cytosolic pathway in cross-presentation in pDCs. Since the vacuolar pathway is reported to be independent of cytosolic proteasomal degradation of polypeptides [376] this may explain the unexpected expression patterns for the HSPs. Another critical issue regardless of the processing pathway is the transportation of antigen and recycling parts within the cell. Concerning this matter, an interesting candidate is the family of Rab GTPases, which

basically organize almost all membrane trafficking within eukaryotic cells [377, 378]. Taking a closer look at available literature, many of these have already been studied specifically in cross-presentation and could be identified as crucial players (*Rab3c*, *Rab14*, *Rab43*, *Rab22a*) facilitating the process [289, 297, 379, 380]. With our NGS data we were able to identify significant differences in expression levels for some of them depending on BATF presence. Strikingly, most of them (*Rab14*, *Rab22a*, *Rab43*) showed a significant downregulation after stimulation in pDCs in *Batf*-deficieny wiping out an explanation for the higher cross-presentation rate within this condition. Thus, regarding antigen processing the emerged gene expression patterns mostly indicate that BATF influences the cross-presenting capacity of pDCs by fine tuning the degrading conditions within phagosomes. Stating this also brings IRAP into focus. IRAP is responsible for trimming of epitope precursors to be presented emerged from phagosomal protease degradation. IRAP is encoded by *Lnpep*, which showed a significant downregulation in *Batf*-deficient pDCs after stimulation (6 h, 12 h). This suggests a protective environment bypassing extensive antigen unbundling thus facilitating cross-presentation.

Another possible explanation for the impact of BATF in cross-presentation of pDCs might be found by studying cell development and differentiation. Recent studies described transitional pDCs, which are related to both, pDCs and cDCs, being found in the isolated population of pDCs used in functional studies [381, 382]. In addition, scRNA sequencing revealed an overlapping pDC/cDC subset in humans. These cells express some pDC markers but exhibit the functionality of cDCs in priming T and B cells. Further analysis suggested that these cells include intermediate myeloid DC populations with a mixture of pDC and cDC characteristics [383-385]. This raises the question whether cDC functions, especially in the context of antigen presentation, observed for pDCs could be due to contamination of these “cDC-like” cells. At this point, I want to put emphasize on the used gating strategy in this thesis, leading to pure pDC isolation. The identification of pDCs in the Flt3-L cultures was started by gating for $CD3^-$ and $CD19^-$ cells excluding T and B cells. Subsequently, DCs were defined by CD11c-positivity. The first differentiation between cDCs and pDCs was made by gating for $CD11b^{low}$ and $B220^+$ cells, B220 representing the first surface marker characterizing pDCs. The $CD11b^{low}B220^+$ cells were further screened for SiglecH and CD317 expression, which led to the final identification of $CD3^-$ $CD19^-$ $CD11c^+$ $CD11b^{low}$ $B220^+$ $SiglecH^+$ $CD317^+$ cells (respectively $CD19^-$ $CD11c^+$ $CD11b^{low}$ $B220^+$ $SiglecH^+$ as presented (see section 3.3.1) in endocytosis experiments) as pDCs. It is well studied, that lineage fate decisions of progenitor cells are subject to different transcription factors [66, 82, 128, 131]. The E2-

2 and Id2 axis determines pDC versus cDC1 lineage decision [130, 131]. The presented surface markers chosen to identify pDCs (B220, SiglecH, CD317) are independent of E2-2 and are controlled by Zeb2 [66]. However, a further development of these purified pDCs to pDC/"cDC-like" cells during re-culture with the T cells in the T cell activation assay following the ACP assay cannot be excluded. Although, if this further differentiation would have happened in BATF KO pDCs explaining their higher ACP potential, it would assign an additional function to BATF in pDCs.

Further complicating this issue, Alculumbre et al. showed that *in vitro* activated canonical pDCs also give rise to distinct populations. These pDC populations mainly differed in function either being characterized by IFN I production or by antigen-presenting functions [386]. Regarding our results this may suggest a critical role for BATF in cell fate in the development of DCs ultimately deciding over their cross-presenting capability. The involvement of BATF in pDCs function is further supported by the recently published results of our working group. Here, the AP-1 family of TFs was defined as potentially important player after pDC activation due to an increased gene expression, an enhanced chromatin accessibility in their promoter region as well as a globally enriched TF DNA binding motif in genomic region exhibited by their members in pDCs after activation [4].

Taking a closer look at the roles of pDCs in cancer, there seems to be a correlation between prognosis and enrichment of pDCs in the tumor [368, 387, 388] supporting the idea that pDCs play a suppressive function in these tumors. Indeed, activated pDCs can induce anti-tumor immunogenic responses and several clinical trials show promising results suggesting pDCs to be a useful tool for the induction of anti-tumor immunity [160, 369, 370, 389]. BATF on the other hand, which we identified as a negative regulator in the context of cross-presentation within our study, seems to act the other way around. High expressions of BATF seem to correlate with cell proliferation in NSCLC [40] and a significantly lower survival rate in acute myeloid leukemia [39]. This suggests that enriching tumor sites with pDCs might have influence on tumor growth behavior. Silencing *Batf* via targeted therapy may protect the functionality of pDCs within this context. Significant progress is being made concerning TFs as targets for therapeutic purposes [390, 391]. The shown impact of BATF on cross-presentation in pDCs together with the knowledge gained by the in silico analyses of the global TF reservoir in pDCs after activation conducted by our working group identifies BATF as a possibly interesting target for further investigations regarding its role in tumor biology and immune responses (with emphasis on cross-presentation) in pDCs. This may lead to the identification of new points of action for the treatment of cancer, infection and autoimmune diseases.

4.3 Antigen uptake suppression regulated by BATF in pDCs

Multiple features are responsible for the efficacy of cDCs in the context of antigen cross-presentation, one of them being their endocytic activity. It is commonly known that pDCs do not share the same endocytic capability with cDCs, but pDCs have been reported to be capable of both, the uptake of soluble as well as particulate antigen [140]. Particles captured via fluid phase pinocytosis are generally cross-presented very poorly while an internalization by an actin-dependent process like phagocytosis show a higher efficacy in cross-presentation [362]. In an experimental setup using soluble FITC-Ova we saw a time-dependent manner of pinocytosis in all cell subsets (pDCs, cDC1, cDC2). BATF did not seem to have any significant impact after stimulation within these cells, at steady state WT pDCs showed a significantly higher uptake rate as compared to BATF KO pDCs. Looking at phagocytosis of beads, we detected a significantly higher capturing rate in *Batf*-deficiency in pDCs at steady state ($FITC^+$ cells KO vs WT: 4.48% vs 1.14%) as well as after stimulation (4.14% vs 1.73%). In cDCs we only measured a significant higher rate of internalized beads after stimulation of the cells comparing BATF KO and WT ($FITC^+$ cells KO vs WT: 6.42% vs 3.51%). In pDCs this observation of an increased antigen uptake rate could have been used as an attempt to explain the results generated in the cross-presentation assay. A higher capturing rate of exogenous antigen would simply lead to a higher cross-presentation capacity. This consideration, to some degree, might still be true. But stimulated cDCs also captured significantly more polystyrene microspheres in *Batf*-deficiency. This is non congruent with the results we obtained in the cross-presentation assay, where cDCs showed significantly lower cross-presenting skills in *Batf*-deficiency measured in the B8-specific T cell line (and the same trend emerged in the OVA-specific T cell line). However, no discrimination between the cDC1 and cDC2 subset was made, neither in the ACP assay nor in the phagocytosis assay. The lower frequencies of cDC1 in *Batf*-defiency may explain the lower efficiency in ACP of the cDC subset in BATF KO. ACP relies on cDC1 to be present as efficient ACPCs. In the context of antigen uptake, the task can be compensated by cDC2.

The uptake of exogenous antigen for cross-presentation is subject to cell surface receptors which target the endocytosed particles to different subcellular compartments that determine their further fate [245, 246]. Especially delivery via C-type lectin receptors (Clec4a, Clec9a, Clec12a) and others (DC-SIGN, DEC-205) enhanced specific $CD8^+$ T cell responses [247, 248, 254, 255, 257]. Strikingly, all of these showed a significant downregulation at some investigation time point (naïve; stimulation with CpG).

Collectively, the incongruency of capturing and cross-presenting rate in cDCs together with the persistent downregulation of trendsetting receptors for endocytosed antigen, suggests other explanations than uptake capacity alone explaining the observed impact of BATF on cross-presentation in pDCs.

4.4 The influence of BATF on MHC I traffic and recycling

Finally, in trying to find the cause for a significant BATF regulated increase of cross-presentation capacity in pDCs, we wanted to investigate the behavior of MHC I expression in dependency of BATF. Gene expression patterns unraveled the trend of upregulated genes in *Batf*-deficiency with a bigger impact in naïve cells that diminished with cell stimulation. With emphasis on H2-D1 and H2-K1 (the latter responsible for the cross-presentation of our two tested epitopes B8 and OVA) a significant difference with a higher expression of both genes in *Batf*-deficiency in the NGS data was only measured at steady state. This could be confirmed by RT-PCR for H2-D1 and the same trend was observed in H2-K1. Nex, we wanted to validate this expression pattern at protein level using FACS analysis after corresponding antibody staining. Surprisingly, MHC I expression at the cell surface showed the exact opposite expression pattern with a significantly lower amount of MHC I molecules present in pDCs derived from BATF KO mice.

MHC I molecules need to be present at the final loading site of peptides. Respectively, this would be the ER or the phagosome considering the two main pathways of antigen processing in cross-presentation [227]. But we also need to understand where these MHC I molecules originate from. One of the possibilities that MHC I get into endosomes and phagosomes for peptide loading is by trafficking from the cell surface [300]. MHC I traffic is suggested to be particularly important in the vacuolar pathway of antigen cross-presentation [284]. Since we hypothesized before about BATF influencing cross-presentation by interfering in the vacuolar pathway, we took MHC I recycling as explanation for the reduced MHC I surface expression. With regard to studies that show the impact of time concerning sub-processes of cross-presentation [61], we claimed to simply have missed the higher amount of MHC I molecules since they have mostly been transported to the loading sites at the timepoint of antibody staining. To rule out misinterpretation of the result we added an intracellular staining which was supposed to reveal the intracellular MHC I molecules. Unfortunately, it did not. MHC I transport to endosomal vesicles is described as a *Rab11a*-dependent mechanism [284]. *Rab11a*

also did not show any upregulation at gene level, supporting the fact that a reduction of MHC I molecules at the cell surface due to transport to recycling or loading compartments is unlikely. Also remarkable is the fact, that CpG stimulation did not lead to an upregulation of MHC I expression on RNA level in neither gene (encoding for H2-D1 or H2-K1) or genotype (BATF WT, KO) tested. The same is seen on protein level, except for MHC I protein expression level on BATF WT pDC surface. In BATF deficient activated pDCs MHC I molecules seem to undergo a recycling process as efficiently as in unstimulated WT pDCs. With a glance to the higher ACP capacity of BATF KO pDCs, this suggests a Rab11a-independent recycling process in BATF deficient pDCs triggered by their activation. This recycling process may damage the epitope recognized by the antibody used to stain the MHC I molecules. Damaged epitopes due to intracellular recycling could be the reason for the impaired ICS of MHC I molecules in this experiment. This suggests a higher intracellular MHC I molecule number, which was not detectable by the antibody, supporting the enhanced ACP capacity.

4.5 Conclusion

Taken together, the data presented in this thesis verifies the ACP capability of pDCs, which can be further enhanced by pDC maturation via activation. BATF is a crucial negative regulator of ACP in pDCs. By coordinating the expression of multiple genes, it dampens the antigen capturing rate of exogenous antigen in pDCs. This thesis positions BATF for the first time as a critical suppressor of ACP in pDCs. Manipulating the expression or functions of BATF in pDCs may provide new therapeutic options for the treatment of cancer and virus infections.

4.6 Outlook

With BATF as a newfound regulator of ACP in pDCs, further research is needed to establish the exact processes and target points used by BATF to exert its influence. We lack a better understanding of the actual impact BATF has on antigen processing as well as peptide loading and presentation via MHC I molecules, yet. In addition, figuring out how BATF related changes in IFN I production may engage in enhancing ACP in pDCs could lead to a completely new understanding of the interplay of IFN I, ACP and BATF. Unraveling these processes may lead to the discovery of new targets for the development of novel therapeutics. With a glance to antitumor immunity, where so-called personalized targeted therapies have been booming within the last years revolutionizing

the field of oncological therapy options, BATF seems to be promising candidate for future research.

4.7 References

1. Dorsey, M., *B-ATF- a novel human bZIP protein that associates with members of the AP-1 transcription factor family.* Oncogene, 1995.

2. Williams, K.L., et al., *Characterization of murine BATF: a negative regulator of activator protein-1 activity in the thymus.* Eur J Immunol, 2001. **31**(5): p. 1620-7.

3. Murphy, T.L., R. Tussiwand, and K.M. Murphy, *Specificity through cooperation: BATF-IRF interactions control immune-regulatory networks.* Nat Rev Immunol, 2013. **13**(7): p. 499-509.

4. Mann-Nuttel, R., et al., *The transcription factor reservoir and chromatin landscape in activated plasmacytoid dendritic cells.* BMC Genom Data, 2021. **22**(1): p. 37.

5. Bader A.G., V.P.K., *Leucine Zipper Transcription Factors- bZIP Proteins.* Encyclopedic Reference of Genomics and Proteomics in Molecular Medicine, 2006.

6. Vogt, P.K. and T.J. Bos, *jun:Oncogene and Transcription Factor*. 1990. p. 1-35.

7. Hai, T. and T. Curran, *Cross-family dimerization of transcription factors Fos/Jun and ATF/CREB alters DNA binding specificity.* Proc Natl Acad Sci U S A, 1991. **88**(9): p. 3720-4.

8. Echlin, *B-ATF functions as a negative regulator of AP-1 mediated transcription and blocks cellular transformation by Ras and Fos.* 2000.

9. Ebright, J.R., M.R. Fairfax, and J.A. Vazquez, *Trichosporon asahii, a non-Candida yeast that caused fatal septic shock in a patient without cancer or neutropenia.* Clinical Infectious Diseases, 2001. **33**(5): p. E28-E30.

10. Li, P., et al., *BATF-JUN is critical for IRF4-mediated transcription in T cells.* Nature, 2012. **490**(7421): p. 543-6.

11. Tussiwand, R., et al., *Compensatory dendritic cell development mediated by BATF-IRF interactions.* Nature, 2012. **490**(7421): p. 502-7.

12. Su, Z.Z., et al., *Cloning and characterization of SARI (suppressor of AP-1, regulated by IFN).* Proc Natl Acad Sci U S A, 2008. **105**(52): p. 20906-11.

13. Hildner, K., et al., *Batf3 deficiency reveals a critical role for CD8alpha+ dendritic cells in cytotoxic T cell immunity.* Science, 2008. **322**(5904): p. 1097-100.

14. Mashayekhi, M., *CD8α(+) dendritic cells are the critical source of interleukin-12 that controls acute infection by Toxoplasma gondii tachyzoites.* 2011.

15. Korn, T., et al., *IL-17 and Th17 Cells.* Annu Rev Immunol, 2009. **27**: p. 485-517.

16. Schraml, B.U., et al., *The AP-1 transcription factor Batf controls T(H)17 differentiation.* Nature, 2009. **460**(7253): p. 405-9.

17. Betz, B.C., et al., *Batf coordinates multiple aspects of B and T cell function required for normal antibody responses.* J Exp Med, 2010. **207**(5): p. 933-42.

18. Jabeen, R., et al., *Th9 cell development requires a BATF-regulated transcriptional network.* J Clin Invest, 2013. **123**(11): p. 4641-53.

19. Ciofani, M., et al., *A validated regulatory network for Th17 cell specification.* Cell, 2012. **151**(2): p. 289-303.

20. Pham, D., et al., *Batf Pioneers the Reorganization of Chromatin in Developing Effector T Cells via Ets1-Dependent Recruitment of Ctcf.* Cell Rep, 2019. **29**(5): p. 1203-1220 e7.

21. Yu, K. and M.R. Lieber, *Current insights into the mechanism of mammalian immunoglobulin class switch recombination.* Crit Rev Biochem Mol Biol, 2019. **54**(4): p. 333-351.

22. Ise, W., et al., *The transcription factor BATF controls the global regulators of class-switch recombination in both B cells and T cells.* Nat Immunol, 2011. **12**(6): p. 536-43.

23. Nurieva, R.I., et al., *Bcl6 mediates the development of T follicular helper cells.* Science, 2009. **325**(5943): p. 1001-5.

24. Yu, D., et al., *The transcriptional repressor Bcl-6 directs T follicular helper cell lineage commitment.* Immunity, 2009. **31**(3): p. 457-68.

25. Bauquet, A.T., et al., *The costimulatory molecule ICOS regulates the expression of c-Maf and IL-21 in the development of follicular T helper cells and TH-17 cells.* Nat Immunol, 2009. **10**(2): p. 167-75.

26. Morman, R.E., et al., *BATF regulates the expression of Nfil3, Wnt10a and miR155hg for efficient induction of antibody class switch recombination in mice.* Eur J Immunol, 2018. **48**(9): p. 1492-1505.

27. Kurachi, M., et al., *The transcription factor BATF operates as an essential differentiation checkpoint in early effector CD8+ T cells.* Nat Immunol, 2014. **15**(4): p. 373-83.

28. Grusdat, M., et al., *IRF4 and BATF are critical for CD8(+) T-cell function following infection with LCMV.* Cell Death Differ, 2014. **21**(7): p. 1050-60.

29. Mjosberg, J.M., et al., *Human IL-25- and IL-33-responsive type 2 innate lymphoid cells are defined by expression of CRTH2 and CD161.* Nat Immunol, 2011. **12**(11): p. 1055-62.

30. Huang, Y., et al., *IL-25-responsive, lineage-negative KLRG1(hi) cells are multipotential 'inflammatory' type 2 innate lymphoid cells.* Nat Immunol, 2015. **16**(2): p. 161-9.

31. Miller, M.M., et al., *BATF acts as an essential regulator of IL-25-responsive migratory ILC2 cell fate and function.* Sci Immunol, 2020. **5**(43).

32. Liang, H.E., et al., *Divergent expression patterns of IL-4 and IL-13 define unique functions in allergic immunity.* Nat Immunol, 2011. **13**(1): p. 58-66.

33. Nussbaum, J.C., et al., *Type 2 innate lymphoid cells control eosinophil homeostasis.* Nature, 2013. **502**(7470): p. 245-8.

34. Bao, K., et al., *BATF Modulates the Th2 Locus Control Region and Regulates CD4+ T Cell Fate during Antihelminth Immunity.* J Immunol, 2016. **197**(11): p. 4371-4381.

35. Vogt, P.K., *Fortuitous convergences: the beginnings of JUN.* Nat Rev Cancer, 2002. **2**(6): p. 465-9.

36. Stolz, M.L. and C. McCormick, *The bZIP Proteins of Oncogenic Viruses.* Viruses, 2020. **12**(7).

37. Liao, J., et al., *Batf promotes growth arrest and terminal differentiation of mouse myeloid leukemia cells.* Mol Cancer Res, 2011. **9**(3): p. 350-63.

38. Fry, E.A. and K. Inoue, *c-MYB and DMTF1 in Cancer.* Cancer Invest, 2019. **37**(1): p. 46-65.

39. Zhang, Y. and L. Xiao, *Identification and validation of a prognostic 8-gene signature for acute myeloid leukemia.* Leuk Lymphoma, 2020. **61**(8): p. 1981-1988.

40. Feng, Y., et al., *BATF acts as an oncogene in non-small cell lung cancer.* Oncol Lett, 2020. **19**(1): p. 205-210.

41. Punkenburg, E., et al., *Batf-dependent Th17 cells critically regulate IL-23 driven colitis-associated colon cancer.* Gut, 2016. **65**(7): p. 1139-50.

42. Hildner, K., et al., *Immunopathogenesis of IBD: Batf as a Key Driver of Disease Activity.* Dig Dis, 2016. **34 Suppl 1**: p. 40-7.

43. Ubel, C., et al., *The activating protein 1 transcription factor basic leucine zipper transcription factor, ATF-like (BATF), regulates lymphocyte- and mast cell-driven immune responses in the setting of allergic asthma.* J Allergy Clin Immunol, 2014. **133**(1): p. 198-206 e1-9.

44. Sopel, N., et al., *The transcription factor BATF modulates cytokine-mediated responses in T cells.* Cytokine Growth Factor Rev, 2016. **30**: p. 39-45.

45. Ora, J., et al., *Advances with glucocorticoids in the treatment of asthma: state of the art.* Expert Opin Pharmacother, 2020. **21**(18): p. 2305-2316.

46. Wang, L.Y., et al., *Increased BATF expression is associated with the severity of liver damage in patients with chronic hepatitis B.* Clin Exp Med, 2018. **18**(2): p. 263-272.

47. Zajac, *Viral immune evasion due to persistence of activated T cells without effector function.* 1998.

48. Gallimore, *Induction and exhaustion of lymphocytic choriomeningitis virus-specific cytotoxic T lymphocytes visualized using soluble tetrameric major histocompatibility complex class I-peptide complexes.* 1998.

49. Barber, D.L., et al., *Restoring function in exhausted CD8 T cells during chronic viral infection.* Nature, 2006. **439**(7077): p. 682-7.

50. Blackburn, S.D., et al., *Coregulation of CD8+ T cell exhaustion by multiple inhibitory receptors during chronic viral infection.* Nat Immunol, 2009. **10**(1): p. 29-37.

51. Riley, J.L., *PD-1 signaling in primary T cells.* Immunol Rev, 2009. **229**(1): p. 114-25.

52. Quigley, M., et al., *Transcriptional analysis of HIV-specific CD8+ T cells shows that PD-1 inhibits T cell function by upregulating BATF.* Nat Med, 2010. **16**(10): p. 1147-51.

53. Worbs, T., S.I. Hammerschmidt, and R. Forster, *Dendritic cell migration in health and disease.* Nat Rev Immunol, 2017. **17**(1): p. 30-48.

54. Sadeghzadeh, M., et al., *Dendritic cell therapy in cancer treatment; the state-of-the-art.* Life Sci, 2020. **254**: p. 117580.

55. Barrat, F.J. and L. Su, *A pathogenic role of plasmacytoid dendritic cells in autoimmunity and chronic viral infection.* J Exp Med, 2019. **216**(9): p. 1974-1985.

56. Steinman, R. and Z. Cohn, *Identification of a novel cell type in eripheral lymphoid organs of mice.* The Journal of experimental medicine 1973. **137**.

57. Banchereau, J. and R.M. Steinman, *Dendritic cells and the control of immunity.* Nature, 1998. **392**(6673): p. 245-52.

58. Steinman, R.M. and M.D. Witmer, *Lymphoid dendritic cells are potent stimulators of the primary mixed leukocyte reaction in mice.* Proc Natl Acad Sci U S A, 1978. **75**(10): p. 5132-6.

59. Merad, M., et al., *The dendritic cell lineage: ontogeny and function of dendritic cells and their subsets in the steady state and the inflamed setting.* Annu Rev Immunol, 2013. **31**: p. 563-604.

60. Gottschalk, C., E. Mettke, and C. Kurts, *The Role of Invariant Natural Killer T Cells in Dendritic Cell Licensing, Cross-Priming, and Memory CD8(+) T Cell Generation.* Front Immunol, 2015. **6**: p. 379.

61. Alloatti, A., et al., *Dendritic cell maturation and cross-presentation: timing matters!* Immunological Reviews, 2016. **272**(1): p. 97-108.

62. Guilliams, M., et al., *Dendritic cells, monocytes and macrophages: a unified nomenclature based on ontogeny.* Nat Rev Immunol, 2014. **14**(8): p. 571-8.

63. Guilliams, M., et al., *Unsupervised High-Dimensional Analysis Aligns Dendritic Cells across Tissues and Species.* Immunity, 2016. **45**(3): p. 669-684.

64. Murphy, T.L., et al., *Transcriptional Control of Dendritic Cell Development.* Annu Rev Immunol, 2016. **34**: p. 93-119.

65. Weissman, I.L. and J.A. Shizuru, *The origins of the identification and isolation of hematopoietic stem cells, and their capability to induce donor-specific transplantation tolerance and treat autoimmune diseases.* Blood, 2008. **112**(9): p. 3543-53.

66. Amon, L., et al., *Transcriptional control of dendritic cell development and functions.* Int Rev Cell Mol Biol, 2019. **349**: p. 55-151.

67. Ogawa, M., *Differentiation and proliferation of hematopoietic stem cells.* Blood, 1993. **81**(11): p. 2844-53.

68. Geissmann, F., et al., *Development of monocytes, macrophages, and dendritic cells.* Science, 2010. **327**(5966): p. 656-61.

69. Iwasaki, H. and K. Akashi, *Myeloid lineage commitment from the hematopoietic stem cell.* Immunity, 2007. **26**(6): p. 726-40.

70. Liu, K., et al., *In vivo analysis of dendritic cell development and homeostasis.* Science, 2009. **324**(5925): p. 392-7.

71. Naik, S.H., et al., *Development of plasmacytoid and conventional dendritic cell subtypes from single precursor cells derived in vitro and in vivo.* Nat Immunol, 2007. **8**(11): p. 1217-26.

72. Onai, N., et al., *Identification of clonogenic common Flt3+M-CSFR+ plasmacytoid and conventional dendritic cell progenitors in mouse bone marrow.* Nat Immunol, 2007. **8**(11): p. 1207-16.

73. Fogg, D.K., et al., *A clonogenic bone marrow progenitor specific for macrophages and dendritic cells.* Science, 2006. **311**(5757): p. 83-7.

74. Naik, S.H., et al., *Intrasplenic steady-state dendritic cell precursors that are distinct from monocytes.* Nat Immunol, 2006. **7**(6): p. 663-71.

75. Reizis, B., *Regulation of plasmacytoid dendritic cell development.* Curr Opin Immunol, 2010. **22**(2): p. 206-11.

76. Shortman, K., et al., *Plasmacytoid dendritic cell development.* Adv Immunol, 2013. **120**: p. 105-26.

77. Schraml, B.U. and C. Reis e Sousa, *Defining dendritic cells.* Curr Opin Immunol, 2015. **32**: p. 13-20.

78. Haniffa, M., M. Collin, and F. Ginhoux, *Ontogeny and functional specialization of dendritic cells in human and mouse.* Adv Immunol, 2013. **120**: p. 1-49.

79. Mackarehtschian, K., et al., *Targeted disruption of the flk2/flt3 gene leads to deficiencies in primitive hematopoietic progenitors.* Immunity, 1995. **3**(1): p. 147-61.

80. Lyman, S.D., *Biologic effects and potential clinical applications of Flt3 ligand.* Curr Opin Hematol, 1998. **5**(3): p. 192-6.

81. Karsunky, H., et al., *Flt3 ligand regulates dendritic cell development from Flt3+ lymphoid and myeloid-committed progenitors to Flt3+ dendritic cells in vivo.* J Exp Med, 2003. **198**(2): p. 305-13.

82. Carotta, S., et al., *The transcription factor PU.1 controls dendritic cell development and Flt3 cytokine receptor expression in a dose-dependent manner.* Immunity, 2010. **32**(5): p. 628-41.

83. Brasel, K., et al., *Hematologic effects of flt3 ligand in vivo in mice.* Blood, 1996. **88**(6): p. 2004-12.

84. Mildner, A. and S. Jung, *Development and function of dendritic cell subsets.* Immunity, 2014. **40**(5): p. 642-56.

85. Edelson, B.T., et al., *Peripheral CD103+ dendritic cells form a unified subset developmentally related to CD8alpha+ conventional dendritic cells.* J Exp Med, 2010. **207**(4): p. 823-36.

86. Gurka, S., et al., *Mouse Conventional Dendritic Cells Can be Universally Classified Based on the Mutually Exclusive Expression of XCR1 and SIRPalpha.* Front Immunol, 2015. **6**: p. 35.

87. Caminschi, I., et al., *The dendritic cell subtype-restricted C-type lectin Clec9A is a target for vaccine enhancement.* Blood, 2008. **112**(8): p. 3264-73.

88. Sichien, D., et al., *IRF8 Transcription Factor Controls Survival and Function of Terminally Differentiated Conventional and Plasmacytoid Dendritic Cells, Respectively.* Immunity, 2016. **45**(3): p. 626-640.

89. Tailor, P., et al., *The BXH2 mutation in IRF8 differentially impairs dendritic cell subset development in the mouse.* Blood, 2008. **111**(4): p. 1942-5.

90. Hambleton, S., et al., *IRF8 mutations and human dendritic-cell immunodeficiency.* N Engl J Med, 2011. **365**(2): p. 127-38.

91. Watchmaker, P.B., et al., *Comparative transcriptional and functional profiling defines conserved programs of intestinal DC differentiation in humans and mice.* Nat Immunol, 2014. **15**(1): p. 98-108.

92. Zhang, T.T., et al., *Dynamic expression of BCL6 in murine conventional dendritic cells during in vivo development and activation.* PLoS One, 2014. **9**(6): p. e101208.

93. Hacker, C., et al., *Transcriptional profiling identifies Id2 function in dendritic cell development.* Nat Immunol, 2003. **4**(4): p. 380-6.

94. Kusunoki, T., et al., *TH2 dominance and defective development of a CD8+ dendritic cell subset in Id2-deficient mice.* J Allergy Clin Immunol, 2003. **111**(1): p. 136-42.

95. Kashiwada, M., et al., *NFIL3/E4BP4 controls type 2 T helper cell cytokine expression.* EMBO J, 2011. **30**(10): p. 2071-82.

96. Lau, C.M., et al., *Transcription factor Etv6 regulates functional differentiation of cross-presenting classical dendritic cells.* J Exp Med, 2018. **215**(9): p. 2265-2278.

97. Bevan, M.J., *Cross-Priming for a Secondary Cytotoxic Response to Minor H-Antigens with H-2 Congenic Cells Which Do Not Cross-React in Cytotoxic Assay.* Journal of Experimental Medicine, 1976. **143**(5): p. 1283-1288.

98. Den Haan, J.M., Lehar, S.M., Bevan, M.J, *CD8(+) but not CD8(-) dendritic cells cross-prime cytotoxic T cells in vivo.* 2000.

99. Boscardin, S.B., et al., *Antigen targeting to dendritic cells elicits long-lived T cell help for antibody responses.* J Exp Med, 2006. **203**(3): p. 599-606.

100. Neubert, K., et al., *Antigen delivery to CD11c+CD8- dendritic cells induces protective immune responses against experimental melanoma in mice in vivo.* J Immunol, 2014. **192**(12): p. 5830-8.

101. Martinez-Lopez, M., et al., *Batf3-dependent CD103+ dendritic cells are major producers of IL-12 that drive local Th1 immunity against Leishmania major infection in mice.* Eur J Immunol, 2015. **45**(1): p. 119-29.

102. Lauterbach, H., et al., *Mouse CD8alpha+ DCs and human BDCA3+ DCs are major producers of IFN-lambda in response to poly IC.* J Exp Med, 2010. **207**(12): p. 2703-17.

103. Satpathy, A.T., et al., *Notch2-dependent classical dendritic cells orchestrate intestinal immunity to attaching-and-effacing bacterial pathogens.* Nat Immunol, 2013. **14**(9): p. 937-48.

104. Lewis, K.L., et al., *Notch2 receptor signaling controls functional differentiation of dendritic cells in the spleen and intestine.* Immunity, 2011. **35**(5): p. 780-91.

105. Tussiwand, R., et al., *Klf4 expression in conventional dendritic cells is required for T helper 2 cell responses.* Immunity, 2015. **42**(5): p. 916-28.

106. Dudziak, D., et al., *Differential antigen processing by dendritic cell subsets in vivo.* Science, 2007. **315**(5808): p. 107-11.

107. Cella, M., et al., *Plasmacytoid monocytes migrate to inflamed lymph nodes and produce large amounts of type I interferon.* Nat Med, 1999. **5**(8): p. 919-23.

108. Siegal, F.P., et al., *The nature of the principal type 1 interferon-producing cells in human blood.* Science, 1999. **284**(5421): p. 1835-7.

109. Reizis, B., et al., *Plasmacytoid dendritic cells: recent progress and open questions.* Annu Rev Immunol, 2011. **29**: p. 163-83.

110. Ito, T., et al., *Specialization, kinetics, and repertoire of type 1 interferon responses by human plasmacytoid predendritic cells.* Blood, 2006. **107**(6): p. 2423-31.

111. Hemmi, H., et al., *The roles of Toll-like receptor 9, MyD88, and DNA-dependent protein kinase catalytic subunit in the effects of two distinct CpG DNAs on dendritic cell subsets.* J Immunol, 2003. **170**(6): p. 3059-64.

112. Izaguirre, A., et al., *Comparative analysis of IRF and IFN-alpha expression in human plasmacytoid and monocyte-derived dendritic cells.* J Leukoc Biol, 2003. **74**(6): p. 1125-38.

113. Kerkmann, M., et al., *Activation with CpG-A and CpG-B oligonucleotides reveals two distinct regulatory pathways of type I IFN synthesis in human plasmacytoid dendritic cells.* J Immunol, 2003. **170**(9): p. 4465-74.

114. Takauji, R., et al., *CpG-DNA-induced IFN-alpha production involves p38 MAPK-dependent STAT1 phosphorylation in human plasmacytoid dendritic cell precursors.* J Leukoc Biol, 2002. **72**(5): p. 1011-9.

115. Jarrossay, D., et al., *Specialization and complementarity in microbial molecule recognition by human myeloid and plasmacytoid dendritic cells.* Eur J Immunol, 2001. **31**(11): p. 3388-93.

116. Edwards, A.D., et al., *Toll-like receptor expression in murine DC subsets: lack of TLR7 expression by CD8 alpha+ DC correlates with*

unresponsiveness to imidazoquinolines. Eur J Immunol, 2003. **33**(4): p. 827-33.

117. Kawai, T., et al., *Interferon-alpha induction through Toll-like receptors involves a direct interaction of IRF7 with MyD88 and TRAF6.* Nat Immunol, 2004. **5**(10): p. 1061-8.

118. Honda, K., et al., *Role of a transductional-transcriptional processor complex involving MyD88 and IRF-7 in Toll-like receptor signaling.* Proc Natl Acad Sci U S A, 2004. **101**(43): p. 15416-21.

119. Uematsu, S. and S. Akira, *Toll-like receptors and Type I interferons.* J Biol Chem, 2007. **282**(21): p. 15319-23.

120. Kumagai, Y., et al., *Cutting Edge: TLR-Dependent viral recognition along with type I IFN positive feedback signaling masks the requirement of viral replication for IFN-{alpha} production in plasmacytoid dendritic cells.* J Immunol, 2009. **182**(7): p. 3960-4.

121. McNab, F., et al., *Type I interferons in infectious disease.* Nat Rev Immunol, 2015. **15**(2): p. 87-103.

122. Ivashkiv, L.B. and L.T. Donlin, *Regulation of type I interferon responses.* Nat Rev Immunol, 2014. **14**(1): p. 36-49.

123. Gilliet, M., W. Cao, and Y.J. Liu, *Plasmacytoid dendritic cells: sensing nucleic acids in viral infection and autoimmune diseases.* Nat Rev Immunol, 2008. **8**(8): p. 594-606.

124. Musumeci, A., et al., *What Makes a pDC: Recent Advances in Understanding Plasmacytoid DC Development and Heterogeneity.* Front Immunol, 2019. **10**: p. 1222.

125. Chopin, M., et al., *Transcription Factor PU.1 Promotes Conventional Dendritic Cell Identity and Function via Induction of Transcriptional Regulator DC-SCRIPT.* Immunity, 2019. **50**(1): p. 77-90 e5.

126. Allman, D., et al., *Ikaros is required for plasmacytoid dendritic cell differentiation.* Blood, 2006. **108**(13): p. 4025-34.

127. Cytlak, U., et al., *Ikaros family zinc finger 1 regulates dendritic cell development and function in humans.* Nat Commun, 2018. **9**(1): p. 1239.

128. Cisse, B., et al., *Transcription factor E2-2 is an essential and specific regulator of plasmacytoid dendritic cell development.* Cell, 2008. **135**(1): p. 37-48.

129. Kee, B.L., *E and ID proteins branch out.* Nat Rev Immunol, 2009. **9**(3): p. 175-84.

130. Spits, H., et al., *Id2 and Id3 inhibit development of CD34(+) stem cells into predendritic cell (pre-DC)2 but not into pre-DC1. Evidence for a lymphoid origin of pre-DC2.* J Exp Med, 2000. **192**(12): p. 1775-84.

131. Satpathy, A.T., et al., *Re(de)fining the dendritic cell lineage.* Nat Immunol, 2012. **13**(12): p. 1145-54.

132. Ghosh, H.S., et al., *Continuous expression of the transcription factor e2-2 maintains the cell fate of mature plasmacytoid dendritic cells.* Immunity, 2010. **33**(6): p. 905-16.

133. Nagasawa, M., et al., *Development of human plasmacytoid dendritic cells depends on the combined action of the basic helix-loop-helix factor E2-2 and the Ets factor Spi-B.* Eur J Immunol, 2008. **38**(9): p. 2389-400.

134. Wu, X., et al., *Bcl11a controls Flt3 expression in early hematopoietic progenitors and is required for pDC development in vivo.* PLoS One, 2013. **8**(5): p. e64800.

135. Sawai, C.M., et al., *Transcription factor Runx2 controls the development and migration of plasmacytoid dendritic cells.* J Exp Med, 2013. **210**(11): p. 2151-9.

136. Chopin, M., et al., *RUNX2 Mediates Plasmacytoid Dendritic Cell Egress from the Bone Marrow and Controls Viral Immunity.* Cell Rep, 2016. **15**(4): p. 866-878.

137. Seth, S., et al., *CCR7 essentially contributes to the homing of plasmacytoid dendritic cells to lymph nodes under steady-state as well as inflammatory conditions.* J Immunol, 2011. **186**(6): p. 3364-72.

138. Wendland, M., et al., *CCR9 is a homing receptor for plasmacytoid dendritic cells to the small intestine.* Proc Natl Acad Sci U S A, 2007. **104**(15): p. 6347-52.

139. Leylek, R. and J. Idoyaga, *The versatile plasmacytoid dendritic cell: Function, heterogeneity, and plasticity.* Int Rev Cell Mol Biol, 2019. **349**: p. 177-211.

140. Villadangos, J.A. and L. Young, *Antigen-presentation properties of plasmacytoid dendritic cells.* Immunity, 2008. **29**(3): p. 352-61.

141. Sapoznikov, A., et al., *Organ-dependent in vivo priming of naive CD4+, but not CD8+, T cells by plasmacytoid dendritic cells.* J Exp Med, 2007. **204**(8): p. 1923-33.

142. Fonteneau, J.F., et al., *Activation of influenza virus-specific CD4+ and CD8+ T cells: a new role for plasmacytoid dendritic cells in adaptive immunity.* Blood, 2003. **101**(9): p. 3520-6.

143. Schlecht, G., et al., *Murine plasmacytoid dendritic cells induce effector/memory CD8+ T-cell responses in vivo after viral stimulation.* Blood, 2004. **104**(6): p. 1808-15.

144. Salio, M., et al., *CpG-matured murine plasmacytoid dendritic cells are capable of in vivo priming of functional CD8 T cell responses to endogenous but not exogenous antigens.* J Exp Med, 2004. **199**(4): p. 567-79.

145. Bjorck, P., et al., *Plasmacytoid dendritic cells take up opsonized antigen leading to CD4+ and CD8+ T cell activation in vivo.* J Immunol, 2008. **181**(6): p. 3811-7.

146. Guery, L. and S. Hugues, *Tolerogenic and activatory plasmacytoid dendritic cells in autoimmunity.* Front Immunol, 2013. **4**: p. 59.

147. Segura, E., M. Durand, and S. Amigorena, *Similar antigen cross-presentation capacity and phagocytic functions in all freshly isolated human lymphoid organ-resident dendritic cells.* J Exp Med, 2013. **210**(5): p. 1035-47.

148. Di Pucchio, T., et al., *Direct proteasome-independent cross-presentation of viral antigen by plasmacytoid dendritic cells on major histocompatibility complex class I.* Nat Immunol, 2008. **9**(5): p. 551-7.

149. Hoeffel, G., et al., *Antigen crosspresentation by human plasmacytoid dendritic cells.* Immunity, 2007. **27**(3): p. 481-92.

150. Tel, J., *Human plasmacytoid dendritic cells efficiently cross-present exogenous Ags to CD8 T cells despite lower Ag uptake than myoloid dendritic cell subsets.* 2013.

151. Mouries, J., et al., *Plasmacytoid dendritic cells efficiently cross-prime naive T cells in vivo after TLR activation.* Blood, 2008. **112**(9): p. 3713-22.

152. Kool, M., et al., *Facilitated antigen uptake and timed exposure to TLR ligands dictate the antigen-presenting potential of plasmacytoid DCs.* J Leukoc Biol, 2011. **90**(6): p. 1177-90.

153. Fu, C., et al., *Plasmacytoid dendritic cells cross-prime naive CD8 T cells by transferring antigen to conventional dendritic cells through exosomes.* Proc Natl Acad Sci U S A, 2020. **117**(38): p. 23730-23741.

154. Yoneyama, H., et al., *Plasmacytoid DCs help lymph node DCs to induce anti-HSV CTLs.* J Exp Med, 2005. **202**(3): p. 425-35.

155. Lou, Y., et al., *Plasmacytoid dendritic cells synergize with myeloid dendritic cells in the induction of antigen-specific antitumor immune responses.* J Immunol, 2007. **178**(3): p. 1534-41.

156. Rogers, G.L., et al., *Plasmacytoid and conventional dendritic cells cooperate in crosspriming AAV capsid-specific CD8(+) T cells.* Blood, 2017. **129**(24): p. 3184-3195.

157. Lozza, L., et al., *Crosstalk between human DC subsets promotes antibacterial activity and CD8+ T-cell stimulation in response to bacille Calmette-Guerin.* Eur J Immunol, 2014. **44**(1): p. 80-92.

158. Aspord, C., et al., *HLA-A(*)0201(+) plasmacytoid dendritic cells provide a cell-based immunotherapy for melanoma patients.* J Invest Dermatol, 2012. **132**(10): p. 2395-2406.

159. Tel, J., et al., *Natural human plasmacytoid dendritic cells induce antigen-specific T-cell responses in melanoma patients.* Cancer Res, 2013. **73**(3): p. 1063-75.

160. Westdorp, H., et al., *Blood-derived dendritic cell vaccinations induce immune responses that correlate with clinical outcome in patients with chemo-naive castration-resistant prostate cancer.* J Immunother Cancer, 2019. **7**(1): p. 302.

161. Bol, K.F., et al., *The clinical application of cancer immunotherapy based on naturally circulating dendritic cells.* J Immunother Cancer, 2019. **7**(1): p. 109.

162. Ali, S., et al., *Sources of Type I Interferons in Infectious Immunity: Plasmacytoid Dendritic Cells Not Always in the Driver's Seat.* Front Immunol, 2019. **10**: p. 778.

163. Channappanavar, R., et al., *Dysregulated Type I Interferon and Inflammatory Monocyte-Macrophage Responses Cause Lethal Pneumonia in SARS-CoV-Infected Mice.* Cell Host Microbe, 2016. **19**(2): p. 181-93.

164. Cervantes-Barragan, L., et al., *Control of coronavirus infection through plasmacytoid dendritic-cell-derived type I interferon.* Blood, 2007. **109**(3): p. 1131-7.

165. Chen, J., et al., *Cellular immune responses to severe acute respiratory syndrome coronavirus (SARS-CoV) infection in senescent BALB/c mice: CD4+ T cells are important in control of SARS-CoV infection.* J Virol, 2010. **84**(3): p. 1289-301.

166. Sa Ribero, M., et al., *Interplay between SARS-CoV-2 and the type I interferon response.* PLoS Pathog, 2020. **16**(7): p. e1008737.

167. Maldonado, S. and P. Fitzgerald-Bocarsly, *Antifungal Activity of Plasmacytoid Dendritic Cells and the Impact of Chronic HIV Infection.* Front Immunol, 2017. **8**: p. 1705.

168. Fitzgerald-Bocarsly, P. and E.S. Jacobs, *Plasmacytoid dendritic cells in HIV infection: striking a delicate balance.* J Leukoc Biol, 2010. **87**(4): p. 609-20.

169. Donaghy, H., et al., *Dysfunction and infection of freshly isolated blood myeloid and plasmacytoid dendritic cells in patients infected with HIV-1.* Blood, 2003. **101**(11): p. 4505-11.

170. Chehimi, J., et al., *Persistent decreases in blood plasmacytoid dendritic cell number and function despite effective highly active antiretroviral therapy and increased blood myeloid dendritic cells in HIV-infected individuals.* J Immunol, 2002. **168**(9): p. 4796-801.

171. Donaghy, H., et al., *Loss of blood CD11c(+) myeloid and CD11c(-) plasmacytoid dendritic cells in patients with HIV-1 infection correlates with HIV-1 RNA virus load.* Blood, 2001. **98**(8): p. 2574-6.

172. O'Brien, M., O. Manches, and N. Bhardwaj, *Plasmacytoid dendritic cells in HIV infection.* Adv Exp Med Biol, 2013. **762**: p. 71-107.

173. Patterson, S., et al., *Plasmacytoid dendritic cells are highly susceptible to human immunodeficiency virus type 1 infection and release infectious virus.* J Virol, 2001. **75**(14): p. 6710-3.

174. Nascimbeni, M., et al., *Plasmacytoid dendritic cells accumulate in spleens from chronically HIV-infected patients but barely participate in interferon-alpha expression.* Blood, 2009. **113**(24): p. 6112-9.

175. Lehmann, C., et al., *Increased interferon alpha expression in circulating plasmacytoid dendritic cells of HIV-1-infected patients.* J Acquir Immune Defic Syndr, 2008. **48**(5): p. 522-30.

176. Schmidt, B., et al., *Low-level HIV infection of plasmacytoid dendritic cells: onset of cytopathic effects and cell death after PDC maturation.* Virology, 2004. **329**(2): p. 280-8.

177. Schmidt, B., et al., *Variations in plasmacytoid dendritic cell (PDC) and myeloid dendritic cell (MDC) levels in HIV-infected subjects on and off antiretroviral therapy.* J Clin Immunol, 2006. **26**(1): p. 55-64.

178. Aiello, A., et al., *The involvement of plasmacytoid cells in HIV infection and pathogenesis.* Cytokine Growth Factor Rev, 2018. **40**: p. 77-89.

179. Mitchell, J.L., et al., *Plasmacytoid dendritic cells sense HIV replication before detectable viremia following treatment interruption.* J Clin Invest, 2020. **130**(6): p. 2845-2858.

180. Pham, T.N.Q., et al., *Flt3L-Mediated Expansion of Plasmacytoid Dendritic Cells Suppresses HIV Infection in Humanized Mice.* Cell Rep, 2019. **29**(9): p. 2770-2782 e5.

181. Ulsenheimer, A., et al., *Plasmacytoid dendritic cells in acute and chronic hepatitis C virus infection.* Hepatology, 2005. **41**(3): p. 643-51.

182. Kanto, T., et al., *Reduced numbers and impaired ability of myeloid and plasmacytoid dendritic cells to polarize T helper cells in chronic hepatitis C virus infection.* J Infect Dis, 2004. **190**(11): p. 1919-26.

183. Xie, Q., et al., *Patients with chronic hepatitis B infection display deficiency of plasmacytoid dendritic cells with reduced expression of TLR9.* Microbes Infect, 2009. **11**(4): p. 515-23.

184. Takahashi, K., et al., *Plasmacytoid dendritic cells sense hepatitis C virus-infected cells, produce interferon, and inhibit infection.* Proc Natl Acad Sci U S A, 2010. **107**(16): p. 7431-6.

185. Doyle, E.H., et al., *Individual liver plasmacytoid dendritic cells are capable of producing IFNalpha and multiple additional cytokines during chronic HCV infection.* PLoS Pathog, 2019. **15**(7): p. e1007935.

186. Golsaz-Shirazi, F., M.M. Amiri, and F. Shokri, *Immune function of plasmacytoid dendritic cells, natural killer cells, and their crosstalk in HBV infection.* Rev Med Virol, 2018. **28**(6): p. e2007.

187. Cao, W.H., et al., *Quantitation of Plasmacytoid Dendritic Cells in Chronic Hepatitis B Patients with HBeAg Positivity During PEG-IFN and Entecavir Therapy.* J Interferon Cytokine Res, 2018. **38**(5): p. 197-205.

188. Dominguez-Molina, B., et al., *Toll-Like Receptor 7 (TLR-7) and TLR-9 Agonists Improve Hepatitis C Virus Replication and Infectivity Inhibition by Plasmacytoid Dendritic Cells.* J Virol, 2018. **92**(23).

189. Li, M.H., et al., *Plasmacytoid Dendritic Cell Function and Cytokine Network Profiles in Patients with Acute or Chronic Hepatitis B Virus Infection.* Chin Med J (Engl), 2018. **131**(1): p. 43-49.

190. Li, G., et al., *Plasmacytoid dendritic cells suppress HIV-1 replication but contribute to HIV-1 induced immunopathogenesis in humanized mice.* PLoS Pathog, 2014. **10**(7): p. e1004291.

191. Feldman, S., et al., *Decreased interferon-alpha production in HIV-infected patients correlates with numerical and functional deficiencies in circulating type 2 dendritic cell precursors.* Clin Immunol, 2001. **101**(2): p. 201-10.

192. Pacanowski, J., et al., *Reduced blood CD123+ (lymphoid) and CD11c+ (myeloid) dendritic cell numbers in primary HIV-1 infection.* Blood, 2001. **98**(10): p. 3016-21.

193. Soumelis, V., et al., *Depletion of circulating natural type 1 interferon-producing cells in HIV-infected AIDS patients.* Blood, 2001. **98**(4): p. 906-12.

194. Royle, C.M., et al., *HIV-1 and HIV-2 differentially mature plasmacytoid dendritic cells into IFN-producing cells or APCs.* J Immunol, 2014. **193**(7): p. 3538-48.

195. Grossman, Z., et al., *CD4+ T-cell depletion in HIV infection: are we closer to understanding the cause?* Nat Med, 2002. **8**(4): p. 319-23.

196. Hazenberg, M.D., et al., *Persistent immune activation in HIV-1 infection is associated with progression to AIDS.* AIDS, 2003. **17**(13): p. 1881-8.

197. Miller, E. and N. Bhardwaj, *Dendritic cell dysregulation during HIV-1 infection.* Immunol Rev, 2013. **254**(1): p. 170-89.

198. O'Brien, M., et al., *Spatiotemporal trafficking of HIV in human plasmacytoid dendritic cells defines a persistently IFN-alpha-producing and partially matured phenotype.* J Clin Invest, 2011. **121**(3): p. 1088-101.

199. Maartens, G., C. Celum, and S.R. Lewin, *HIV infection: epidemiology, pathogenesis, treatment, and prevention.* The Lancet, 2014. **384**(9939): p. 258-271.

200. Sapienza, M.R., et al., *Molecular profiling of blastic plasmacytoid dendritic cell neoplasm reveals a unique pattern and suggests selective sensitivity to NF-kB pathway inhibition.* Leukemia, 2014. **28**(8): p. 1606-16.

201. Khoury, J.D., *Blastic Plasmacytoid Dendritic Cell Neoplasm.* Curr Hematol Malig Rep, 2018. **13**(6): p. 477-483.

202. Venugopal, S., et al., *Blastic Plasmacytoid Dendritic Cell Neoplasm-Current Insights.* Clin Lymphoma Myeloma Leuk, 2019. **19**(9): p. 545-554.

203. Pagano, L., et al., *Blastic plasmacytoid dendritic cell neoplasm: diagnostic criteria and therapeutical approaches.* Br J Haematol, 2016. **174**(2): p. 188-202.

204. Sweet, K., *Blastic plasmacytoid dendritic cell neoplasm: diagnosis, manifestations, and treatment.* Curr Opin Hematol, 2020. **27**(2): p. 103-107.

205. Lucas, N., et al., *Biology and prognostic impact of clonal plasmacytoid dendritic cells in chronic myelomonocytic leukemia.* Leukemia, 2019. **33**(10): p. 2466-2480.

206. Kong, Q.T., et al., *Blastic plasmacytoid dendritic cell neoplasm of the skin associated with myelodysplastic syndrome.* Dermatol Online J, 2014. **21**(3).

207. Chamoun, K., et al., *Early detection of transformation to BPDCN in a patient with MDS.* Exp Hematol Oncol, 2018. **7**: p. 26.

208. Zalmai, L., et al., *Plasmacytoid dendritic cells proliferation associated with acute myeloid leukemia: phenotype profile and mutation landscape.* Haematologica, 2020. **Online ahead of print**.

209. Xiao, W., et al., *Plasmacytoid dendritic cell expansion defines a distinct subset of RUNX1* 2020.

210. Xiao, W., et al., *Loss of plasmacytoid dendritic cell differentiation is highly predictive for post-induction measurable residual disease and inferior outcomes in acute myeloid leukemia.* Haematologica, 2019. **104**(7): p. 1378-1387.

211. Zhu, L., et al., *Plasmacytoid Dendritic Cell Infiltration in Acute Myeloid Leukemia.* Cancer Manag Res, 2020. **12**: p. 11411-11419.

212. Panda, S.K., R. Kolbeck, and M.A. Sanjuan, *Plasmacytoid dendritic cells in autoimmunity.* Curr Opin Immunol, 2017. **44**: p. 20-25.

213. Le Bon, A., et al., *Cross-priming of CD8+ T cells stimulated by virus-induced type I interferon.* Nat Immunol, 2003. **4**(10): p. 1009-15.

214. Kurts, C., B.W. Robinson, and P.A. Knolle, *Cross-priming in health and disease.* Nat Rev Immunol, 2010. **10**(6): p. 403-14.

215. Chaplin, D.D., *Overview of the immune response.* J Allergy Clin Immunol, 2010. **125**(2 Suppl 2): p. S3-23.

216. Akira, S., S. Uematsu, and O. Takeuchi, *Pathogen recognition and innate immunity.* Cell, 2006. **124**(4): p. 783-801.

217. Medzhitov, R., *Recognition of microorganisms and activation of the immune response.* Nature, 2007. **449**(7164): p. 819-26.

218. Vyas, J.M., A.G. Van der Veen, and H.L. Ploegh, *The known unknowns of antigen processing and presentation.* Nat Rev Immunol, 2008. **8**(8): p. 607-18.

219. Rock, K.L., E. Reits, and J. Neefjes, *Present Yourself! By MHC Class I and MHC Class II Molecules.* Trends Immunol, 2016. **37**(11): p. 724-737.

220. Neefjes, J., et al., *Towards a systems understanding of MHC class I and MHC class II antigen presentation.* Nat Rev Immunol, 2011. **11**(12): p. 823-36.

221. Kotsias, F., I. Cebrian, and A. Alloatti, *Antigen processing and presentation.* Int Rev Cell Mol Biol, 2019. **348**: p. 69-121.

222. Huang, A.Y., et al., *Role of bone marrow-derived cells in presenting MHC class I-restricted tumor antigens.* Science, 1994. **264**(5161): p. 961-5.

223. Sigal, L.J., et al., *Cytotoxic T-cell immunity to virus-infected non-haematopoietic cells requires presentation of exogenous antigen.* Nature, 1999. **398**(6722): p. 77-80.

224. den Haan, J.M. and M.J. Bevan, *Antigen presentation to CD8+ T cells: cross-priming in infectious diseases.* Curr Opin Immunol, 2001. **13**(4): p. 437-41.

225. Zinkernagel, R.M. and P.C. Doherty, *Immunological surveillance against altered self components by sensitised T lymphocytes in lymphocytic choriomeningitis.* Nature, 1974. **251**(5475): p. 547-8.

226. Joffre, O.P., et al., *Cross-presentation by dendritic cells.* Nat Rev Immunol, 2012. **12**(8): p. 557-69.

227. Blander, J.M., *Regulation of the Cell Biology of Antigen Cross-Presentation.* Annu Rev Immunol, 2018. **36**: p. 717-753.

228. Embgenbroich, M. and S. Burgdorf, *Current Concepts of Antigen Cross-Presentation.* Front Immunol, 2018. **9**: p. 1643.

229. Kovacsovics-Bankowski, M. and K.L. Rock, *A phagosome-to-cytosol pathway for exogenous antigens presented on MHC class I molecules.* Science, 1995. **267**(5195): p. 243-6.

230. Palmowski, M.J., et al., *Role of immunoproteasomes in cross-presentation.* J Immunol, 2006. **177**(2): p. 983-90.

231. Koch, J. and R. Tampe, *The macromolecular peptide-loading complex in MHC class I-dependent antigen presentation.* Cell Mol Life Sci, 2006. **63**(6): p. 653-62.

232. Firat, E., et al., *The role of endoplasmic reticulum-associated aminopeptidase 1 in immunity to infection and in cross-presentation.* J Immunol, 2007. **178**(4): p. 2241-8.

233. Shen, L., et al., *Important role of cathepsin S in generating peptides for TAP-independent MHC class I crosspresentation in vivo.* Immunity, 2004. **21**(2): p. 155-65.

234. Pfeifer, J.D., et al., *Phagocytic Processing of Bacterial-Antigens for Class-I Mhc Presentation to T-Cells.* Nature, 1993. **361**(6410): p. 359-362.

235. Liu, T., et al., *TAP peptide transporter-independent presentation of heat-killed Sendai virus antigen on MHC class I molecules by splenic antigen-presenting cells.* J Immunol, 1997. **159**(11): p. 5364-71.

236. Saveanu, L., et al., *IRAP identifies an endosomal compartment required for MHC class I cross-presentation.* Science, 2009. **325**(5937): p. 213-7.

237. Kurotaki, T., et al., *Efficient cross-presentation by heat shock protein 90-peptide complex-loaded dendritic cells via an endosomal pathway.* J Immunol, 2007. **179**(3): p. 1803-13.

238. Bertholet, S., et al., *Leishmania antigens are presented to CD8+ T cells by a transporter associated with antigen processing-independent pathway in vitro and in vivo.* J Immunol, 2006. **177**(6): p. 3525-33.

239. Ackerman, A.L., et al., *Early phagosomes in dendritic cells form a cellular compartment sufficient for cross presentation of exogenous antigens.* Proc Natl Acad Sci U S A, 2003. **100**(22): p. 12889-94.

240. Doherty, G.J. and H.T. McMahon, *Mechanisms of endocytosis.* Annu Rev Biochem, 2009. **78**: p. 857-902.

241. Conner, S.D. and S.L. Schmid, *Regulated portals of entry into the cell.* Nature, 2003. **422**(6927): p. 37-44.

242. Kovacsovics-Bankowski, M., *Eflicient major histocompatibility complex class I presentation of exogenous antigenupon phagocytosis by macrophages.* 1993.

243. Kumari, S., S. Mg, and S. Mayor, *Endocytosis unplugged: multiple ways to enter the cell.* Cell Res, 2010. **20**(3): p. 256-75.

244. Aderem, A. and D.M. Underhill, *Mechanisms of phagocytosis in macrophages.* Annu Rev Immunol, 1999. **17**: p. 593-623.

245. Burgdorf, S., et al., *Distinct pathways of antigen uptake and intracellular routing in CD4 and CD8 T cell activation.* Science, 2007. **316**(5824): p. 612-6.

246. Lakadamyali, M., M.J. Rust, and X. Zhuang, *Ligands for clathrin-mediated endocytosis are differentially sorted into distinct populations of early endosomes.* Cell, 2006. **124**(5): p. 997-1009.

247. Klechevsky, E., et al., *Cross-priming CD8+ T cells by targeting antigens to human dendritic cells through DCIR.* Blood, 2010. **116**(10): p. 1685-97.

248. Schreibelt, G., et al., *The C-type lectin receptor CLEC9A mediates antigen uptake and (cross-)presentation by human blood BDCA3+ myeloid dendritic cells.* Blood, 2012. **119**(10): p. 2284-92.

249. Jongbloed, S.L., et al., *Human CD141+ (BDCA-3)+ dendritic cells (DCs) represent a unique myeloid DC subset that cross-presents necrotic cell antigens.* J Exp Med, 2010. **207**(6): p. 1247-60.

250. Bachem, A., et al., *Superior antigen cross-presentation and XCR1 expression define human CD11c+CD141+ cells as homologues of mouse CD8+ dendritic cells.* J Exp Med, 2010. **207**(6): p. 1273-81.

251. Poulin, L.F., et al., *Characterization of human DNGR-1+ BDCA3+ leukocytes as putative equivalents of mouse CD8alpha+ dendritic cells.* J Exp Med, 2010. **207**(6): p. 1261-71.

252. Sancho, D., et al., *Identification of a dendritic cell receptor that couples sensing of necrosis to immunity.* Nature, 2009. **458**(7240): p. 899-903.

253. Zelenay, S., et al., *The dendritic cell receptor DNGR-1 controls endocytic handling of necrotic cell antigens to favor cross-priming of CTLs in virus-infected mice.* J Clin Invest, 2012. **122**(5): p. 1615-27.

254. Saluja, S.S., et al., *Targeting human dendritic cells via DEC-205 using PLGA nanoparticles leads to enhanced cross-presentation of a melanoma-associated antigen.* Int J Nanomedicine, 2014. **9**: p. 5231-46.

255. Fehres, C.M., et al., *In situ Delivery of Antigen to DC-SIGN(+)CD14(+) Dermal Dendritic Cells Results in Enhanced CD8(+) T-Cell Responses.* J Invest Dermatol, 2015. **135**(9): p. 2228-2236.

256. Lahoud, M.H., et al., *The C-type lectin Clec12A present on mouse and human dendritic cells can serve as a target for antigen delivery and enhancement of antibody responses.* J Immunol, 2009. **182**(12): p. 7587-94.

257. Hutten, T.J., et al., *CLEC12A-Mediated Antigen Uptake and Cross-Presentation by Human Dendritic Cell Subsets Efficiently Boost Tumor-Reactive T Cell Responses.* J Immunol, 2016. **197**(7): p. 2715-25.

258. Burgdorf, S., et al., *Spatial and mechanistic separation of cross-presentation and endogenous antigen presentation.* Nat Immunol, 2008. **9**(5): p. 558-66.

259. Alloatti, A., et al., *Toll-like Receptor 4 Engagement on Dendritic Cells Restrains Phago-Lysosome Fusion and Promotes Cross-Presentation of Antigens.* Immunity, 2015. **43**(6): p. 1087-100.

260. Chatterjee, B., et al., *Internalization and endosomal degradation of receptor-bound antigens regulate the efficiency of cross presentation by human dendritic cells.* Blood, 2012. **120**(10): p. 2011-20.

261. Accapezzato, D., et al., *Chloroquine enhances human CD8+ T cell responses against soluble antigens in vivo.* J Exp Med, 2005. **202**(6): p. 817-28.

262. Samie, M. and P. Cresswell, *The transcription factor TFEB acts as a molecular switch that regulates exogenous antigen-presentation pathways.* Nat Immunol, 2015. **16**(7): p. 729-36.

263. Lennon-Dumenil, A.M., et al., *Analysis of protease activity in live antigen-presenting cells shows regulation of the phagosomal proteolytic contents during dendritic cell activation.* J Exp Med, 2002. **196**(4): p. 529-40.

264. Delamarre, L., et al., *Differential lysosomal proteolysis in antigen-presenting cells determines antigen fate.* Science, 2005. **307**(5715): p. 1630-4.

265. Savina, A., et al., *NOX2 controls phagosomal pH to regulate antigen processing during crosspresentation by dendritic cells.* Cell, 2006. **126**(1): p. 205-18.

266. Mantegazza, A.R., et al., *NADPH oxidase controls phagosomal pH and antigen cross-presentation in human dendritic cells.* Blood, 2008. **112**(12): p. 4712-22.

267. Jancic, C., et al., *Rab27a regulates phagosomal pH and NADPH oxidase recruitment to dendritic cell phagosomes.* Nat Cell Biol, 2007. **9**(4): p. 367-78.

268. Matheoud, D., et al., *Leishmania evades host immunity by inhibiting antigen cross-presentation through direct cleavage of the SNARE VAMP8.* Cell Host Microbe, 2013. **14**(1): p. 15-25.

269. Savina, A., et al., *The small GTPase Rac2 controls phagosomal alkalinization and antigen crosspresentation selectively in CD8(+) dendritic cells.* Immunity, 2009. **30**(4): p. 544-55.

270. Graham, D.B., et al., *An ITAM-signaling pathway controls cross-presentation of particulate but not soluble antigens in dendritic cells.* J Exp Med, 2007. **204**(12): p. 2889-97.

271. Hall, A.B., et al., *Requirements for Vav guanine nucleotide exchange factors and Rho GTPases in FcgammaR- and complement-mediated phagocytosis.* Immunity, 2006. **24**(3): p. 305-16.

272. Murrow, L. and J. Debnath, *Autophagy as a stress-response and quality-control mechanism: implications for cell injury and human disease.* Annu Rev Pathol, 2013. **8**: p. 105-37.

273. Ravindran, R., et al., *Vaccine activation of the nutrient sensor GCN2 in dendritic cells enhances antigen presentation.* Science, 2014. **343**(6168): p. 313-317.

274. Grotzke, J.E. and P. Cresswell, *Are ERAD components involved in cross-presentation?* Mol Immunol, 2015. **68**(2 Pt A): p. 112-5.

275. Imai, J., et al., *Exogenous antigens are processed through the endoplasmic reticulum-associated degradation (ERAD) in cross-presentation by dendritic cells.* Int Immunol, 2005. **17**(1): p. 45-53.

276. Yihong, *The AAA ATPase Cdc48:p97 and its partners transport proteins from the ER into the cytosol.* 2001.

277. Ackerman, A.L., A. Giodini, and P. Cresswell, *A role for the endoplasmic reticulum protein retrotranslocation machinery during crosspresentation by dendritic cells.* Immunity, 2006. **25**(4): p. 607-17.

278. Zehner, M., et al., *Mannose receptor polyubiquitination regulates endosomal recruitment of p97 and cytosolic antigen translocation for cross-presentation.* Proc Natl Acad Sci U S A, 2011. **108**(24): p. 9933-8.

279. Imai, T., et al., *Heat shock protein 90 (HSP90) contributes to cytosolic translocation of extracellular antigen for cross-presentation by dendritic cells.* Proc Natl Acad Sci U S A, 2011. **108**(39): p. 16363-8.

280. Zehner, M., et al., *The translocon protein Sec61 mediates antigen transport from endosomes in the cytosol for cross-presentation to CD8(+) T cells.* Immunity, 2015. **42**(5): p. 850-63.

281. Grotzke, J.E., et al., *Sec61 blockade by mycolactone inhibits antigen cross-presentation independently of endosome-to-cytosol export.* Proc Natl Acad Sci U S A, 2017. **114**(29): p. E5910-E5919.

282. Hornung, V., et al., *Silica crystals and aluminum salts activate the NALP3 inflammasome through phagosomal destabilization.* Nat Immunol, 2008. **9**(8): p. 847-56.

283. Guermonprez, P., et al., *ER-phagosome fusion defines an MHC class I cross-presentation compartment in dendritic cells.* Nature, 2003. **425**(6956): p. 397-402.

284. Cruz, F.M., et al., *The Biology and Underlying Mechanisms of Cross-Presentation of Exogenous Antigens on MHC-I Molecules.* Annu Rev Immunol, 2017. **35**: p. 149-176.

285. Sengupta, D., et al., *Proteasomal degradation within endocytic organelles mediates antigen cross-presentation.* EMBO J, 2019. **38**(16): p. e99266.

286. Rock, K.L., I.A. York, and A.L. Goldberg, *Post-proteasomal antigen processing for major histocompatibility complex class I presentation.* Nat Immunol, 2004. **5**(7): p. 670-7.

287. Serwold, T., et al., *ERAAP customizes peptides for MHC class I molecules in the endoplasmic reticulum.* Nature, 2002. **419**(6906): p. 480-3.

288. York, I.A., et al., *The ER aminopeptidase ERAP1 enhances or limits antigen presentation by trimming epitopes to 8-9 residues.* Nat Immunol, 2002. **3**(12): p. 1177-84.

289. Weimershaus, M., et al., *Conventional dendritic cells require IRAP-Rab14 endosomes for efficient cross-presentation.* J Immunol, 2012. **188**(4): p. 1840-6.

290. Blum, J.S., P.A. Wearsch, and P. Cresswell, *Pathways of antigen processing.* Annu Rev Immunol, 2013. **31**: p. 443-73.

291. Rapoport, T.A., L. Li, and E. Park, *Structural and Mechanistic Insights into Protein Translocation.* Annual Review of Cell and Developmental Biology, Vol 33, 2017. **33**: p. 369-390.

292. Paulsson, K. and P. Wang, *Chaperones and folding of MHC class I molecules in the endoplasmic reticulum.* Biochimica et Biophysica Acta (BBA) - Molecular Cell Research, 2003. **1641**(1): p. 1-12.

293. Abe, F., et al., *Interaction of Bap31 and MHC class I molecules and their traffic out of the endoplasmic reticulum.* J Immunol, 2009. **182**(8): p. 4776-83.

294. Spiliotis, *Selective Export of MHC Class I Molecules from the ER after Their Dissociation from TAP.* 2000.

295. Appenzeller-Herzog, C. and H.P. Hauri, *The ER-Golgi intermediate compartment (ERGIC): in search of its identity and function.* J Cell Sci, 2006. **119**(Pt 11): p. 2173-83.

296. Dejgaard, S.Y., et al., *Rab18 and Rab43 have key roles in ER-Golgi trafficking.* J Cell Sci, 2008. **121**(Pt 16): p. 2768-81.

297. Kretzer, N.M., et al., *RAB43 facilitates cross-presentation of cell-associated antigens by CD8alpha+ dendritic cells.* J Exp Med, 2016. **213**(13): p. 2871-2883.

298. Cebrian, I., et al., *Sec22b regulates phagosomal maturation and antigen crosspresentation by dendritic cells.* Cell, 2011. **147**(6): p. 1355-68.

299. McNew, J.A., et al., *Compartmental specificity of cellular membrane fusion encoded in SNARE proteins.* Nature, 2000. **407**(6801): p. 153-9.

300. Basha, G., et al., *A CD74-dependent MHC class I endolysosomal cross-presentation pathway.* Nat Immunol, 2012. **13**(3): p. 237-45.

301. Radhakrishna, H. and J.G. Donaldson, *ADP-ribosylation factor 6 regulates a novel plasma membrane recycling pathway.* J Cell Biol, 1997. **139**(1): p. 49-61.

302. Naslavsky, N., R. Weigert, and J.G. Donaldson, *Characterization of a nonclathrin endocytic pathway: membrane cargo and lipid requirements.* Mol Biol Cell, 2004. **15**(8): p. 3542-52.

303. Jovic, *The early endosome- a busy sorting station for proteins at the crossroads.* 2010.

304. Ullrich, O., et al., *Rab11 regulates recycling through the pericentriolar recycling endosome.* Journal of Cell Biology, 1996. **135**(4): p. 913-924.

305. Perrin, L., et al., *Rab4b controls an early endosome sorting event by interacting with the gamma-subunit of the clathrin adaptor complex 1.* J Cell Sci, 2013. **126**(Pt 21): p. 4950-62.

306. Klinkert, K. and A. Echard, *Rab35 GTPase: A Central Regulator of Phosphoinositides and F-actin in Endocytic Recycling and Beyond.* Traffic, 2016. **17**(10): p. 1063-77.

307. van de Weijer, M.L., R.D. Luteijn, and E.J. Wiertz, *Viral immune evasion: Lessons in MHC class I antigen presentation.* Semin Immunol, 2015. **27**(2): p. 125-37.

308. Smiley, J.R., *Herpes simplex virus virion host shutoff protein: immune evasion mediated by a viral RNase?* J Virol, 2004. **78**(3): p. 1063-8.

309. Fruh, K., et al., *A viral inhibitor of peptide transporters for antigen presentation.* Nature, 1995. **375**(6530): p. 415-8.

310. Hill, A., et al., *Herpes simplex virus turns off the TAP to evade host immunity.* Nature, 1995. **375**(6530): p. 411-5.

311. Hewitt, E.W., S.S. Gupta, and P.J. Lehner, *The human cytomegalovirus gene product US6 inhibits ATP binding by TAP.* EMBO J, 2001. **20**(3): p. 387-96.

312. Lehner, P.J., et al., *The human cytomegalovirus US6 glycoprotein inhibits transporter associated with antigen processing-dependent peptide translocation.* Proc Natl Acad Sci U S A, 1997. **94**(13): p. 6904-9.

313. Ahn, K., et al., *Molecular mechanism and species specificity of TAP inhibition by herpes simplex virus ICP47.* EMBO J, 1996. **15**(13): p. 3247-55.

314. Ahn, K., et al., *The ER-luminal domain of the HCMV glycoprotein US6 inhibits peptide translocation by TAP.* Immunity, 1997. **6**(5): p. 613-21.

315. Wiertz, E.J., et al., *The human cytomegalovirus US11 gene product dislocates MHC class I heavy chains from the endoplasmic reticulum to the cytosol.* Cell, 1996. **84**(5): p. 769-79.

316. Park, B., et al., *The HCMV membrane glycoprotein US10 selectively targets HLA-G for degradation.* J Exp Med, 2010. **207**(9): p. 2033-41.

317. Reusch, U., et al., *A cytomegalovirus glycoprotein re-routes MHC class I complexes to lysosomes for degradation.* EMBO J, 1999. **18**(4): p. 1081-91.

318. Schwartz, *Endocytosis of major histocompatibility complex class I molecules is induced by the HIV-1 Nef protein.* 1996.

319. Cohen, G.B., et al., *The selective downregulation of class I major histocompatibility complex proteins by HIV-1 protects HIV-infected cells from NK cells.* Immunity, 1999. **10**(6): p. 661-71.

320. Busche, A., et al., *Priming of CD8+ T cells against cytomegalovirus-encoded antigens is dominated by cross-presentation.* J Immunol, 2013. **190**(6): p. 2767-77.

321. Nopora, K., et al., *MHC class I cross-presentation by dendritic cells counteracts viral immune evasion.* Front Immunol, 2012. **3**: p. 348.

322. Orr, M.T., et al., *Inhibition of MHC class I is a virulence factor in herpes simplex virus infection of mice.* PLoS Pathog, 2005. **1**(1): p. e7.

323. Ribeiro-Gomes, F.L., et al., *Apoptotic cell clearance of Leishmania major-infected neutrophils by dendritic cells inhibits CD8(+) T-cell priming in vitro by Mer tyrosine kinase-dependent signaling.* Cell Death Dis, 2015. **6**: p. e2018.

324. Palmer, E., *Negative selection--clearing out the bad apples from the T-cell repertoire.* Nat Rev Immunol, 2003. **3**(5): p. 383-91.

325. Starr, T.K., S.C. Jameson, and K.A. Hogquist, *Positive and negative selection of T cells.* Annu Rev Immunol, 2003. **21**: p. 139-76.

326. von Boehmer, H., et al., *Thymic selection revisited: how essential is it?* Immunol Rev, 2003. **191**: p. 62-78.

327. Kurts, C., et al., *Class I-restricted cross-presentation of exogenous self-antigens leads to deletion of autoreactive CD8(+) T cells.* J Exp Med, 1997. **186**(2): p. 239-45.

328. Heath, W.R., et al., *Cross-tolerance: a pathway for inducing tolerance to peripheral tissue antigens.* J Exp Med, 1998. **187**(10): p. 1549-53.

329. Zehn, D. and M.J. Bevan, *T cells with low avidity for a tissue-restricted antigen routinely evade central and peripheral tolerance and cause autoimmunity.* Immunity, 2006. **25**(2): p. 261-70.

330. Nakayama, M., et al., *Priming and effector dependence on insulin B:9-23 peptide in NOD islet autoimmunity.* J Clin Invest, 2007. **117**(7): p. 1835-43.

331. de Jersey, J., et al., *Beta cells cannot directly prime diabetogenic CD8 T cells in nonobese diabetic mice.* Proc Natl Acad Sci U S A, 2007. **104**(4): p. 1295-300.

332. Heymann, F., et al., *Kidney dendritic cell activation is required for progression of renal disease in a mouse model of glomerular injury.* J Clin Invest, 2009. **119**(5): p. 1286-97.

333. Galea, I., et al., *An antigen-specific pathway for CD8 T cells across the blood-brain barrier.* J Exp Med, 2007. **204**(9): p. 2023-30.

334. Perchellet, A., T. Brabb, and J.M. Goverman, *Crosspresentation by nonhematopoietic and direct presentation by hematopoietic cells induce central tolerance to myelin basic protein.* Proc Natl Acad Sci U S A, 2008. **105**(37): p. 14040-5.

335. Huseby, E.S., et al., *A pathogenic role for myelin-specific CD8(+) T cells in a model for multiple sclerosis.* J Exp Med, 2001. **194**(5): p. 669-76.

336. Limmer, A., et al., *Efficient presentation of exogenous antigen by liver endothelial cells to CD8+ T cells results in antigen-specific T-cell tolerance.* Nat Med, 2000. **6**(12): p. 1348-54.

337. Ichiki, Y., et al., *T cell immunity in autoimmune hepatitis.* Autoimmun Rev, 2005. **4**(5): p. 315-21.

338. Brazillet, M.P., et al., *Induction of experimental autoimmune thyroiditis by heat-denatured porcine thyroglobulin: a Tc1-mediated disease.* Eur J Immunol, 1999. **29**(4): p. 1342-52.

339. Zhao, Y. and X. Li, *Cross-immune tolerance: conception and its potential significance on transplantation tolerance.* Cell Mol Immunol, 2010. **7**(1): p. 20-5.

340. Gokmen, M.R., G. Lombardi, and R.I. Lechler, *The importance of the indirect pathway of allorecognition in clinical transplantation.* Curr Opin Immunol, 2008. **20**(5): p. 568-74.

341. Calzascia, T., et al., *Cutting edge: cross-presentation as a mechanism for efficient recruitment of tumor-specific CTL to the brain.* J Immunol, 2003. **171**(5): p. 2187-91.

342. McDonnell, A.M., et al., *Tumor-infiltrating dendritic cells exhibit defective cross-presentation of tumor antigens, but is reversed by chemotherapy.* Eur J Immunol, 2015. **45**(1): p. 49-59.

343. Ramakrishnan, R., et al., *Oxidized lipids block antigen cross-presentation by dendritic cells in cancer.* J Immunol, 2014. **192**(6): p. 2920-31.

344. Nelson, D.J., et al., *Tumor progression despite efficient tumor antigen cross-presentation and effective "arming" of tumor antigen-specific CTL.* J Immunol, 2001. **166**(9): p. 5557-66.

345. Nowak, A.K., et al., *Induction of tumor cell apoptosis in vivo increases tumor antigen cross-presentation, cross-priming rather than cross-tolerizing host tumor-specific CD8 T cells.* J Immunol, 2003. **170**(10): p. 4905-13.

346. Schnurr, M., et al., *ISCOMATRIX adjuvant induces efficient cross-presentation of tumor antigen by dendritic cells via rapid cytosolic antigen delivery and processing via tripeptidyl peptidase II.* J Immunol, 2009. **182**(3): p. 1253-9.

347. Bendz, H., et al., *Human heat shock protein 70 enhances tumor antigen presentation through complex formation and intracellular antigen delivery without innate immune signaling.* J Biol Chem, 2007. **282**(43): p. 31688-702.

348. Dhodapkar, K.M., et al., *Antitumor monoclonal antibodies enhance cross-presentation ofcCellular antigens and the generation of myeloma-specific killer T cells by dendritic cells.* J Exp Med, 2002. **195**(1): p. 125-33.

349. Met, O., et al., *Principles of adoptive T cell therapy in cancer.* Semin Immunopathol, 2019. **41**(1): p. 49-58.

350. Herve, J., et al., *beta2-Adrenoreceptor agonist inhibits antigen cross-presentation by dendritic cells.* J Immunol, 2013. **190**(7): p. 3163-71.

351. Hunzeker, J.T., et al., *A marked reduction in priming of cytotoxic CD8+ T cells mediated by stress-induced glucocorticoids involves multiple deficiencies in cross-presentation by dendritic cells.* J Immunol, 2011. **186**(1): p. 183-94.

352. Bauer, J., et al., *Cutting Edge: IFN-beta Expression in the Spleen Is Restricted to a Subpopulation of Plasmacytoid Dendritic Cells Exhibiting a Specific Immune Modulatory Transcriptome Signature.* J Immunol, 2016. **196**(11): p. 4447-51.

353. Barnowski, C., et al., *Efficient Induction of Cytotoxic T Cells by Viral Vector Vaccination Requires STING-Dependent DC Functions.* Front Immunol, 2020. **11**: p. 1458.

354. Hulsen, T., J. de Vlieg, and W. Alkema, *BioVenn - a web application for the comparison and visualization of biological lists using area-proportional Venn diagrams.* BMC Genomics, 2008. **9**: p. 488.

355. Green, M.R. and J. Sambrook, *Estimation of Cell Number by Hemocytometry Counting.* Cold Spring Harb Protoc, 2019. **2019**(11).

356. Green, M.R. and J. Sambrook, *Quantifying and Storing RNA.* Cold Spring Harb Protoc, 2020. **2020**(3): p. 101709.

357. Livak, K.J. and T.D. Schmittgen, *Analysis of relative gene expression data using real-time quantitative PCR and the 2(-Delta Delta C(T)) Method.* Methods, 2001. **25**(4): p. 402-8.

358. Macey, M.G., *Flow cytometry: principles and clinical applications.* Med Lab Sci, 1988. **45**(2): p. 165-73.

359. Wilkerson, M.J., *Principles and applications of flow cytometry and cell sorting in companion animal medicine.* Vet Clin North Am Small Anim Pract, 2012. **42**(1): p. 53-71.

360. Qin, D., *Next-generation sequencing and its clinical application.* Cancer Biol Med, 2019. **16**(1): p. 4-10.

361. Reizis, B., *Plasmacytoid Dendritic Cells: Development, Regulation, and Function.* Immunity, 2019. **50**(1): p. 37-50.

362. Kovacsovics-Bankowski, M., et al., *Efficient major histocompatibility complex class I presentation of exogenous antigen upon phagocytosis by macrophages.* Proc Natl Acad Sci U S A, 1993. **90**(11): p. 4942-6.

363. Sheng, J., et al., *A Discrete Subset of Monocyte-Derived Cells among Typical Conventional Type 2 Dendritic Cells Can Efficiently Cross-Present.* Cell Rep, 2017. **21**(5): p. 1203-1214.

364. Fu, C., et al., *Plasmacytoid Dendritic Cells and Cancer Immunotherapy.* Cells, 2022. **11**(2).

365. Oberkampf, M., et al., *Mitochondrial reactive oxygen species regulate the induction of CD8(+) T cells by plasmacytoid dendritic cells.* Nat Commun, 2018. **9**(1): p. 2241.

366. Hemann, E.A., et al., *Plasmacytoid Dendritic Cells Require Direct Infection To Sustain the Pulmonary Influenza A Virus-Specific CD8 T Cell Response.* J Virol, 2015. **90**(6): p. 2830-7.

367. Moffat, J.M., et al., *Targeting antigen to bone marrow stromal cell-2 expressed by conventional and plasmacytoid dendritic cells elicits efficient antigen presentation.* Eur J Immunol, 2013. **43**(3): p. 595-605.

368. Aspord, C., et al., *Melanoma hijacks plasmacytoid dendritic cells to promote its own progression.* Oncoimmunology, 2014. **3**(1): p. e27402.

369. Lombardi, V.C., S.F. Khaiboullina, and A.A. Rizvanov, *Plasmacytoid dendritic cells, a role in neoplastic prevention and progression.* Eur J Clin Invest, 2015. **45 Suppl 1**: p. 1-8.

370. Charles, J., et al., *An innovative plasmacytoid dendritic cell line-based cancer vaccine primes and expands antitumor T-cells in melanoma patients in a first-in-human trial.* Oncoimmunology, 2020. **9**(1): p. 1738812.

371. Guery, L., et al., *Ag-presenting CpG-activated pDCs prime Th17 cells that induce tumor regression.* Cancer Res, 2014. **74**(22): p. 6430-40.

372. Kranz, L.M., et al., *Systemic RNA delivery to dendritic cells exploits antiviral defence for cancer immunotherapy.* Nature, 2016. **534**(7607): p. 396-401.

373. Giodini, A. and P. Cresswell, *Hsp90-mediated cytosolic refolding of exogenous proteins internalized by dendritic cells.* EMBO J, 2008. **27**(1): p. 201-11.

374. Johnson, J.L., *Evolution and function of diverse Hsp90 homologs and cochaperone proteins.* Biochim Biophys Acta, 2012. **1823**(3): p. 607-13.

375. Kato, Y., et al., *HSP70 and HSP90 Differentially Regulate Translocation of Extracellular Antigen to the Cytosol for Cross-Presentation.* Autoimmune Dis, 2012. **2012**: p. 745962.

376. Rock, K.L. and L. Shen, *Cross-presentation: underlying mechanisms and role in immune surveillance.* Immunol Rev, 2005. **207**: p. 166-83.

377. Stenmark, H., *Rab GTPases as coordinators of vesicle traffic.* Nat Rev Mol Cell Biol, 2009. **10**(8): p. 513-25.

378. Agola, J.O., et al., *Rab GTPases as regulators of endocytosis, targets of disease and therapeutic opportunities.* Clin Genet, 2011. **80**(4): p. 305-18.

379. Zou, L., et al., *The GTPase Rab3b/3c-positive recycling vesicles are involved in cross-presentation in dendritic cells.* Proc Natl Acad Sci U S A, 2009. **106**(37): p. 15801-6.

380. Cebrian, I., et al., *Rab22a controls MHC-I intracellular trafficking and antigen cross-presentation by dendritic cells.* EMBO Rep, 2016. **17**(12): p. 1753-1765.

381. Bryant, C., et al., *A CD2 high-expressing stress-resistant human plasmacytoid dendritic-cell subset.* Immunol Cell Biol, 2016. **94**(5): p. 447-57.

382. Zhang, H., et al., *A distinct subset of plasmacytoid dendritic cells induces activation and differentiation of B and T lymphocytes.* Proc Natl Acad Sci U S A, 2017. **114**(8): p. 1988-1993.

383. Villani, A.C., et al., *Single-cell RNA-seq reveals new types of human blood dendritic cells, monocytes, and progenitors.* Science, 2017. **356**(6335).

384. See, P., et al., *Mapping the human DC lineage through the integration of high-dimensional techniques.* Science, 2017. **356**(6342).

385. Alcantara-Hernandez, M., et al., *High-Dimensional Phenotypic Mapping of Human Dendritic Cells Reveals Interindividual Variation and Tissue Specialization.* Immunity, 2017. **47**(6): p. 1037-1050 e6.

386. Alculumbre, S.G., et al., *Diversification of human plasmacytoid predendritic cells in response to a single stimulus.* Nat Immunol, 2018. **19**(1): p. 63-75.

387. Swiecki, M. and M. Colonna, *The multifaceted biology of plasmacytoid dendritic cells.* Nat Rev Immunol, 2015. **15**(8): p. 471-85.

388. Mitchell, D., S. Chintala, and M. Dey, *Plasmacytoid dendritic cell in immunity and cancer.* J Neuroimmunol, 2018. **322**: p. 63-73.

389. Liu, C., et al., *Plasmacytoid dendritic cells induce NK cell-dependent, tumor antigen-specific T cell cross-priming and tumor regression in mice.* J Clin Invest, 2008. **118**(3): p. 1165-75.

390. Rezaei Araghi, R., et al., *Iterative optimization yields Mcl-1-targeting stapled peptides with selective cytotoxicity to Mcl-1-dependent cancer cells.* Proc Natl Acad Sci U S A, 2018. **115**(5): p. E886-E895.

391. Ball, D.P., et al., *Signal transducer and activator of transcription 3 (STAT3) inhibitor, S3I-201, acts as a potent and non-selective alkylating agent.* Oncotarget, 2016. **7**(15): p. 20669-79.

Acknowledgements

First and foremost, I would like to thank my doctoral supervisor, Professor Stefanie Scheu. She gave me the opportunity to get to know an exceptionally motivating, supportive and goal-oriented atmosphere in a scientific study group. I was shown an extremely exciting and certainly inspiring field for my professional future in addition to my clinical work. I am looking forward to taking what I have learned with me on my way and to benefit from it in further projects.

I would also like to thank my study group, especially Dr. Shafaqat Ali, for the numerous exciting discussions about this thesis and the interpersonal support during this project. Another supporting hand that I would not have wanted to miss is Sonja Schavier.

The study group of Professor Ingo Drexler should not remain unmentioned, above all I would like to thank for the possibility of the realization of the antigen cross-presentation assay. This would not have been possible without the great input by Cornelia Barnowski.

A very special thanks goes to my family and friends for their tireless support.